

UC San Diego

UC San Diego Electronic Theses and Dissertations

Title

Electrospinning of Nanofibrous Scaffolds for Meniscal Tissue Engineering

Permalink

<https://escholarship.org/uc/item/2cr8c0d3>

Author

Baek, Jihye

Publication Date

2015

Peer reviewed|Thesis/dissertation

UNIVERSITY OF CALIFORNIA, SAN DIEGO

Electrospinning of Nanofibrous Scaffolds for Meniscal Tissue Engineering

A dissertation submitted in partial satisfaction of the
requirements for the degree Doctor of Philosophy

in

Materials Science and Engineering

by

Jihye Baek

Committee in Charge:

Professor Sungho Jin, Chair
Professor Renkun Chen
Professor Darryl D'Lima
Professor Ratneshwar Lal
Professor Vlado A. Lubarda
Professor Shyni Varghese

2015

Copyright

Jihye Baek, 2015

All rights reserved

The dissertation of Jihye Baek is approved, and it is acceptable in
quality and form for publication on microfilm:

Chair

University of California, San Diego

2015

DEDICATION

*Dedicated to my loving family
who have always shown unfailing love*

EPIGRAPH

“I can do all this through him who gives me strength.”

-The Bible, Philippians 4:13

TABLE OF CONTENTS

SIGNATURE PAGE.....	iii
DEDICATION.....	iv
EPIGRAPH.....	v
TABLE OF CONTENTS.....	vi
LIST OF FIGURES.....	xi
LIST OF TABLES.....	xiv
ACKNOWLEDGEMENTS.....	xv
VITA.....	xviii
ABSTRACT OF THE DISSERTATION.....	xx
CHAPTER 1: INTRODUCTION.....	1
1.1 Motivations and Background.....	1
1.1.1 Structure –function, and composition of the meniscus	1
1.1.2. Meniscus lesions and their treatment	7
1.1.3 Meniscal Tissue Engineering	9
1.1.4 Electrospinning and nanofibrous scaffolds for meniscal tissue engineering.....	11
1.2 Thesis objective	15
1.3 Overview of the dissertation.....	16
1.4 References.....	17
CHAPTER 2: MENISCUS TISSUE ENGINEERING USING A NOVEL COMBINATION OF ELECTROSPUN SCAFFOLDS AND HUMAN MENISCUS CELLS EMBEDDED WITHIN AN EXTRACELLULAR MATRIX HYDROGEL.	21
2.1 Introduction.....	21

2.2 Materials and Methods.....	25
2.2.1 Fabrication of poly lactic acid (PLA) scaffolds	25
2.2.2 Structural morphology of PLA scaffolds	26
2.2.3 Tissues and cell isolation.....	26
2.2.4 Cell cultures on single layered ES PLA scaffolds.....	27
2.2.5 Mechanical properties of PLA scaffolds	28
2.2.6 Multilayer construct formation.....	29
2.2.7 Cell viability assessments.....	30
2.2.8 Cellular morphology of avascular meniscus cells on single layer PLA scaffolds.....	30
2.2.9 Histology and immunohistochemistry.....	31
2.2.10 RNA isolation and RT-PCR.....	31
2.2.11 Statistical analysis	32
2.3 Results.....	33
2.3.1 Controlled production of electrospun random and aligned PLA fibrous scaffolds.....	33
2.3.2 Controlled production of electrospun random and aligned PLA fibrous scaffolds.....	33
2.3.3 Meniscus cell phenotype is not altered by fiber orientation or from region of isolation	35
2.3.4 High tensile mechanical properties of aligned electrospun PLA scaffolds.	36
2.3.5 Multi-layer PLA cell-seeded scaffold support meniscus-like neotissue formation	38
2.4 Discussion.....	41
2.5 Conclusion	45
2.6 Acknowledgments.....	46
2.7 References.....	47

CHAPTER 3: REPAIR OF AVASCULAR MENISCUS TEARS WITH ELECTROSPUN COLLAGEN SCAFFOLDS SEEDED WITH HUMAN CELLS.51

3.1 Introduction.....	51
3.2.1 Fabrication of electrospun collagen type I scaffolds.....	54
3.2.2 Structural morphology of collagen type I scaffold.....	54
3.2.3 Tissues harvesting and cell isolation.....	55
3.2.4 Cell seeding in electrospun collagen type I scaffolds	55
3.2.5 Mechanical properties of collagen type I scaffold	56
3.2.6 Cell viability assessments.....	57
3.2.7 Cellular morphology of meniscus cells on collagen type I scaffolds by SEM	57
3.2.8 Measurement of newly deposited collagen type I.....	58
3.2.9 RNA isolation and RT-PCR.....	58
3.2.10 Ex-vivo meniscal repair.....	59
3.2.11 Histology, immunohistochemistry (IHC), and histomorphometry	60
3.2.12 MRI for ex-vivo model with coronal defect.....	61
3.2.13 Mechanical testing of repair in ex-vivo model.....	61
3.2.14 Statistical analysis	62
3.3 Results.....	63
3.3.1 Controlled production of ES collagen fibrous scaffolds	63
3.3.2 Scaffold organization influences cell response while maintaining high cell viability.....	63
3.3.3 Mechanical properties of scaffolds influenced by fiber alignment and culture conditions	64
3.3.4 A meniscus-like phenotype supported by scaffold and specific gene responses differed between cell source and scaffold organization.....	70
3.3.5 Integration and neotissue formation of ES cell seeded scaffolds in an ex vivo meniscus defect model.	71
3.4 Discussion.....	75

3.5 Conclusion	80
3.6 Acknowledgments.....	80
3.7 References.....	81
CHAPTER 4: MENISCAL TISSUE ENGINEERING USING ELECTROSPUN	
NATURAL/COLLAGEN: COMPARISON OF DIFFERENT CELL SOURCES.. 88	
4.1 Introduction.....	88
4.2 Materials and Methods.....	92
4.2.1 Fabrication of electrospun collagen type I scaffolds.....	92
4.2.2 Tissues and cell isolation.....	92
4.2.3 Single layer scaffold cell culturing.....	94
4.2.4 Multi-layer construct formation	94
4.2.5 Cell viability assessments.....	95
4.2.6 Cellular morphology of avascular meniscus cells on collagen type I scaffolds by SEM.....	95
4.2.7 Histology	96
4.2.8 RNA isolation and RT-PCR.....	96
4.2.9 Mechanical properties of multilayered constructs.....	97
4.2.10 Statistical analysis	97
4.3 Results.....	99
4.3.1 Cell morphology and organization on a single layer of scaffold	99
4.3.2 Multi-layer collagen scaffolds encapsulated cells with or without hydrogel.....	99
4.3.3 Multilayered collagen construct support meniscus-like neotissue formation	103
4.3.4 A meniscus-like phenotype supported by scaffold and specific gene responses differed between cell source and scaffold organization.....	106
4.3.5 Tensile mechanical property of multilayered construct dependent on existing cells or cell types	109
4.4 Discussion.....	111

4.5 Conclusion	115
4.6 Acknowledgments.....	115
4.7 References.....	116
CHAPTER 5: CONCLUSIONS	120

LIST OF FIGURES

Figure 1.1 Anatomic location of the meniscus. Anterior view of the human knee joint illustrating semilunar disc shaped fibrocartilaginous menisci. Courtesy of student consult.com	2
Figure 1.2 Schematic chart of the biochemical content in meniscus by wet weight	3
Figure 1.3 Synoptic drawing (upper part). And SEM pictures of three distinct areas, 1. Superficial network, 2. Lamellar layer, and 3. Central main layer is correlated with the synoptic drawing (under part). Adapted from (Petersen et al. 1998)[5]	4
Figure 1.4 Schematic diagram of different types of meniscal injuries. Courtesy of http://www.inkymousestudios.com/portfolio/medical-illustration/human/tibial-plateau-meniscus-tears.php	7
Figure 1.5 Schematic diagram of categorized scaffolds for tissue engineering of the meniscus.....	9
Figure 1.6 Schematic diagram of scaffolds for meniscal tissue engineering graded on three standards from 1-4 blocks[2].	11
Figure 1.7 Scanning electron microscopy (SEM) image of electrospun nanofibers compared to a human hair (left) and schematic of different fibers according to diverse diameters. Courtesy of http://www.epa.gov/ncer/events/news/2002/09_05_02a.html	12
Figure 1.8 Schematic of electrospinning device to generate nanofibers.....	14
Figure 2.1 Overview of the electrospinning equipment	26
Figure 2.2 Geometry and size (mm) of the dog-bone shaped tensile test specimens	29
Figure 2.3 Three-dimensional cultures of human meniscus cells on electrospun PLA scaffolds embedded in the tricomponent hydrogel.	30
Figure 2.4 Scanning electron micrographs (SEM) of electrospun (ES) PLA scaffolds (A) SEM of random and (B) aligned ES PLA fibers (Mag. 1250x, scale bar: 20 μ m). ..	33
Figure 2.5 Scanning electron micrographs (SEM) and confocal microscope images demonstrating viability (live/dead) of cellular response on electrospun (ES) PLA scaffolds.	34
Figure 2.6 Relative fold change in gene expression of human vascular and avascular meniscus cells cultivated on either random or aligned PLA electrospun scaffolds(n = 4–5 donors). Expression levels are relative to monolayer controls (dotted line).....	35

Figure 2.7 Mechanical testing of random and aligned ES PLA scaffolds.	37
Figure 2.8 Mechanical testing of random and aligned ES PLA scaffolds over time in culture with or without cells (one week and three weeks) (A) Young’s modulus (MPa) (B) Ultimate stress (MPa).....	39
Figure 2.9 Histology and immunohistochemistry of multi-layer aligned PLA cell seeded scaffolds.	40
Figure 3.1 Fabrication of avascular section of meniscus.....	59
Figure 3.2 Images of the cell/collagen scaffold implant during the tensile testing process.	61
Figure 3.3 Scanning electron micrographs (SEM) of electrospun (ES) collagen scaffolds. (A) SEM of random and (B) aligned ES collagen fibers (Mag. 1250x; scale bar: 10 μm).....	63
Figure 3.4 Scanning electron micrographs (SEM) of cellular response on electrospun (ES) collagen scaffolds..	65
Figure 3.5 Mechanical testing of random and aligned ES collagen scaffolds... ..	68
Figure 3.6 ELISA quantification for collagen type I and gene expression levels of human vascular and avascular meniscus cells cultivated on either random or aligned collagen electrospun scaffolds. Expression levels are relative to monolayer controls (dotted line).....	69
Figure 3.7 Mechanical strength of bovine meniscus ex-vivo repair model. Collagen membranes were seeded with human meniscus avascular cells to create a human meniscus avascular cells/electrospun collagen scaffold implant, as described under material and methods.	70
Figure 3.8 Overview of defect formation, histology and immunohistochemistry of bovine meniscus ex-vivo repair model	72
Figure 3.9 Histomorphometric analysis of integration was significantly different between acellular and cell-seeded scaffolds \.....	73
Figure 3.10 MRI images of bovine meniscus ex-vivo repair model.....	74
Figure 4.1 Scanning electron micrographs (SEM) and confocal microscope images demonstrating viability (live/dead) of cellular response on electrospun (ES) collagen scaffolds.....	98
Figure 4.2 Three –dimensional cultures of human meniscus and BM-MSc on electrospun collagen scaffolds embedded in the tricomponent hydrogel As a	

screening tool, hBM-MSC were seeded upon electrospun collagen scaffold sheets I the hydrogel.	99
Figure 4.3 Layers of scaffold (square or disc shaped) and cells within hydrogel were constructed The constructs were maintained in serum-free medium with either TGFβ1, TGFβ3(10 ng/ml) or without growth factors (control) for 14 days.....	101
Figure 4.4 Layers of scaffold (square or disc shaped) and cells without hydrogel were constructed The constructs were maintained in serum-free medium with either TGFβ1, TGFβ3(10 ng/ml) or without growth factors (control) for 14 days.....	102
Figure 4.5 Histological analysis (H&E) of three-dimensional cultures of human meniscus, BM-MSCs, Synovial, and IPFP cells on electrospun collagen scaffolds embedded in the tricomponent hydrogel.....	104
Figure 4.6 Histological analysis (Safranin O fast green) of three-dimensional cultures of human meniscus, BM-MSCs, Synovial, and IPFP cells on electrospun collagen scaffolds embedded in the tricomponent hydrogel.	105
Figure 4.7 Relative fold change in COL1A1 gene expression of human vascular and avascular meniscus cells, MSCs, synovial, and IPFP cells of multilayered collagen constructs. Expression levels are relative to monolayer controls (dotted line).....	107
Figure 4.8 Relative fold change in COMP gene expression of human vascular and avascular meniscus cells, MSCs, synovial, and IPFP cells of multilayered collagen constructs. Expression levels are relative to monolayer controls (dotted line).....	108
Figure 4.9 The mechanical properties of multilayered construct were quantified via tensile testing (n = 9 per group). (A) Young’s modulus (p<0.05) and (B) ultimate tensile strength of three-dimensional constructs (no significant difference)	110

LIST OF TABLES

Table 1.1 Biomechanical properties of the knee meniscus	5
Table 1.2 Tensile properties of the knee meniscus	6
Table 3.1 Ultimate tensile strength and Young's modulus (MPa) of freshly made and non-cultured random and aligned ES collagen scaffolds. (NC, noncrosslinked scaffolds; CL, crosslinked)	66
Table 3.2 Ultimate tensile strength and Young's modulus (MPa) of random & aligned ES collagen scaffolds over time in culture with or without cells (1 week and 3 weeks).	67

ACKNOWLEDGEMENTS

During my graduate studies at University of California at San Diego, I have been blessed to meet so many talented people. Firstly, I cannot thank my advisor enough for being my mentor; I would like to express my sincerest gratitude to Professor Darryl D’Lima and Prof. Sungho Jin for giving me a wonderful opportunity to be part of the greatest journey that I have experienced thus far. His heartfelt encouragement, guidance, and passion for science and clinic always inspire me to joyfully follow my own trail without any hesitation.

I would like to thank my committee members, Prof. Ratneshwar Lal, Prof. Shyni Varghese, Prof. Vlado A. Lubarda, and Prof. Renkun Chen for helpful discussions and valuable suggestions on my dissertation.

I am indebted to all my former and present members of the D’Lima group who are my colleagues as well as good friends of mine. In particular, I am truly grateful to Dr. Clifford C. Colwell for his wonderful support and encouragement, Dr. Martin K. Lotz for allowing me to use his lab and collaborate with his members, and Dr. Shawn P. Grogan for being a dependable friend and giving me the indispensable foundation of proper cell culture. Without his help, I would not have been able to succeed. Prof. Peter Chen for his biomechanical advices and consideration. Many thanks to MD Shantanu Patil and MD Wonchul Choi for their kind suggestions, and advices from their clinical experience and Many thanks to Sujata Sovani and Merissa Olmer for kindly teaching me cell analyzing and histology and for helpful discussion and encouragement. I appreciate

Judy Blake and Cathi Rabago for the administrative paper works, numerous informative notices and their smiles and Tammy Lee, and Erik W Dorthé for all their help.

Also, I would like to express my gratitude to the other members of Dr. Martin K. Lotz: Lilo Creighton-Achermann for teaching me histology and immunohistochemistry, Stuart Duffy, Oscar Alvarez-Garcia, Josan Chung, Connie Jo Choate, Cathy Klasen.

I'm so thanks for other members in Sungho Jin's lab: Taekyoung Kim for being so valuable friends and giving me advices and encouragements, Youngjin Kim for helping me to modify an electrospinner, Cihan Kuru for being a good friend and giving me cooperation with him, and Chulmin Choi for his advice.

I am also thankful to my colleagues: Prof. Jaeyun Moon for spending time with me at night together, being a great friend, and providing me all the valuable suggestions for being a great friend and Prof. Youngsung Hwang for helpful discussion about tissue engineering, his encouragement, and his consideration. Prof. Jiang Du for his wonderful collaboration on Margnetic Resonance Imaging (MRI).

I would like to recognize and thank Charlotte Lauve and Patrick Mallon for the administrative paperwork, invaluable advice, and numerous informative notices.

I would truly like to thank my wonderful friends who are like family and made this incredible journey possible: Sungwoon Kim, Anna Park, Helen Lee, Sunju Choi, Boram Lee, Joon Lee, Sooyoung Jang, Dajung Lee, Soohyun Nam, Yeejin Lee.

Lastly, I would like to express my deepest gratitude and love to my friend, Russell Lindsey, and my family: Namchul Baek, Kumsun Kim, Mihye Baek, Jaeha Baek, and his wife Sohee oh for their unfailing love, support, and prayer. Also, I would like to thank

my relatives Kyoung Ok Cho, Nohyuk Myung, Yeun Ju Myung, Yiyeon Myung, and Jacob Myung for their love and support.

Chapter 2, in full, is a reprint of the material as it appears in *Journal of Orthopaedic Research*, Volume 33, 2015. Jihye Baek, Xian Chen, Sujata Sovani, Sungho Jin, Shawn P. Grogan, Darryl D. D’Lima. The dissertation author was the primary investigator and author of this paper.

Chapter 3, in full, is currently being prepared for submission for publication of the material. Jihye Baek, Sujata Sovani, Nicholas E. Glembofski, Jiang Du, Sungho Jin, Shawn P. Grogan, Darryl D. D’Lima. The dissertation author was the primary investigator and author of this paper.

Chapter 4, in full, is currently being prepared for submission for publication of the material. Jihye Baek, Sujata Sovani, Wonchul Choi, Sungho Jin, Shawn P. Grogan, Darryl D. D’Lima. The dissertation author was the primary investigator and author of this paper.

VITA

- 2007 Bachelor of Engineering in Textile Engineering/Organic Materials and Fiber Engineering, Soongsil University, Seoul, Korea
- 2009 Master of Science in Textile Engineering/Organic Materials and Fiber Engineering, Soongsil University, Seoul, Korea
- 2015 Doctor of Philosophy in Materials Science and Engineering, University of California, San Diego

LIST OF PUBLICATIONS

- [1] **Jihye Baek**, Xian Chen, Sujata Sovani, Sungho Jin, Shawn P. Grogan, Darryl D. D’Lima, Meniscus Tissue Engineering Using a Novel Combination of Electrospun Scaffolds and Human Meniscus Cells Embedded Within an Extracellular Matrix Hydrogel, *Journal of Orthopaedic Research*, **33**, 572-583 (2015)
- [2] **Jihye Baek**, Sujata Sovani, Nicholas E. Glembofski, Jiang Du, Sungho Jin, Shawn P. Grogan, Darryl D. D’Lima, Repair of avascular meniscus tears with electrospun collagen scaffolds seeded with human cells. (*manuscript in preparation*)
- [3] **Jihye Baek**, Sujata Sovani, Wonchul Choi, Sungho Jin, Shawn P. Grogan, Darryl D. D’Lima, Meniscal Tissue Engineering using Electrospun Natural/Collagen: Comparison of Different Cell Sources. (*manuscript in preparation*)

LIST OF PRESENTATIONS

- [1] **Jihye Baek**, Sungho Jin, Sujata Sovani, Xian Chen, Darryl D. D’Lima, Grogan Shawn P. Meniscal Tissue Engineering: Cell Encapsulation of Electrospun Collagen, Podium, 60th Annual Meeting of the Orthopaedic Research Society (ORS), New Orleans, LA, March 15–18, 2014.

[2] **Jihye Baek**, Sungho Jin, Xian Chen, Darryl D D’Lima, Shawn P Grogan, “Meniscal tissue engineering using electrospun matrix systems” Poster., 59th Annual Meeting, Orthopaedic Research Society (ORS), San Antonio, TX, January 26-29, 2013.

ABSTRACT OF THE DISSERTATION

Electrospinning of Nanofibrous Scaffolds for Meniscal Tissue Engineering

by

Jihye Baek

Doctor of Philosophy in Materials Science and Engineering

University of California, San Diego, 2015

Professor Sungho Jin, Chair

Meniscus injury and degeneration have been linked to the development of secondary osteoarthritis. Therapies that successfully repair or replace the meniscus are therefore likely to prevent or delay OA progression. We investigated the novel approach of building layers of aligned polylactic acid (PLA) electrospun scaffolds with human meniscus cells embedded in extracellular matrix (ECM) hydrogel to lead to formation of neotissues that resemble meniscus-like tissue. PLA ES scaffolds with randomly oriented or aligned fibers were seeded with human meniscus cells derived from vascular or

avascular regions. Morphology and mechanical properties of PLA scaffolds (with and without cells) were influenced by fiber direction of the scaffolds.

Also, the self-healing capacity of an injured meniscus is limited to the vascularized regions and is especially challenging in the inner avascular regions. Thus, we investigated the use of human meniscus cell-seeded electrospun collagen type I scaffolds to produce meniscus tissue and explored whether these cell seeded scaffolds can be implanted in repair defects created in meniscus avascular tissue explants. To determine potential for repair of meniscal defects, meniscus cells were seeded and cultured on aligned electrospun collagen scaffolds for 4 weeks before implantation. Surgical defects resembling “longitudinal tears” were created in the avascular zone of live bovine meniscus explants and implanted with cell-seeded collagen scaffolds and cultured for 3 weeks. Ex-vivo implantation with cell-seeded collagen scaffolds resulted in neo-tissue that was significantly better integrated with the native tissue. Meniscus cell-seeded electrospun collagen scaffolds may therefore be useful in facilitating meniscal repair in the repair of avascular meniscus tears.

Hydrogels and electrospun scaffolds materials support cell attachment and neo tissue development and can be tuned to structurally and mechanically resemble native ECM by altering either electrospun fiber or hydrogel properties. We examined meniscus tissue generation from different cell sources including several human meniscus, bone-marrow mesenchymal stem, synovial, and infrapatellar fat pad cells. All cells were seeded onto electrospun collagen scaffolds while encapsulated in an ECM hydrogel or directly seeded on the scaffolds. Collagen scaffolds supported meniscus tissue formation and cell seeded scaffolds generated higher stiffness relative to acellular scaffolds.

Overall, electrospun materials support neotissue formation and show potential for use in cell-based meniscus regeneration strategies.

CHAPTER 1: INTRODUCTION

“The secret of life, though, is to fall seven times and to get up eight times.”

—Paulo Coelho

1.1 Motivations and Background

1.1.1 Structure –function, and composition of the meniscus

Menisci are semilunar disc-shaped fibrocartilaginous tissues located on the tibial plateau within the medial and lateral compartments of the knee (Figure 1.1). The major functions of this tissue include transmission of load and contribution to joint lubrication[1]. The menisci can be divided into outer and inner regions containing cells that are responsible for maintaining tissue homeostasis under the high shear and compressive forces experienced in the knee joint. The wedge shape semilunar sections of meniscus and its horn attachment contribute to alter the perpendicular compressive tibiofemoral forces to horizontal hoop stresses[2]. Simultaneously, shear forces are developed between the collagen fibers within the meniscus while the meniscus is deformed outspread. Meniscal existence in diverse animal species already proves their significance[3].

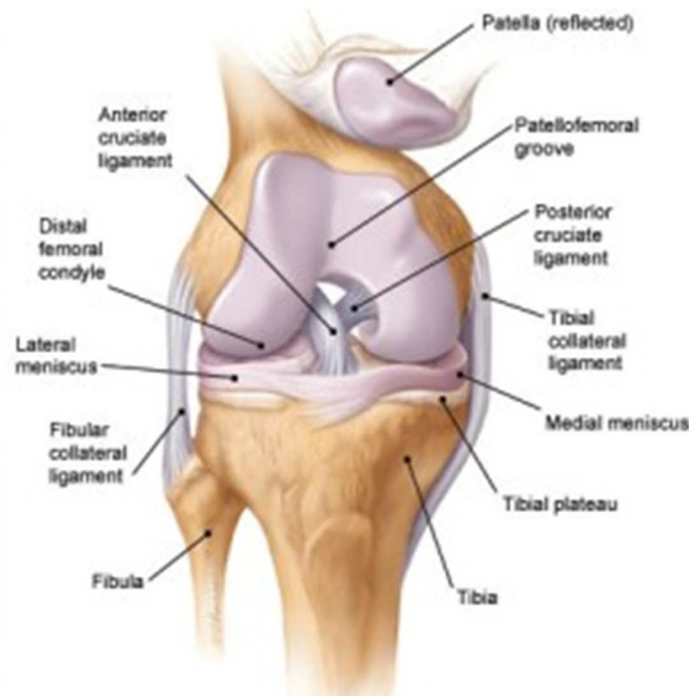


Figure 1.1 Anatomic location of the meniscus. Anterior view of the human knee joint illustrating semilunar disc shaped fibrocartilaginous menisci. Courtesy of student consult.com

The peripheral section of the meniscus is comprised of vascularized tissue and covered by synovial membrane tissues, including major fibroblast-like cells while the inner section of the meniscus is avascular along with more chondrocyte-like cells[2]. In terms of biochemical composition, the meniscus is highly hydrated since water forms approximately 72% of the wet weight of the meniscus.[4] The remaining 28% is consists of organic matter comprised of mostly extracellular matrix (ECM) and cells. The bulk of the organic matter consist of collagens (75%), GAGs (17%), DNA (2%), adhesion glycoproteins (<1%), and elastin (<1%) (Figure 1.2[2]).

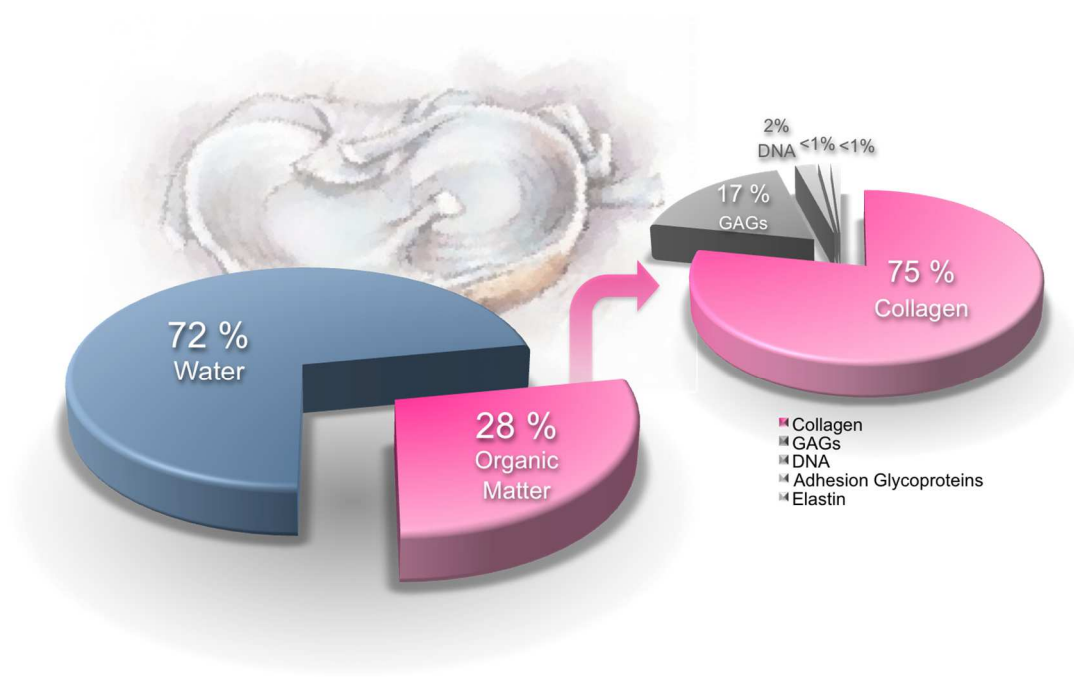


Figure 1.2 Schematic chart of the biochemical content in meniscus by wet weight

The collagen fibrils are mostly organized in a circumferential direction while some collagen fibers are oriented radially (Figure 1.3). This can be correlated with mechanical forces that meniscus withstands during everyday activity. Petersen et al.[5] conducted scanning electron microscopy (SEM) of human meniscus tissues, and described three distinct layers in the meniscus cross section (Figure 1.3) including i) Superficial network, a fibril network, woven into a mesh-like matrix, enclosing the femoral and tibial areas. ii) Lamellar layer, which lies below the superficial network that is comprised of radially oriented bundles of collagen fibrils. iii) Central main layer that is the primary bulk part of the meniscus, consisting of collagen fibrils that are organized in a circumferential orientation.

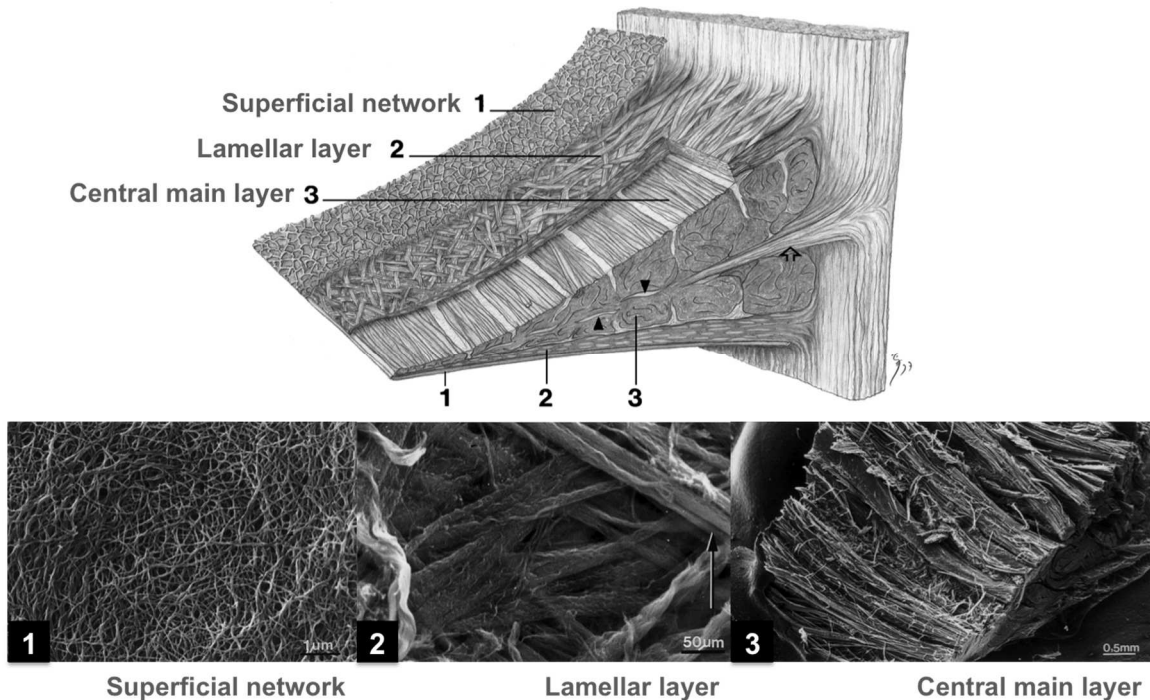


Figure 1.3 Synoptic drawing (upper part). And SEM pictures of three distinct areas, 1. Superficial network, 2. Lamellar layer, and 3. Central main layer is correlated with the synoptic drawing (under part). Adapted from (Petersen et al. 1998)[5]

The biomechanical properties of the meniscus in the knee are adapted to resist many different forces such as shear, tension, and compression. Several studies have investigated the properties of the meniscus tissue both in humans and in animal models as outlined in in Tables 1.1 and 1.2[6-9]. As reported by these studies, the meniscus withstands vertical compression with an aggregate modulus of about 100-140 kPa. The tensile mechanical property of the meniscus vary with the direction (between circumferential and radial directions). Even though biomechanical properties vary by species, the meniscus has a characteristic anisotropy turned to the forces exerted on the tissue.

Table 1.1 Biomechanical properties of the knee meniscus

Study	Species	Segment	Aggregate Modulus [H _A] (±SD;MPa)	Shear Modulus [δμs] (±SD;MPa)	Permeability (±SD; 10 ⁻¹⁵ m ⁴ N ⁻¹ s ⁻¹)
Sweigart et al. [8]	Human	Medial Superior:			
		<i>Anterior</i>	0.15 ± 0.03	0.08 ± 0.01	1.84 ± 0.64
		<i>Central</i>	0.10 ± 0.03	0.05 ± 0.01	1.54 ± 0.71
		<i>Posterior</i>	0.11 ± 0.02	0.05 ± 0.01	2.74 ± 2.49
		Medial inferior:			
		<i>Anterior</i>	0.16 ± 0.05	0.08 ± 0.02	1.71 ± 0.48
	Bovine	<i>Central</i>	0.11 ± 0.04	0.06 ± 0.02	1.54 ± 0.49
		<i>Posterior</i>	0.09 ± 0.03	0.05 ± 0.01	1.32 ± 0.61
		Medial Superior:			
		<i>Anterior</i>	0.21 ± 0.06	0.11 ± 0.03	6.22 ± 2.55
		<i>Central</i>	0.14 ± 0.05	0.08 ± 0.02	5.73 ± 6.19
		<i>Posterior</i>	0.11 ± 0.04	0.06 ± 0.02	4.73 ± 2.56
		Medial inferior:			
		<i>Anterior</i>	0.16 ± 0.06	0.08 ± 0.03	5.79 ± 4.31
		<i>Central</i>	0.11 ± 0.03	0.06 ± 0.02	5.65 ± 4.13
		<i>Posterior</i>	0.13 ± 0.06	0.07 ± 0.03	5.40 ± 5.36

Table 1.2 Tensile properties of the knee meniscus

Study	Species	Direction	Location	Stiffness (\pm SD;MPa)
Fithian et al. [6]	Human	Circumferential	Lateral Meniscus	
			<i>Anterior</i>	159.1 \pm 47.4
			<i>Central</i>	228.8 \pm 51.4
			<i>Posterior</i>	294.1 \pm 90.4
			Medial Meniscus	
			<i>Anterior</i>	159.6 \pm 26.2
			<i>Central</i>	228.8 \pm 51.4
			<i>Posterior</i>	294.1 \pm 90.4
			Tissakht et al.[9]	Human
<i>Anterior</i>	124.58 \pm 39.51			
<i>Central</i>	91.37 \pm 23.04			
<i>Posterior</i>	143.73 \pm 38.91			
Medial Meniscus				
<i>Anterior</i>	106.21 \pm 77.95			
<i>Central</i>	77.95 \pm 25.09			
<i>Posterior</i>	82.36 \pm 22.23			
Radial	Lateral Meniscus			
	<i>Anterior</i>	48.47 \pm 25.67		
	<i>Central</i>	45.86 \pm 24.20		
	<i>Posterior</i>	29.85 \pm 12.77		
	Medial Meniscus			
	<i>Anterior</i>	48.31 \pm 24.35		
<i>Central</i>	46.20 \pm 27.56			
<i>Posterior</i>	32.55 \pm 11.27			
Lechner et al.[7]	Human	Circumferential	Medial Meniscus	
			<i>Anterior</i>	141.2 \pm 56.7
			<i>Central</i>	116.4 \pm 47.5
			<i>Posterior</i>	108.4 \pm 42.9

1.1.2. Meniscus lesions and their treatment

Meniscus tears are a major consequence of intra-articular knee injury and meniscal surgery is the most common orthopedic procedure in the United States[10, 11]. To be specific, approximately 1.5 million arthroscopic surgical procedures of the knee are performed each year in the United States alone and of these more than half involve the meniscus[12]. Meniscus lesions commonly occur young people as a consequence of sporting injuries, typically in females between 11 to 20 years of age and males between 21 and 30 years of age. Also, males are more prone to meniscal injury than females (male:female ratio between 2.5:1 to 4:1)[13, 14]. Meniscal injury in the medial meniscus take places more frequently than in the lateral meniscus with a ratio of about 2:1[15].

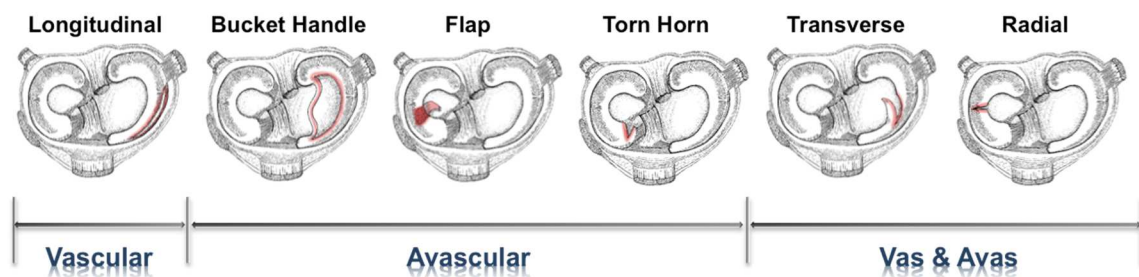


Figure 1.4 Schematic diagram of different types of meniscal injuries. Courtesy of <http://www.inkymousestudios.com/portfolio/medical-illustration/human/tibial-plateau-meniscus-tears.php>

The meniscus also exhibits regional variations in vascularization. Even though the menisci are fully vascularized at birth, the blood vessels in the meniscus regress over time. Therefore, the peripheral outer region (i.e. the red-red region) receives the

overwhelming bulk of blood vessels while inner section of the meniscus becomes avascular. Since this regional diversity of vascularization of the meniscus is correlated with healing capacity, juvenile meniscus injuries heal readily and have greater self-healing capacity than adult meniscus lesions, which only tend to heal in the vascularized region[16]. Thus, the vascularized periphery of the meniscus has some self-healing capacity, and minor or simple tears can be repaired with 63 – 91% repair rate[17]. However, large or complex tears, especially those within the avascular region have no self-healing capacity and are extremely difficult to repair[2, 4].

The treatment of meniscus injuries has progressed substantially over the last three decades. Diverse techniques and approaches have been attempted in patients in order to improve the repair and substitute damaged menisci. In order to relieve pain, enhance function, and prevent cartilage degeneration, meniscus allograft transplantation has been proposed as one solution[18-20]. Another approach is the direct replacement of meniscal tissue using synthetic or natural biomaterial, including periosteal tissue[21], small intestine submucosa SIS[22], acellular porcine meniscal tissue[23], perichondral tissue[24], and bacterial cellulose[25]. Even though a number of techniques have been developed to repair meniscal tears: involving sutures, screws, arrows, and darts[27], partial or total meniscectomy is currently the most common and recommended treatment for meniscus tears[26]. These meniscal repair procedures can relieve pain, locking, and instability in the short-term. However, in the long term, no significant benefit has been documented with respect to preventing degenerative joint changes and accelerated osteoarthritis (OA) due to deficient meniscal function[28-30].

1.1.3 Meniscal Tissue Engineering

Tissue engineering typically uses scaffolds to contribute transitory support for cells in order to stimulate the formation of new extracellular matrix (ECM) to replace tissue that has been damaged or destroyed by injury, disease, or innate defects. Native ECM comprises of diverse molecules that is critical for cell survival, proliferation, and function. It is comprised of proteins such as collagens, and carbohydrate biopolymers such as glycosaminoglycan (GAGs). The scaffolds for tissue engineering should imitate both the structure and the function of natural ECM. A number of studies have been conducted to tissue engineer the meniscus with different kinds of scaffold materials to mimic natural ECM and promote cell function in a natural microenvironment.

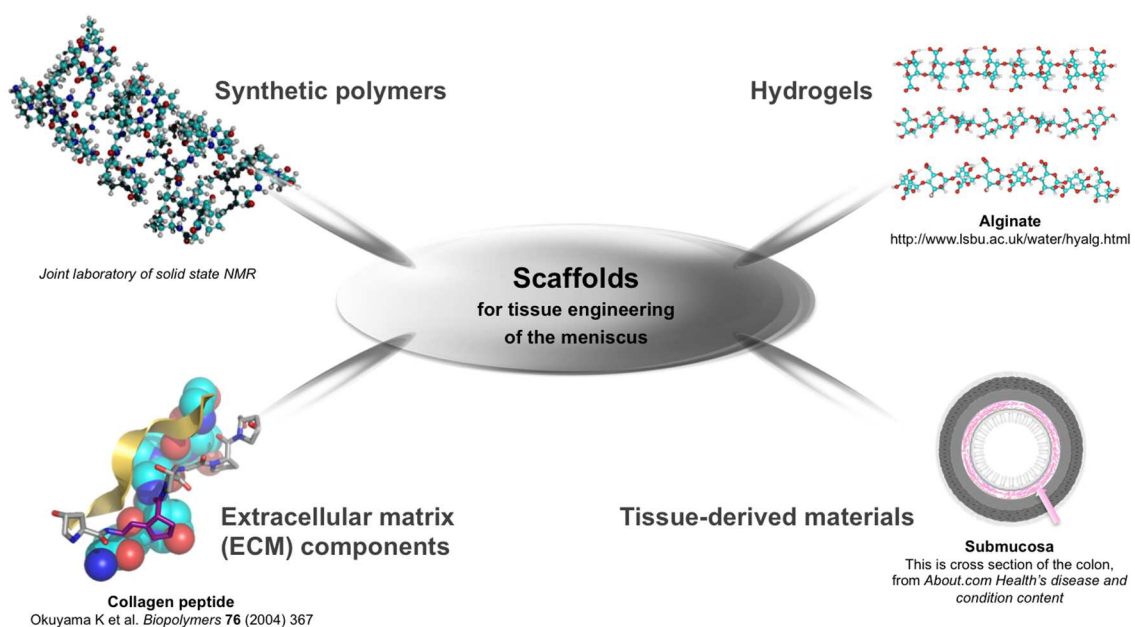


Figure 1.5 Schematic diagram of categorized scaffolds for tissue engineering of the meniscus

Scaffolds for meniscal tissue engineering can be classified into four broad groups: synthetic polymers, hydrogels, ECM components, or tissue-derived materials (Figure 1.5). Synthetic polymers such as polyurethane (PU), polycaprolactone (PCL), polyglycolic acid (PGA), polylactic acid (PLA), and polylactic co-glycolic acid (PLGA) are materials that can be biodegraded, and have several advantages including desirable mechanical properties, amenable to diverse methods to fabricate, and feasibility of tuning suitable pore size[31, 32]. Hydrogels are hydrophilic colloids, which can hold water, and are derived from synthetic materials such as poly N-isopropyl acrylamids (PNIPAAm) or natural materials like alginate[2]. Since hydrogels can hold a large amount of water, the water content largely determines the physical properties of the hydrogels. ECM component scaffolds are derived from macromolecules of natural materials like gelatin or collagen. ECM scaffolds establish a native environment for cultured cells and enhance bioactivity. However, the mechanical property of the ECM component scaffolds is not optimal. Lastly, tissue-derived materials consist of processed whole tissue such as decellularized ECM. Although tissue-derived materials have advantages of providing natural environment for cell seeding, migration, and ECM deposition, the supply of tissue-derived materials is limited[2].

The optimal scaffold for meniscal tissue engineering has to perform exceptionally well in at least three standards; mechanical properties, bioactivity, and logistics. The above four categories of scaffolds are graded based on this three standards outlined in Figure 1.6[2]. Because during everyday activity, the meniscus withstands many different kinds of forces such as shear, compression, and tension, scaffolds for meniscal tissue engineering should possess relevant mechanical properties. Also, ideal scaffolds should

support adequate cell viability in order to permit the production of new ECM, integrate into host tissue, have low immunogenicity, and maintain a final stable cell phenotype. Finally, scaffolds need to be easily accessed and available in plentiful and convenient supplies, able to be sterilized, and are able to be surgically handled and implanted into the knee joint.

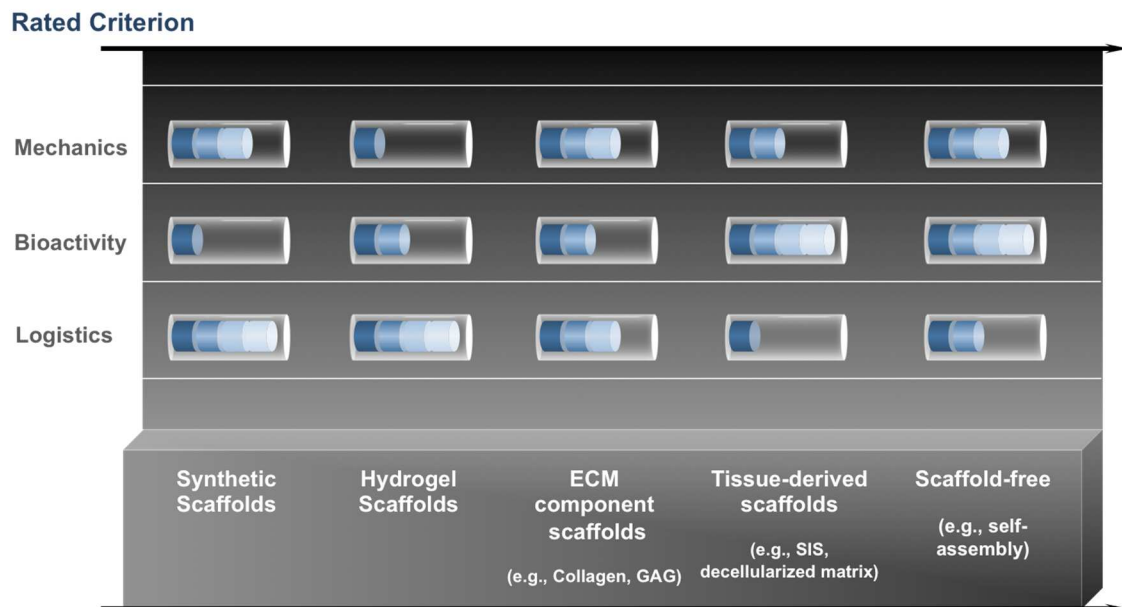


Figure 1.6 Schematic diagram of scaffolds for meniscal tissue engineering graded on three standards from 1-4 blocks[2].

1.1.4 Electrospinning and nanofibrous scaffolds for meniscal tissue engineering

A porous, and interconnected 3D construct with high surface area is needed for meniscal tissue engineering in order facilitate cell attachment, allow the diffusion of nutrients from the blood or synovial fluid, and mimic the mechanical properties of the tissue. Compared to macroscale-structural scaffolds, nanoscale-structural scaffolds have a

much larger surface area to present more surface proteins and enhance cell adhesions through cell membrane receptor interactions.

Many techniques have been investigated for fabricating porous scaffolds of tissue engineering to mimic ECM such as gas-foamed, salt-leached, freeform fabrication, topography library, phase separation, molecular self-assembly and hydrogels[33-36]. However, these methods have not been able to mimic ECM structure and function with the desired porosity. One method to emulate meniscus nano- and microstructure with appropriate anisotropic mechanical properties, and with high cell compatibility, may be achieved using a process called electrospinning.

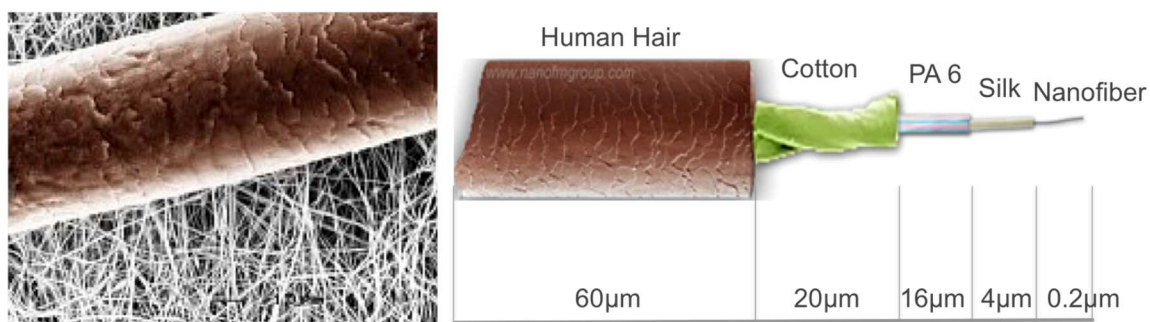


Figure 1.7 Scanning electron microscopy (SEM) image of electrospun nanofibers compared to a human hair (left) and schematic of different fibers according to diverse diameters. Courtesy of http://www.epa.gov/ncer/events/news/2002/09_05_02a.html

In the electrospinning process, a high voltage is applied to charge a liquid droplet of homogeneous polymer solution at the tip of spinneret, which serves as an electrode. At a critical point, a stream of liquid erupts and dries and is collected as a fiber on grounded or charged collectors, which serve as the counter-electrode. This point of eruption forms a Taylor cone, which accelerates the formation of continuous fibers (Figure 1.8). The

working parameters of electrospinning can be largely categorized into three parts: solution parameter, process parameters, and ambient parameters[37]. The solution parameters are comprised of the concentration of polymer solution, molecular weight of the polymer, solution viscosity, surface tension, and solution conductivity, which is dependent on the type of polymer and solvent. There are four different process parameters that affect the electrospinning process: the applied voltage that should be higher than the threshold voltage needed to eject a stream of liquid as fibers, the flow rate to control the emitted volume of solution onto a spinneret, the collector acting as the conductive substrate, and the distance between the collector and the tip of the syringe that affects the fiber diameter and morphology.

Electrospun scaffolds comprised of natural or synthetic materials in dimensions that mimic native collagen fiber bundles[2] can be efficiently produced by electrospinning.[13, 38] The combination of mechanical strength and biocompatible qualities of electrospun nanofibers provide an advantage over other 3-dimensional (3-D) scaffolds formed with techniques such as gas-foamed, salt-leached, freeform fabrication, topography library, and hydrogels [33, 35, 36]. The high surface-to-volume ratio, and porosity generated by electrospun fibers facilitates cell attachment, cell proliferation, and deliver of nutrients through the scaffold[39]. Specifically for meniscus tissue engineering, a scaffold that provides the requisite mechanical properties of the meniscus may be useful to enhance repair of meniscal tear defects, and may permit early rehabilitation. Active joint motion during the early phase of repair also helps prevent restrictive adhesions and scar tissue formation that affect range of motion and limit recovery of function[40].

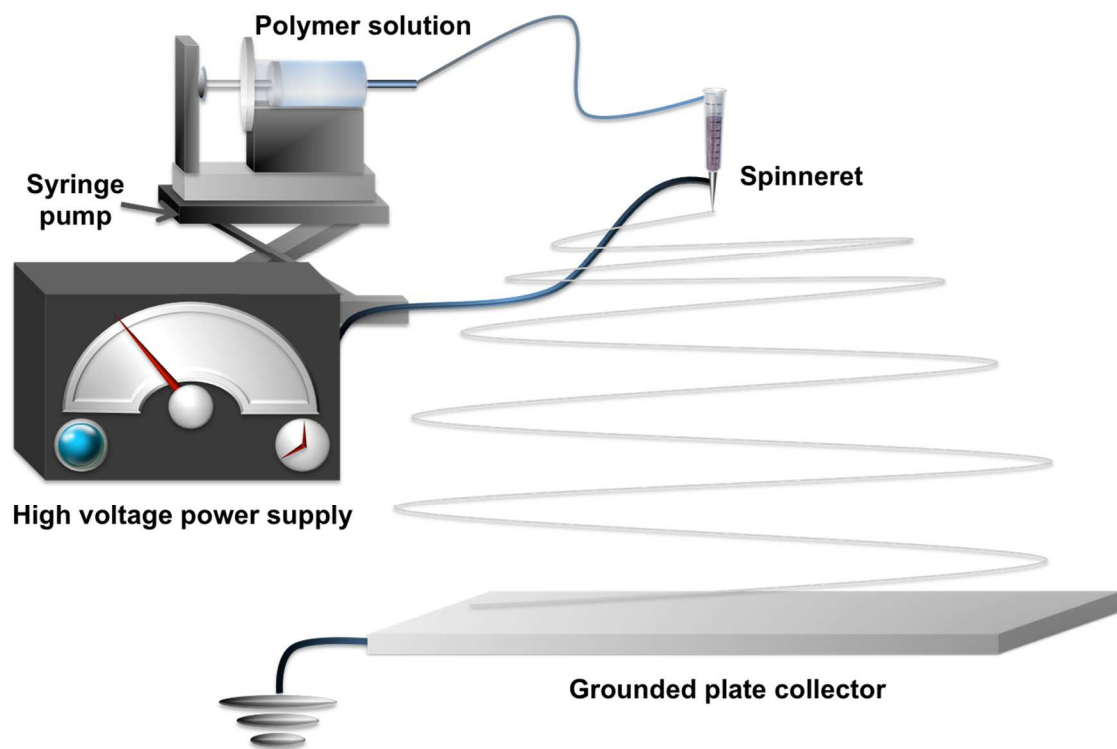


Figure 1.8 Schematic of electrospinning device to generate nanofibers

1.2 Thesis objective

The central focus of this thesis is to design electrospun nanofibrous scaffolds that can mimic the native extracellular matrix, especially circumferential collagen fibrils within meniscus, and to assess cell-attachment, cell viability, cellular morphological responses, extracellular matrix production, mechanical properties and stem cell differentiation.

To achieve these goals, the following issues were addressed:

- To develop and optimize the electrospinning processes to enhance cell-matrix interactions by tailoring specific scaffold parameters affecting nanostructural architecture, namely pore size, pore network geometry, hierarchical nanostructures, and anisotropy of internal pore structures.
- To design tunable natural materials as 3-dimensional constructs with appropriate mechanical properties, capable of promoting expansion of human meniscus cells or stem cells while maintaining their function.
- To investigate the healing effect of cell seeded engineered constructs with native meniscal tissue.

1.3 Overview of the dissertation

Chapter 1 provides a brief introduction to the structure, function, and composition of the meniscus, to meniscal tissue engineering, to the process of electrospinning, and summarizes the current status of meniscal tissue engineering.

Chapter 2 describes the design, development and characterization of electrospun artificial fibrous scaffolds and engineered multilayered architectures with human meniscus cells.

Chapter 3 further extends the application of electrospinning with a natural polymer, a major component of the meniscus ECM, and provides proof of concept healing of a meniscal tear.

Chapter 4 investigates the meniscogenic potential of different types of human cells when seeded on a nanofibrous scaffolds comprised of natural polymer.

Chapter 5 summarizes the dissertation and outlines potential future directions.

1.4 References

- [1] Ghosh P and Taylor T 1987 The knee joint meniscus: A fibrocartilage of some distinction *Clin Orthop Relat Res* 224 52-63
- [2] Makris E A, Hadidi P and Athanasiou K A 2011 The knee meniscus: Structure-function, pathophysiology, current repair techniques, and prospects for regeneration *Biomaterials* 32 7411-31
- [3] Arnoczky S P, Warren R F and Spivak J M 1988 Meniscal repair using an exogenous fibrin clot. An experimental study in dogs *The Journal of Bone & Joint Surgery* 70 1209-17
- [4] Scotti C, Hirschmann M T, Antinolfi P, Martin I and Peretti G M 2013 Meniscus repair and regeneration: Review on current methods and research potential *Eur Cell Mater* 26 150-70
- [5] Petersen W and Tillmann B 1998 Collagenous fibril texture of the human knee joint menisci *Anatomy and embryology* 197 317-24
- [6] Fithian D C, Kelly M A and Mow V C 1990 Material properties and structure-function relationships in the menisci *Clin Orthop Relat Res* 252 19-31
- [7] Lechner K, Hull M L and Howell S M 2000 Is the circumferential tensile modulus within a human medial meniscus affected by the test sample location and cross-sectional area? *Journal of Orthopaedic Research* 18 945-51
- [8] Sweigart M A, Zhu C F, Burt D M, deHoll P D, Agrawal C M, Clanton T O and Athanasiou K A 2004 Intraspecies and interspecies comparison of the compressive properties of the medial meniscus *Annals of Biomedical Engineering* 32 1569-79
- [9] Tissakht M and Ahmed A M 1995 Tensile stress-strain characteristics of the human meniscal material *Journal of Biomechanics* 28 411-22
- [10] Morgan C D, Wojtys E M, Casscells C D and Casscells S W 1991 Arthroscopic meniscal repair evaluated by second-look arthroscopy *Am J Sports Med* 19 632-7
- [11] Salata M J, Gibbs A E and Sekiya J K 2010 A systematic review of clinical outcomes in patients undergoing meniscectomy *Am J Sports Med* 38 1907-16
- [12] Rodkey W G, Steadman J R and Li S-T 1999 A clinical study of collagen meniscus implants to restore the injured meniscus *Clin Orthop Relat Res* 367S S281-S92

- [13] Baker B E, Peckham A C, Pupparo F and Sanborn J C 1985 Review of meniscal injury and associated sports Am J Sports Med 13 1-4
- [14] Hede A, Jensen D B, Blyme P and Sonne-Holm S 1990 Epidemiology of meniscal lesions in the knee. 1,215 open operations in copenhagen 1982-84 Acta Orthop Scand 61 435-7
- [15] Campbell S E, Sanders T G and Morrison W B 2001 Mr imaging of meniscal cysts: Incidence, location, and clinical significance AJR Am J Roentgenol 177 409-13
- [16] Petrosini A V and Sherman O H 1996 A historical perspective on meniscal repair Clin Sports Med 15 445-53
- [17] Barber F A 1994 Accelerated rehabilitation for meniscus repairs Arthroscopy: The Journal of Arthroscopic & Related Surgery 10 206-10
- [18] Izuta Y, Ochi M, Adachi N, Deie M, Yamasaki T and Shinomiya R 2005 Meniscal repair using bone marrow-derived mesenchymal stem cells: Experimental study using green fluorescent protein transgenic rats The Knee 12 217-23
- [19] Peretti G M 2004 Cell-based therapy for meniscal repair: A large animal study American Journal of Sports Medicine 32 146-58
- [20] Port J, Jackson D W, Lee T Q and Simon T M 1996 Meniscal repair supplemented with exogenous fibrin clot and autogenous cultured marrow cells in the goat model American Journal of Sports Medicine 24 547-55
- [21] Walsh C J, Goodman D, Caplan A I and Goldberg V M 1999 Meniscus regeneration in a rabbit partial meniscectomy model Tissue Engineering 5 327-37
- [22] Cook J L, Fox D B, Malaviya P, Tomlinson J L, Kuroki K, Cook C R and Kladakis S 2006 Long-term outcome for large meniscal defects treated with small intestinal submucosa in a dog model Am J Sports Med 34 32-42
- [23] Stapleton T W, Ingram J, Fisher J and Ingham E 2011 Investigation of the regenerative capacity of an acellular porcine medial meniscus for tissue engineering applications Tissue Engineering Part A 17 231-42
- [24] Bruns J, Kahrs J, Kampen J, Behrens P and Plitz W 1998 Autologous perichondral tissue for meniscal replacement The Journal of Bone & Joint Surgery Br 80 918-23
- [25] Bodin A, Concaro S, Brittberg M and Gatenholm P 2007 Bacterial cellulose as a potential meniscus implant Journal of Tissue Engineering and Regenerative Medicine 1 406-8

- [26] van Tienen T G, Hannink G and Buma P 2009 Meniscus replacement using synthetic materials *Clinics in Sports Medicine* 28 143-56
- [27] Lozano J, Ma Cb Fau - Cannon W D and Cannon W D 2007 All-inside meniscus repair: A systematic review *Clin Orthop Relat Res* 134-41
- [28] Chang A, Moisio K, Chmiel J S, Eckstein F, Guermazi A, Almagor O, Cahue S, Wirth W, Prasad P and Sharma L 2011 Subregional effects of meniscal tears on cartilage loss over 2 years in knee osteoarthritis *Annals of the Rheumatic Diseases* 70 74-49
- [29] Englund M, Guermazi A, Roemer F W, Yang M, Zhang Y, Nevitt M C, Lynch J A, Lewis C E, Torner J and Felson D T 2010 Meniscal pathology on mri increases the risk for both incident and enlarging subchondral bone marrow lesions of the knee: The most study *Annals of the Rheumatic Diseases* 69 1796-802
- [30] Roos H, Lauren M, Adalberth T, Roos E M, Jonsson K and Lohmander L S 1998 Knee osteoarthritis after meniscectomy: Prevalence of radiographic changes after twenty-one years, compared with matched controls *Arthritis and Rheumatism* 41 687-93
- [31] Agrawal C M and Ray R B 2001 Biodegradable polymeric scaffolds for musculoskeletal tissue engineering *Journal of Biomedical Materials Research* 55 141-50
- [32] Liang R, Fisher M, Yang G, Hall C and Woo S L Y 2011 Alpha1,3-galactosyltransferase knockout does not alter the properties of porcine extracellular matrix bioscaffolds *Acta Biomaterialia* 7 1719-27
- [33] Annabi N, Nichol J W, Zhong X, Ji C, Koshy S, Khademhosseini A and Dehghani F 2010 Controlling the porosity and microarchitecture of hydrogels for tissue engineering *Tissue Engineering Part B, Reviews* 16 371-83
- [34] Chatterjee K, Kraigsley A M, Bolikal D, Kohn J and Jr. C G S 2012 Gas-foamed scaffold gradients for combinatorial screening in 3d *J Funct Biomater* 3 173-82
- [35] Hong J K and Madihally S V 2011 Next generation of electrosprayed fibers for tissue regeneration *Tissue Engineering Part B, Reviews* 17 125-42
- [36] Kumar G, Tison C K, Chatterjee K, Pine P S, McDaniel J H, Salit M L, Young M F and Simon C G 2011 The determination of stem cell fate by 3d scaffold structures through the control of cell shape *Biomaterials* 32 9188-96

- [37] Thompson C J, Chase G G, Yarin A L and Reneker D H 2007 Effects of parameters on nanofiber diameter determined from electrospinning model *Polymer* 48 6913-22
- [38] Ionescu L C and Mauck R L 2013 Porosity and cell pre seeding influence electrospun scaffold maturation and meniscus integration in vitro *Tissue engineering Part A* 19 538-47
- [39] Kumbar S G, James R, Nukavarapu S P and Laurencin C T 2008 Electrospun nanofiber scaffolds: Engineering soft tissues *Biomed Mater* 3 034002
- [40] Platt M A 2005 Tendon repair and healing *Clin Podiatr Med Surg* 22 553-60

CHAPTER 2: MENISCUS TISSUE ENGINEERING USING A NOVEL COMBINATION OF ELECTROSPUN SCAFFOLDS AND HUMAN MENISCUS CELLS EMBEDDED WITHIN AN EXTRACELLULAR MATRIX HYDROGEL.

“We are what we repeatedly do. Excellence, then, is not an act, but a habit.”

—Aristotle

2.1 Introduction

Menisci are semilunar disc-shaped fibrocartilaginous tissues located on the tibial plateau. The major functions of this tissue include transmission of load and contribution to joint lubrication.[1] The menisci can be divided into outer and inner regions containing cells that are responsible for maintaining tissue homeostasis under the high shear and compressive forces experienced in the knee joint. The wedge shape of meniscus and its horn attachments serve to convert the vertical compressive tibiofemoral forces to horizontal hoop stresses. Simultaneously, shear forces are developed between the collagen fibers within the meniscus while the meniscus is deformed radially.[2] The outer region hosts blood vessels and is thus also termed the vascular region. Cells within the vascular region are mainly fibroblast-like and are elongated or spindle-shaped. The inner or avascular region is devoid of blood vessels and contains mainly chondrocyte-like cells that are rounded or spherical.[3]

Compromised meniscus function due to degeneration or injury is the most common risk factor for the development of knee osteoarthritis. The most common orthopaedic procedure is partial meniscectomy, which also alters normal meniscus function.[4] Approximately 1.5 million arthroscopic surgical procedures of the knee are performed each year in the United States alone and of these more than half involve the meniscus.[5] Clinical interventions aim to preserve the meniscus structure and function. A number of techniques are being used to repair meniscal tears: polymer-based arrows, darts, screws, staples, and other suture devices.[6] However, because of the low probability of successfully repairing a torn meniscus, partial or total meniscus replacement is being actively developed.[7, 8]

To satisfy this need, a number of tissue engineering strategies have attempted to enhance the repair and replacement of damaged meniscus. Meniscus allograft transplantation has been explored as a solution to replace lost meniscal tissue to prevent cartilage degeneration, relieve pain, as well as to improve function.[9] Another approach is the direct replacement of meniscal tissue, in part or in whole, using natural or synthetic biomaterial scaffolds, including collagen-based grafts, subintestinal submucosa, cell-free hydrogels, degradable porous foams, multilayered, multiporous silk scaffolds and macro- and microporous polymeric meshes.[10, 2] Many of the above studies employing in vivo animal models or in human clinical trials show some chondroprotection by the implants but with a low success rate. With the exception of allografts, this failure is likely because the implants do not mimic the complex internal architecture and native mechanical properties as well as possess the appropriate resident cells.[11-14]

An alternative means to emulate meniscus nano- and microstructure with mechanical properties, and with high cell compatibility, may be achieved using a process called electrospinning. Electrospun scaffolds comprised of natural or synthetic materials in dimensions that mimic native collagen fiber bundles[2] can be efficiently produced by electrospinning.[15, 16] The combination of mechanical strength and biocompatibility qualities of electrospun nanofibers provide an advantage over other 3-dimensional (3-D) scaffolds using other techniques such as gas-foamed, salt-leached, freeform fabrication, topography library, and hydrogels. The high surface-to-volume ratio and porosity generated by the electrospun fibers facilitates cell attachment, cell proliferation, and transport of nutrients through the scaffold.[17] A scaffold that provides the requisite mechanical properties of the meniscus may be useful for repair of meniscal tear defects and may permit early rehabilitation. Active joint motion during the early phase of repair also helps prevent restrictive adhesions and scar tissue formation that affect range of motion and limit recovery of function.[18]

In the past decade, biodegradable materials, such as polylactic acid (PLA) and poly(glycolic acid) (PGA), have been preferred especially in intra-articular procedures.[19] PLA has been more useful for biodegradable meniscal repair devices because the wet-strength half-life is 6 months.[20] The critical period for meniscal repair is 6 to 12 weeks[21] and PLA meniscal repair devices (e.g., Biostinger, meniscal screw, and meniscus arrow) preserve their initial strength even after six months.[22-24] Polylactides of varying molecular weights have been shown to be biocompatible,[25] Pure PLA has excellent mechanical properties including a tensile strength of 50 MPa and a modulus of 3.4 GPa.[26] The biocompatibility, suitable degradation time, and strength

of PLA materials allow it to better mimic the structure, biological, and mechanical function of native extracellular matrix (ECM) proteins, which provide support and regulate tissue formation and regeneration.

In this study we aimed to: i) produce electrospun PLA scaffolds with random or aligned fiber arrangements similar to the collagen fiber arrangements in native meniscus,[27] which were examined for their mechanical properties and were observed under scanning electron microscopy (SEM); ii) examine the response of cultured human meniscus cells isolated from the vascular and avascular regions on these electrospun scaffolds in terms of cell viability, morphology and gene expression profiles; and iii) produce multilayered PLA constructs in an effort toward generating engineered meniscus-like graft tissue. These constructs were made by encapsulating human avascular meniscus cells in an extracellular matrix hydrogel sandwiched between layers of electrospun PLA. After culture, these engineered tissues were characterized by histology and immunohistochemistry to examine whether this approach would produce a meniscus-like tissue.

2.2 Materials and Methods

2.2.1 Fabrication of poly lactic acid (PLA) scaffolds

PLA ($M_w = 100,000$, NatureWorks LLC, Minnetonka, MN) was dissolved in a mixed solvent of dichloromethane and N,N-dimethylacetamide (8/2 w/w) by stirring for 48 h at room temperature to obtain homogeneous 10 wt% solution. The PLA solution was loaded in a syringe, which was driven by a syringe pump (KDS200, KD Scientific Inc., Holliston, MA) at a feeding rate of 2.0 mL/h. A Teflon tube was used to connect the syringe and a 21G needle (inner diameter of 0.5 mm), which was set up horizontally. A voltage regulated DC power supply (NNC-30kV-2mA portable type, NanoNC, South Korea) was used to apply a voltage varying from 15 to 20 kV to the PLA solution to generate the polymer jet. The electrospun fibers were deposited in the form of a web on collectors covered by aluminum foil. For collecting random fibers, the tip-to-collector distance (TCD) was set to 16 cm on a flat plate as a collector. For collecting aligned fibers, a rotating drum (~2400 rpm) was placed at 12 cm from the tangent of the drum to the needle tip. To account for different collector sizes and effect of gravity, the TCD distances were optimized for the formation of electrospun PLA fibers of consistent and of comparable diameter. An overview of the systems used to generate random and aligned electrospun scaffolds is shown in Figures 2.1A and B.

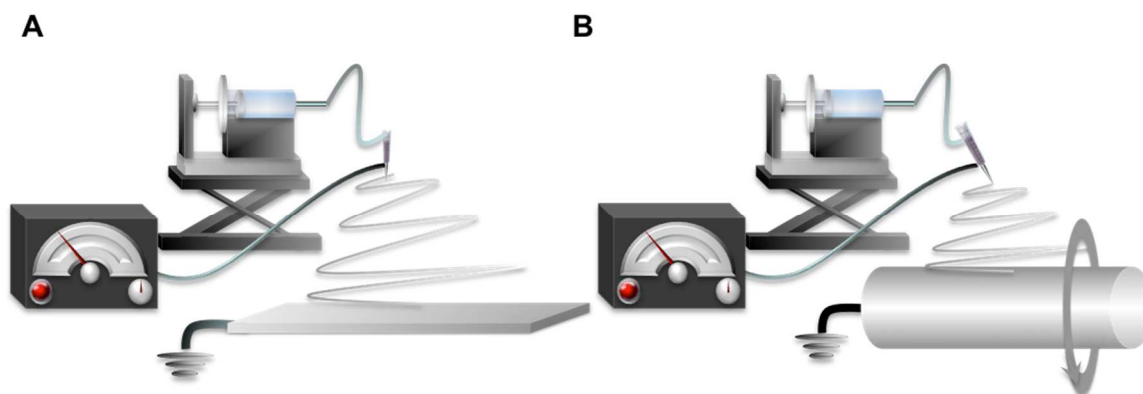


Figure 2.1 Overview of the electrospinning equipment (A) A grounded plate collector produced random PLA fibers and (B) a rotating drum collector was used to deposit aligned PLA fibers

2.2.2 Structural morphology of PLA scaffolds

The morphology of electrospun PLA scaffolds was studied under scanning electron microscopy (SEM) (Philips XL30, FEI Co., Andover, MA) with an accelerating voltage of 10 kV. Scaffolds were coated with iridium using a sputter coater (Emitech K575X, EM Technologies Ltd, England). The diameter of individual electrospun fibers was measured from the SEM images using image processing software (Image J, National Institutes of Health, Bethesda, MD).

2.2.3 Tissues and cell isolation

Normal human menisci (medial and lateral) were obtained from tissue banks (with Scripps Institutional Review Board approval), from six donors (mean age: 29.8 ± 4.7 ; age range: 23–35 years; two females, four males). Normal menisci were selected

following a previously reported macroscopic and histologic grading system.[28] The inner 2/3 (avascular region) and the outer 1/3 of the meniscus (vascular region) was separated with a scalpel and enzymatically digested using collagenase (2 mg/mL; C5138, Sigma-Aldrich, St. Louis, MO) in DMEM (Mediatech Inc, Manassas, VA) and 1% Penicillin-Streptomycin-Fungizone (Life Technologies, Carlsbad, CA) for 5–6 hours. The digested tissues were filtered through 100 μm cell strainers (BD Biosciences, San Jose, CA) and seeded in monolayer culture medium (MCM) consisting of DMEM (Mediatech) supplemented with 10% calf serum (Omega Scientific Inc. Tarzana, CA) and 1% Penicillin/Streptomycin/Gentamycin (Life Technologies). Cells were cultured for 1 passage before use in scaffold seeding experiments.

2.2.4 Cell cultures on single layered ES PLA scaffolds

Human cells from avascular or vascular regions of the meniscus were separately seeded onto 2 cm (length) x 1 cm (width) rectangular shape of random and aligned PLA scaffolds at a density of 0.5×10^6 per scaffold (0.25×10^6 per cm^2) in 6-well plates. Cells were cultured in DMEM supplemented with 10% calf serum and 1% Penicillin, Streptomycin, and Gentamycin for 3 days to permit cell attachment and scaffold colonization. Subsequently, the medium was changed to serum free ITS+ medium (Sigma-Aldrich) supplemented with 10 ng/mL TGF β 1 (PeproTech, Rocky Hill, NJ). The serum-free ITS+ medium used in ES scaffolds culture consisted of DMEM (Cellgro, Manassas, VA), 1 x ITS + (Sigma-Aldrich) (i.e. 10 mg ml⁻¹ insulin 5.5 mg ml⁻¹ transferrin, 5 ng ml⁻¹ selenium, 0.5 mg ml⁻¹ bovine serum albumin, 4.7 mg ml⁻¹ linoleic acid), 1.25 mg ml⁻¹ human serum albumin (Bayer, Leverkusen, Germany), 100 nM

dexamethasone (Sigma-Aldrich), 0.1 mM ascorbic acid 2-phosphate (Sigma-Aldrich), and penicillin/streptomycin/gentamycin (Gibco, Carlsbad, CA).[29] After 2 weeks in culture with medium changes every 3 to 4 days, the cells on the scaffolds were assessed for cell viability by confocal microscopy and for cell morphology by histology and SEM.

2.2.5 Mechanical properties of PLA scaffolds

The mechanical properties of PLA scaffolds were quantified via tensile testing ($n = 10$ per group). Both random and aligned scaffolds were tested under three different conditions: i) freshly electrospun dry scaffolds were tested within 1 day of production; ii) scaffolds were seeded with avascular human meniscus cells and cultured for one and three weeks; and iii) scaffolds were cultured for one and three weeks without cells. For mechanical testing, the electrospun scaffolds were cut into dog-bone-shaped scaffolds using a custom-made aluminum template to guide reproducible testing shapes. The template was 50 mm in length, with a 5 mm width on each end and a central width of 2 mm (Fig. 2.2). The thickness of each scaffold was measured using a digital caliper and reported as mean \pm standard deviation (SD). For mechanical testing of cultured cell-seeded and acellular scaffolds, human avascular cells (0.5×10^6 cells/each scaffold) were seeded on aligned PLA scaffolds. All cultures were in DMEM supplemented with 10% calf serum and 1% Penicillin, Streptomycin, and Gentamycin for 3 days to permit cell attachment and scaffold colonization. Subsequently, the medium was changed to serum-free ITS+ medium (Sigma-Aldrich) supplemented with 10 ng/mL TGF β 1 (PeproTech). After 1 week and 3 weeks in culture with medium changes every 3 to 4 days, the cell-

seeded and non-seeded scaffolds were cut into the same dog-bone shaped specimens as the dry specimens and were evaluated for mechanical properties.

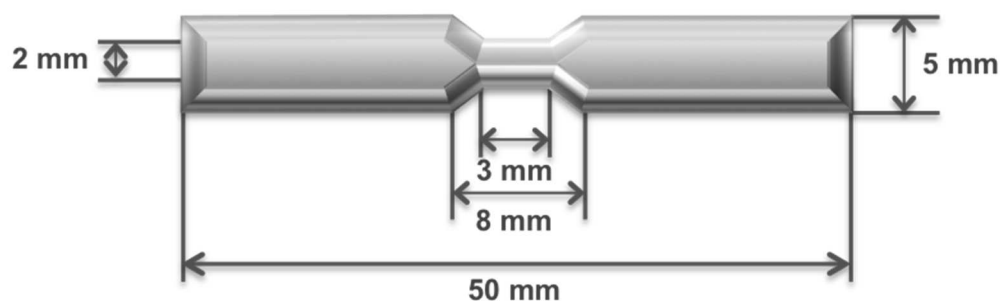


Figure 2.2 Geometry and size (mm) of the dog-bone shaped tensile test specimens

The specimens were mounted in the grips at their two ends of a uniaxial testing machine (Instron® Universal Testing Machine, 3342 Single Column Model; Norwood, MA) with a 500 N load cell and tested to failure at a crosshead speed of 1 mm min⁻¹ at a gauge length of 20 cm under ambient conditions. Young's modulus was calculated from the slope of the linear segment of the stress-strain curve. Ultimate tensile strength (UTS) was calculated at the maximum load before failure. Values were presented as mean \pm SD.

2.2.6 Multilayer construct formation

Human avascular meniscus cells (passage 1) were suspended in a hydrogel consisting of collagen type II (3 mg/mL), chondroitin sulfate (1 mg/mL) and hyaluronan (1 mg/mL) at 1×10^6 cells per mL. Cells suspended in hydrogel were seeded onto one aligned PLA scaffold (50 μ L), followed by layering another scaffold sheet on top. Another cell layer was applied, followed by a final, third scaffold on the top (Fig.2.3). To

stabilize the scaffold layers, a layer of 2% alginate (PRONOVA UP LVG; Novamatrix, Sandvika, Norway) was dispensed over the construct and crosslinked in calcium chloride (120 mM; Sigma-Aldrich) for 20 minutes. Layered constructs were cultured in serum-free medium supplemented with TGF β 1 (10 ng/mL).

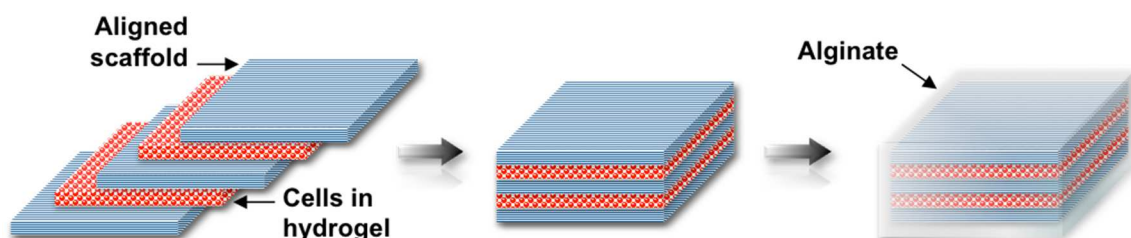


Figure 2.3 Process of production of multiple layers. Human meniscus cells encapsulated in a hydrogel consisting of collagen type II, chondroitin sulfate and hyaluronan were seeded onto a base aligned PLA scaffold, followed by placement of another scaffold above in the same fiber orientation. This was followed by another layer of cells and one more scaffold layer. To hold the layers together, a layer of 2% alginate was deposited over the entire stack and crosslinked.

2.2.7 Cell viability assessments

The viability of cells cultured on PLA scaffolds was observed using the live/dead kit consisting of Calcein-AM and Ethidium Homodimer-1 (Life Technologies) and a laser confocal microscope (LSM-510, Zeiss, Jena, Germany) as previously described.[30]

2.2.8 Cellular morphology of avascular meniscus cells on single layer PLA scaffolds

SEM was employed to observe high-resolution features of cells grown on the electrospun PLA scaffolds. After a culture time of 7 and 14 days, the cells on the substrates were washed with PBS and fixed with 2.5% weight/volume glutaraldehyde

(Sigma-Aldrich) in PBS for 1 h. After fixation the samples were washed 3 times with PBS for 10 minutes each. The samples were then dehydrated in a graded series of ethanol (50%, 70%, and 90%) for 30 minutes each and left in 100% ethanol for 24 h at temperatures below 4° C. Next, the samples were kept in 100% ethanol until they were completely dried in a critical point dryer (Autosamdri-815, Series A, Tousimis Inc., Rockville, MD). The dried samples were then surface metalized by sputter coating with iridium for SEM examination. The morphology of the scaffolds and the adherent cells was observed by SEM (Philips XL30, FEI Co., Andover, MA).

2.2.9 Histology and immunohistochemistry

PLA scaffold layers seeded with avascular meniscus cells were fixed in Z-Fix (ANATECH, Battle Creek, MI) and embedded in paraffin. Sections of 5–7 µm were stained with H&E and Safranin O Fast Green. For detection of collagen type I by immunohistochemistry, cut sections were treated with hyaluronidase for 2 h,[31] and incubated with a primary antibody against collagen type I (clone: I-8H5; MP Biomedicals, Santa Ana, CA) at 10 µg/mL. For detection of collagen type II, (II-II6B3, Hybridoma Bank, University of Iowa) used at 10 µg/mL. Secondary antibody staining and detection procedures were followed as previously described.[32] An isotype control was used to monitor nonspecific staining.

2.2.10 RNA isolation and RT-PCR

Total RNA was isolated from single layer PLA constructs using the RNeasy mini kit (Qiagen, Hilden, Germany) and first strand cDNA was made according to the

manufacturer's protocol (Applied Biosystems, Foster City, CA). Quantitative RT-PCR was performed using TaqMan® gene expression reagents. COL1A1, aggrecan, SOX9, COMP and GAPDH were detected using Assays-on-Demand™ primer/probe sets (Applied Biosystems). To normalize gene expression levels, GAPDH was employed using the Δ Ct method.[33]

2.2.11 Statistical analysis

ANOVA and post-hoc student's t-test was used to assess the statistical significance of differences in fiber diameter, mechanical properties, and gene expression levels. P-values less than 0.05 were considered significant.

2.3 Results

2.3.1 Controlled production of electrospun random and aligned PLA fibrous scaffolds

The morphological structures of aligned and random electrospun PLA fibers are shown in Figure 2.4. The rotating drum speed (~2400 rpm) and delivery parameters used produced scaffold structures with a high degree of alignment (Fig. 2.4B). The average diameter of aligned fibers was $1.25 \pm 0.31 \mu\text{m}$ (range: 0.46–2.32 μm) and that for random PLA fibers was $1.31 \pm 0.56 \mu\text{m}$ (range, 0.70–3.84 μm). There was no statistically significant difference between the fiber diameters. Random scaffolds had a thickness of $0.15 \pm 0.04 \text{ mm}$; the thickness of aligned scaffolds was $0.09 \pm 0.03 \text{ mm}$.

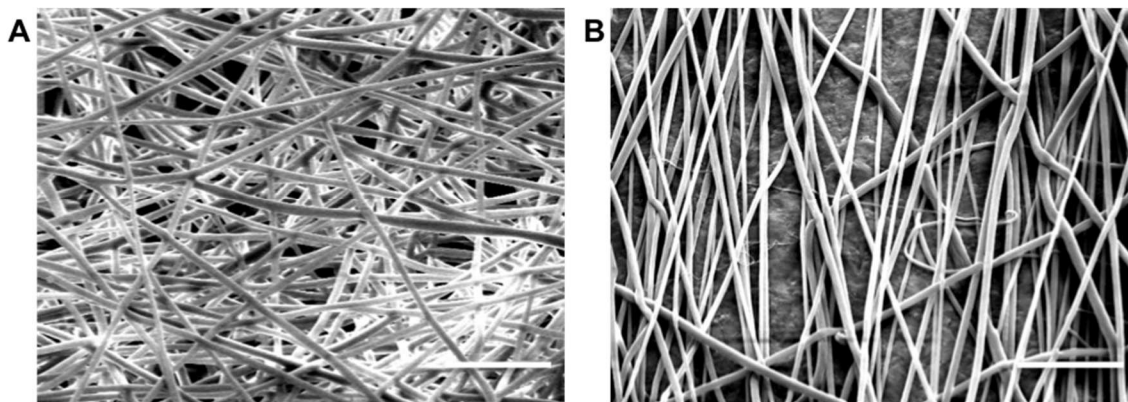


Figure 2.4 Scanning electron micrographs (SEM) of electrospun (ES) PLA scaffolds (A) SEM of random and (B) aligned ES PLA fibers (Mag. 1250x, scale bar: 20 μm).

2.3.2 Controlled production of electrospun random and aligned PLA fibrous scaffolds

Cells seeded upon randomly spun PLA scaffolds were flattened and spread-out with multi-directional extensions (Fig. 2.5A), while cells on aligned PLA scaffolds were

elongated in line with the direction of the fibers (Fig. 2.5B). These differences in morphology and alignment were also reflected in the confocal images (Figs. 2.5C-D), which provided evidence of high cell viability for both scaffolds. No obvious differences in cell morphology were seen between the vascular or avascular cells.

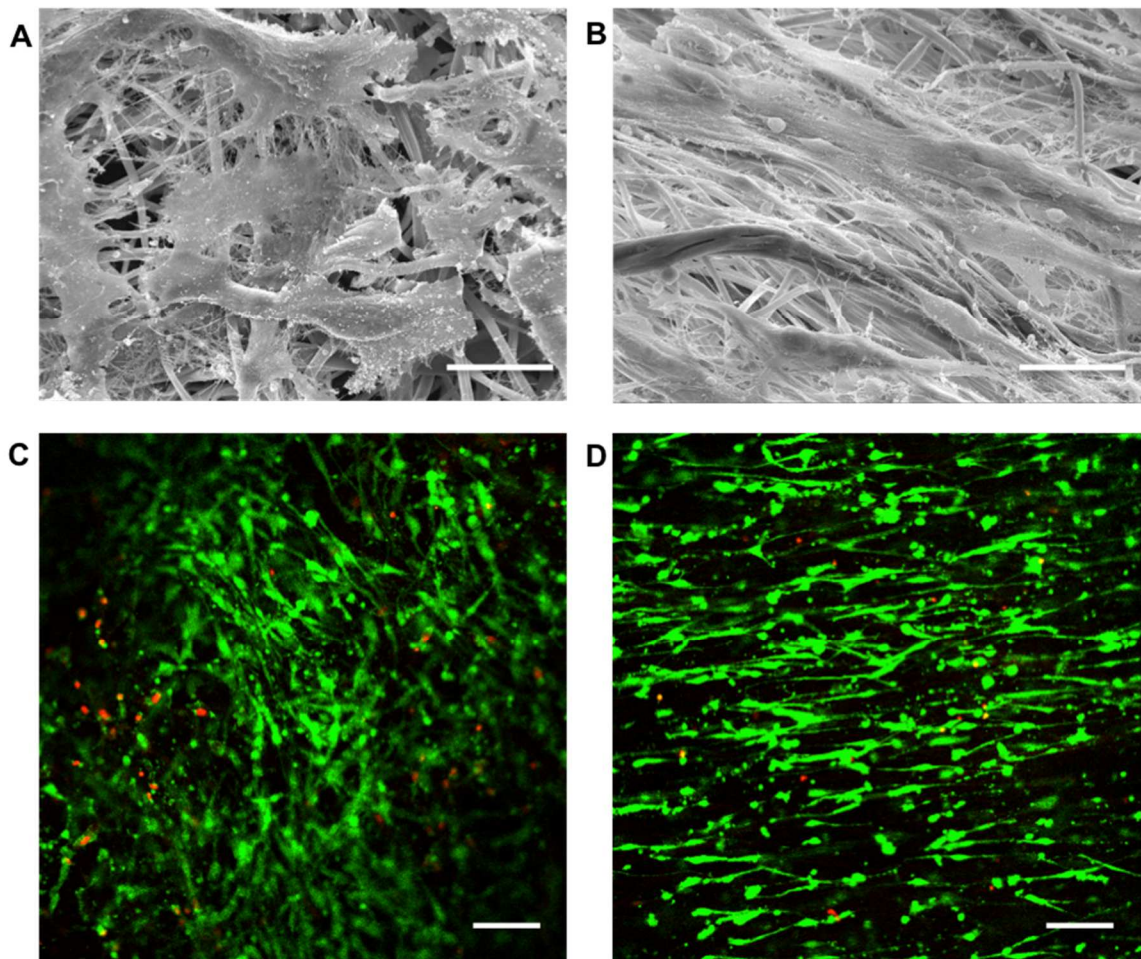


Figure 2.5 Scanning electron micrographs (SEM) of cellular response on electrospun (ES) PLA scaffolds. (A) SEM of avascular human meniscus cells cultivated on random and (B) vascular human meniscus cells seeded on aligned ES PLA fibers (Mag. 1250x), scale bar: 20 μm in SEM images. (C) Confocal microscopy of vascular human meniscus cells cultivated on random scaffolds and (D) avascular human meniscus cells cultivated on aligned scaffolds demonstrating viability (live/dead) and alignment cells cultivated on PLA scaffolds (Mag. 10x; scale bar: 200 μm in confocal images)

2.3.3 Meniscus cell phenotype is not altered by fiber orientation or from region of isolation

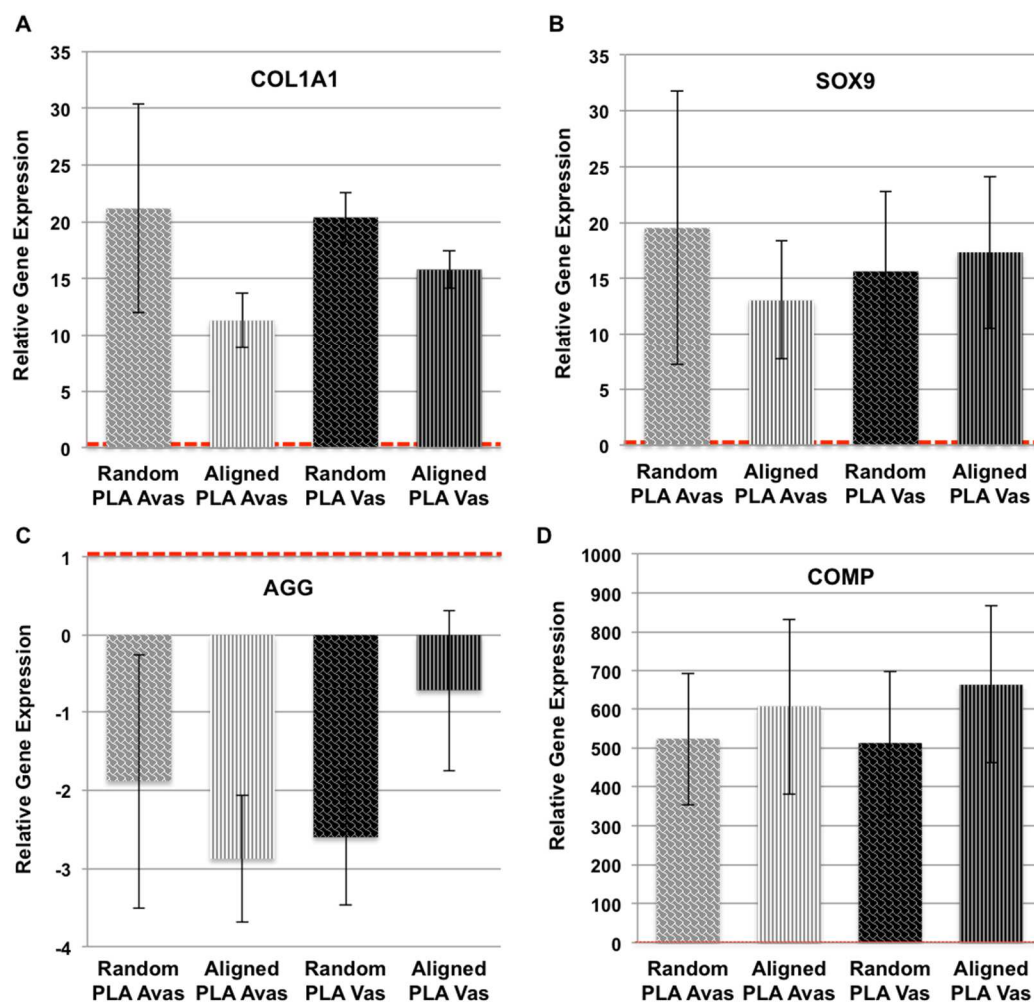


Figure 2.6 Relative fold change in gene expression of human vascular and avascular meniscus cells cultivated on either random or aligned PLA electrospun scaffolds. (A) Increased COL1A1 gene expression. (B) Increased SOX9 gene expression. (C) Reduced Aggrecan expression relative to monolayer controls. (D) COMP expression on random and aligned PLA electrospun scaffolds (n = 4–5 donors). Expression levels are relative to monolayer controls (dotted line).

In comparison to meniscal cells maintained in MCM (baseline control gene expression levels indicated by dotted line in Fig. 2.6), cells derived from either vascular and avascular regions cultivated on both random and aligned ES PLA scaffolds in serum-free ITS medium the presence of TGF β 1 (10 ng/ml) displayed significantly ($p < 0.05$) increased COL1A1, SOX9 (Figs. 2.6A and 2.6B), and COMP (Fig. 2.6D) gene expression levels relative to monolayer cultured cells. Although decreased aggrecan mRNA was seen (approximately 2-fold) in cells on both scaffolds (Fig. 2.6C), this expression was not significantly different from the monolayer cultured cells.

2.3.4 High tensile mechanical properties of aligned electrospun PLA scaffolds

Young's modulus and UTS in the random and aligned scaffolds are presented in Figure 4. Random scaffolds possess an average tensile modulus of 67.31 ± 2.04 MPa. Aligned scaffolds, tested in the direction parallel to the aligned nanofibers generated a significantly greater ($p < 0.001$) tensile modulus of 322.42 ± 34.40 MPa, compared to random scaffolds. However, the tensile modulus perpendicular to the aligned direction was 7.18 ± 1.27 MPa, significantly weaker than random scaffolds ($p < 0.001$). Similarly, UTS of aligned scaffolds was significantly ($p < 0.001$) higher: 14.24 ± 1.45 MPa (parallel to direction of alignment) compared to 3.8 ± 0.21 MPa measured in the random ES scaffolds.

Random and aligned scaffolds tested in the direction of fiber orientation generated a sharper increase in stress with a "toe region" in the pre-yield region. While random scaffolds extended nonlinearly after yield, aligned scaffolds generated crack straining

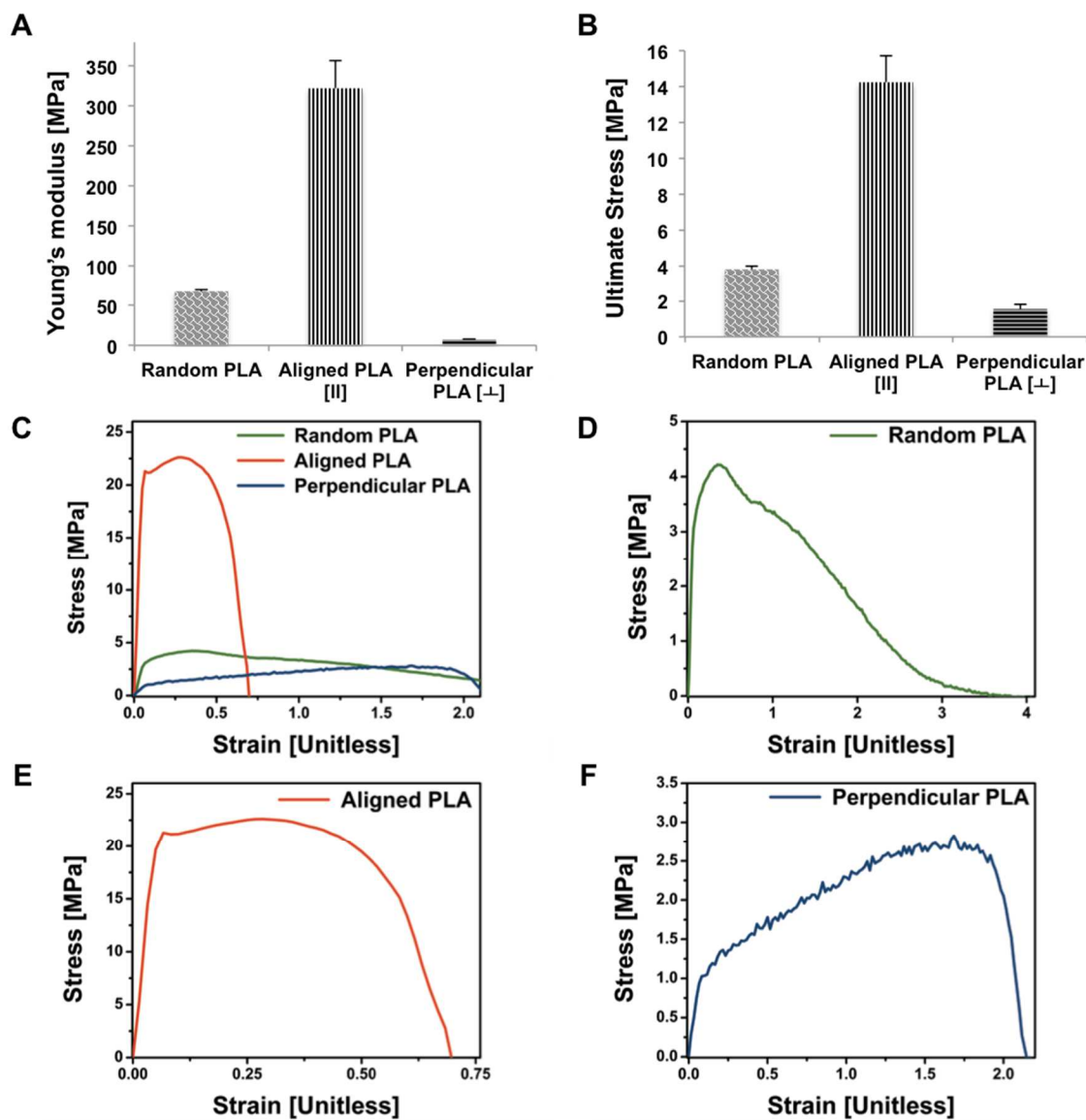


Figure 2.7 Mechanical testing of random and aligned ES PLA scaffolds. (A) Young's modulus (MPa) for random, aligned (along fiber orientation), and perpendicular to fiber orientation. (B) Ultimate stress readings (MPa) for each condition. (C) Stress/strain curve for each condition and (D) random PLA scaffold. (E) aligned PLA scaffold (F) perpendicular oriented PLA scaffold.

(Figs. 2.7C-E), yielded, and failed at comparatively adjacent points earlier in the strain region. Aligned scaffolds measured in the direction perpendicular to fiber orientation, exhibiting a much lower stress-strain response (Figs. 2.7C and 2.7F).

Mechanical properties of cell-seeded and paired acellular scaffolds were assessed over time in culture via tensile testing. The stiffness of all scaffolds showed some decrease with time in culture. However, cell-seeded scaffolds tended to possess higher stiffness and reached a higher ultimate tensile stress, although no significant difference was established in Figure 2.8.

2.3.5 Multi-layer PLA cell-seeded scaffold support meniscus-like neotissue formation

Since the random PLA scaffolds yielded a much lower average tensile modulus (67 MPa) than the aligned scaffolds (>300 MPa), we chose to make multilayers of scaffolds using only aligned fibers to mimic the circumferential collagen fibrous bundles in native meniscus. Human avascular meniscus cells were seeded onto three scaffolds within a biomimetic gel composed of collagen type II, chondroitin sulfate and hyaluronan (1 mg /mL each) and held in place with a layer of 2% alginate crosslinked with calcium chloride (Fig. 2.9D). Following 2 weeks of culture, a construct was developed that comprised of a fusion of the PLA scaffold layers, newly synthesized ECM and cells that had infiltrated and distributed inside and throughout the triple-layered construct (Figs. 2.9A–F). The neotissue was Safranin-O negative (Figs 2.9A and 2.9B), and possessed an ECM composed of collagen type I (Fig. 2.9C) and with cells elongated in the same direction/orientation as the ES PLA fibers. Immunostaining for collagen type II was negative for these neotissues (data not shown).

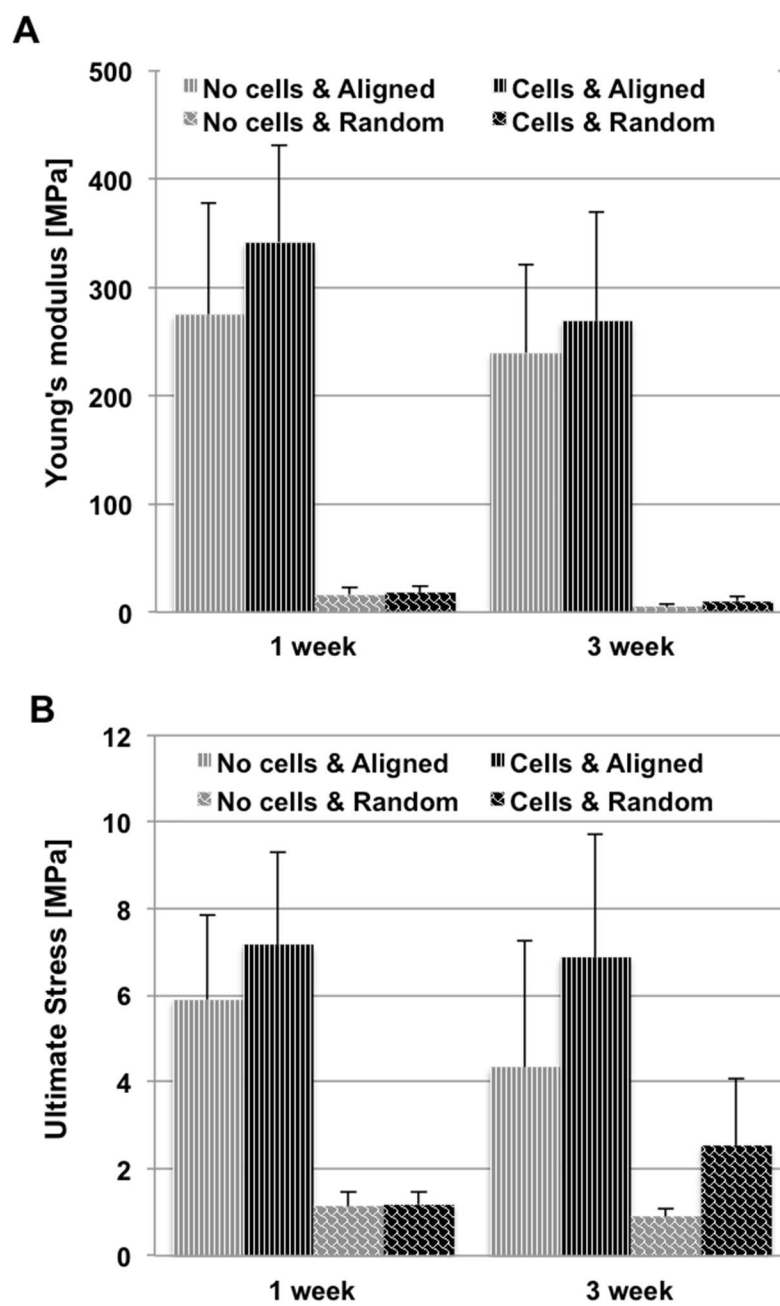


Figure 2.8 Mechanical testing of random and aligned ES PLA scaffolds over time in culture with or without cells (one week and three weeks) (A) Young's modulus (MPa) (B) Ultimate stress (MPa)

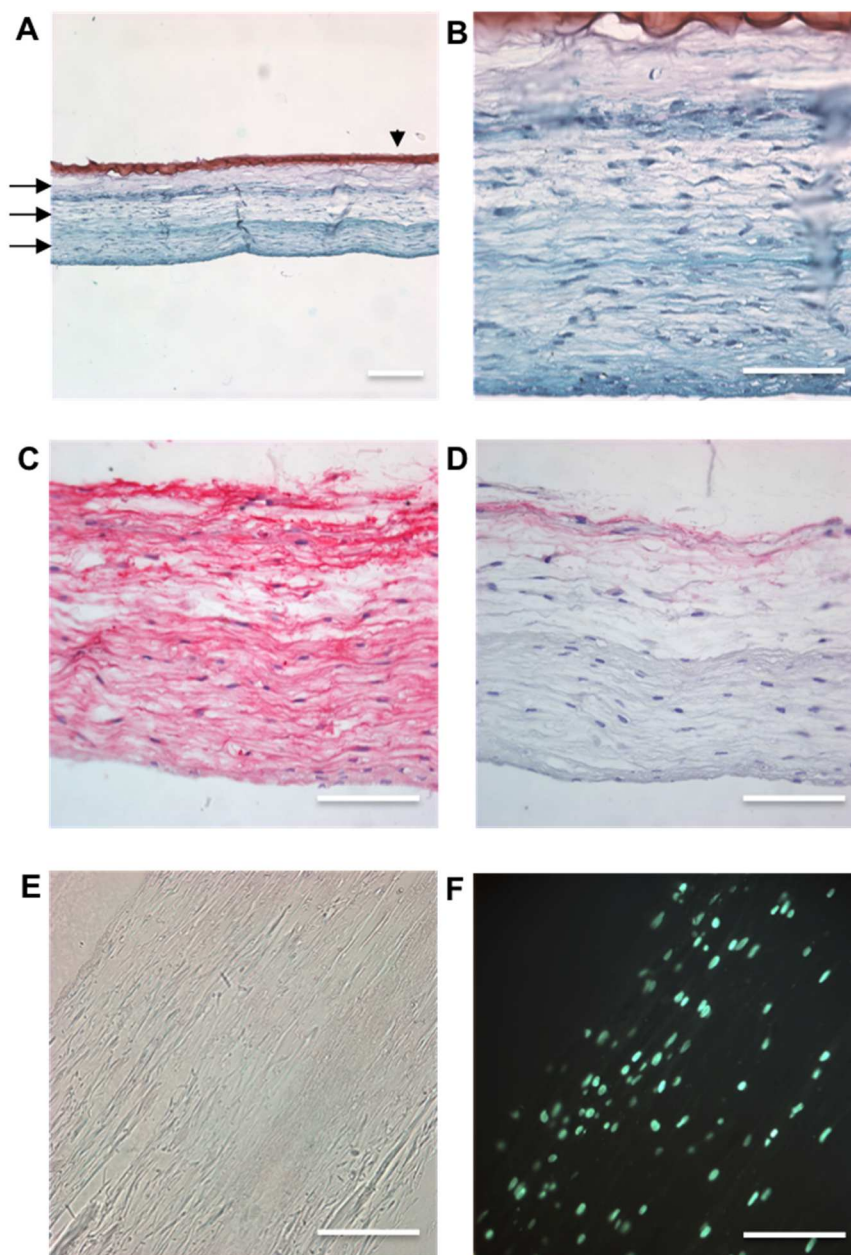


Figure 2.9 Histology and immunohistochemistry of multi-layer aligned PLA cell seeded scaffolds. (A–B) Safranin O/Fast-green stain. Arrows indicate three aligned PLA scaffold layers and the arrowhead points to the layer of alginate. (C) Collagen type I immunostain. (D) Isotype control stain. (E) Light microscope image of two weeks cultured construct. (F) DAPI stain. (Mag. A = 10x, scale bar: 200 μm ; Mag. B, C, D, E, and F = 40x, scale bar: 100 μm).

2.4 Discussion

The ultrastructural arrangement of collagen fibers in the superficial and laminar layers of the meniscus comprises of random collagen fibers. However, the main central layer is made up of circumferentially aligned collagen bundles that are critical for the mechanical function of the meniscus.[27] We demonstrated the capacity to create both random and aligned electrospun scaffolds, which resemble the architecture of the native meniscus, by using electrospinning technology. We investigated the potential of combining human meniscus cells with nanofibrous scaffolds for meniscus tissue engineering. These electrospun PLA scaffolds possessed anisotropic mechanical properties, mimicked the native central layer of the meniscus tissue (the main bulk of meniscus tissue consisting of collagen fibrils[27]), and supported cell growth to permit production of the major ECM components seen in meniscus tissue. Our data also show that electrospinning can be employed in conjunction with a novel cell-seeded biomimetic hydrogel to produce higher order constructs that promote neotissue formation and scaffold integration. These results demonstrate proof of concept of using such scaffolds for meniscus tissue engineering.

Production of scaffolds via electrospinning has been carried out with numerous synthetic polymers including polyurethanes, PLA, poly- ϵ -caprolactone (PCL), and polydioxanone. The attachment and proliferation of cells, deposition of matrix, and the development of mechanical properties of the scaffolds over time is highly dependent on the type of material.[34] The initial high strength and relatively long degradation time of

PLA helps to mimic the structure and biological function of native ECM proteins, which may support the formation and maturation of the tissue.

However, the initial mechanical properties of scaffold are important for implant survival before eventual replacement and remodeling of regenerated tissue. We established that the tensile modulus of aligned scaffolds was approximately 5-fold higher than randomly oriented scaffolds and was comparable to the high end of the tensile modulus of human meniscus in the circumferential direction. The pronounced ‘toe’ region seen in the stress-strain curve of circumferential parts of meniscus was also seen in ES aligned PLA scaffolds in the present study (Figs. 4C and 4E).

The mechanical properties of our PLA scaffolds were significantly higher than those reported elsewhere for aligned nanofiber scaffolds.[35-37] For example, random PCL scaffolds had an isotropic tensile modulus of 2.1 ± 0.4 MPa, compared to highly anisotropic PCL scaffolds whose modulus was 11.6 ± 3.1 MPa in the presumed fiber direction.[35] To increase mechanical strength of electrospun PLA, Seth et al,[38] produced randomly electrospun nanocomposite scaffolds by encapsulating multi-walled carbon nanotubes (MWNT) in PLA. The combined PLA and MWNT increased the modulus of the randomly oriented electrospun scaffolds to 55 MPa.[38] However, this modulus is in the low end of the range of moduli reported for human menisci, and even lower than the tensile properties of the randomly oriented scaffolds reported in the present study.

Electrospun nanofibers (50–1000 nm) are similar in diameter to the native extracellular matrix.[39] This nano-sized fiber diameter has been shown to promote matrix-forming activities in seeded cells, for instance, chondrocytes seeded on PLLA

nanofibers produce more matrix than when seeded on PLLA microfibers.[40] We therefore focused on the generation of engineered meniscus constructs using nanofibrous biodegradable scaffolds produced via electrospinning in this range (nominally 500–1000 nm). Human meniscus cells infiltrated and distributed within aligned electrospun scaffolds with an elongated morphology resembling cells in native meniscal tissue. We also observed the production of ECM with high collagen type I content by human meniscus cells between the PLA fibers and throughout the multiple electrospun PLA layers within 14 days of culture. The low GAG staining is also consistent with normal human meniscus.[28]

Notably, fiber orientation affected the morphology of cells on these scaffolds. Meniscus cells seeded on random PLA scaffolds were flattened with multi-directional extensions, while they were more elongated and in line with the direction of the fibers on the aligned PLA scaffolds. In this current study, both random and aligned scaffolds induced meniscus-like gene expression profiles as previously reported.[41, 42] Despite differences in the observed cell morphology and in the observed via confocal and SEM images, we could not detect significant differences in gene expression due to fiber alignment, cell morphology, or due to region of origin (vascular or avascular). This result was likely because in both cases, the cell morphology remained fibroblast-like. Similar to our study with human meniscus cells, others have also reported that bovine meniscus fibrochondrocytes or bovine mesenchymal stem cells derived from bone marrow preferentially aligned in the predominant fiber direction, whereas cells on nonaligned scaffolds were randomly oriented.[15] In addition, Baker et al [15] noted a significant increase in mechanical properties after 70 days for aligned PCL scaffolds compared to

random constructs seeded with either cell type. In this current study, the mechanical properties of cell-seeded scaffolds were higher than non-cell seeded scaffolds at every time point. Importantly, this indicates that these improvements in mechanical property can be attributed to the neotissue deposited by the cells on each scaffold.

Hydrogels consist of entangled polymer chains that have an amorphous to semi-fibrous character, whereas ES scaffolds display distinct nano- to microscale topography that can be easily tuned.[43] Hydrogels reinforced with nanofibers are therefore an attractive approach to tissue engineering since nanofibers can enhance the poor mechanical properties of hydrogels. One study used a blend of PCL and gelatin but only reported a compressive strength of about 20 kPa.[44] Synthetically reinforced hydrogel-electrospun scaffold composite materials improved cell proliferation, and attachment and spreading of neuroblastoma and rat cortical neuron cells that was attributed to the topography of the electrospun fibers.[45, 44] We used a different approach to assemble nanofibrous scaffolds into complex architectures by stacking multiple layers of fibers sequentially deposited on top of one another (~1.5 mm total thickness) for proof-of-concept engineering of fiber-reinforced meniscal tissues. The motivation for developing multilayered constructs was to mimic regions of native tissue with respect to its biochemical, structural, and mechanical properties at a clinically relevant scale.[42, 46] Combining electrospinning with a biomimetic gel also provided cells with a growth environment to support neotissue development similar to the ECM found in native avascular meniscus tissue and aided in fusing multiple layers together. Although cells typically spread out on the surface of electrospun scaffolds, these cells also infiltrated inside each of the PLA scaffold layers.

Several issues remain to be addressed in the production of a functional construct for meniscus repair. While PLA is an FDA-approved biomaterial and is widely used clinically, resorbed PLA scaffolds can lead to synovitis and chondral lesions.[22, 23] Hence, a natural scaffold or more biocompatible material with nonreactive degradation products is more desirable. Since only one group was studied, we could not test specific hypotheses about the impact of the various components of the constructs. Assays of biochemical composition are also important to assess potential for clinical translation. We did not test the delamination strength of layered constructs due to technical challenges. While our primary intention in the present study was to demonstrate proof of concept with respect to biocompatibility, meniscal cell phenotype, and neotissue formation, in future studies we aim to test whether these constructs can be used to repair defects created in an *ex vivo* tissue model.

2.5 Conclusion

In summary, we electrospun PLA to generate biodegradable and biomimetic nanofibrous scaffolds. Aligned electrospun PLA fibers generated an anisotropic tensile modulus that better approximated the properties of meniscal tissue than random electrospun PLA fibers. Cells from avascular and vascular regions of human menisci survived, attached, and infiltrated the PLA nanofibrous scaffold, and secreted the major proteins found in meniscal matrix. Moreover, we were also able to demonstrate the novel approach of combining nanofibrous scaffolds with human meniscus cells in an ECM hydrogel to create thicker multilayered constructs in the dimensions necessary for partial meniscus replacement.

2.6 Acknowledgments

This chapter, in full, is a reprint of the material as it appears in *Journal of Orthopaedic Research*, Volume 33, 2015. Jihye Baek, Xian Chen, Sujata Sovani, Sungho Jin, Shawn P. Grogan, Darryl D. D’Lima. The dissertation author was the primary investigator and author of this paper.

2.7 References

- [1] Ghosh P and Taylor T 1987 The knee joint meniscus: A fibrocartilage of some distinction *Clin Orthop Relat Res* 224 52-63
- [2] Makris E A, Hadidi P and Athanasiou K A 2011 The knee meniscus: Structure-function, pathophysiology, current repair techniques, and prospects for regeneration *Biomaterials* 32 7411-31
- [3] McDevitt C A, Mukherjee S, Kambic H and Parker R 2002 Emerging concepts of the cell biology of the meniscus *Curr Opin Orthop* 13 345-50
- [4] Katz J N and Martin S D 2009 Meniscus--friend or foe: Epidemiologic observations and surgical implications *Arthritis and rheumatism* 60 633-5
- [5] Rodkey W G, Steadman J R and Li S-T 1999 A clinical study of collagen meniscus implants to restore the injured meniscus *Clin Orthop Relat Res* 367S S281-S92
- [6] Lozano J, Ma C and Cannon W 2007 All-inside meniscus repair: A systematic review *Clin Orthop Relat Res* 455 134-41
- [7] Englund M, Roos E M and Lohmander L S 2003 Impact of type of meniscal tear on radiographic and symptomatic knee osteoarthritis: A sixteen-year followup of meniscectomy with matched controls *Arthritis and rheumatism* 48 2178-87
- [8] Scotti C, Hirschmann M T, Antinolfi P, Martin I and Peretti G M 2013 Meniscus repair and regeneration: Review on current methods and research potential *Eur Cell Mater* 26 150-70
- [9] Lee A S, Kang R W, Kroin E, Verma N N and Cole B J 2012 Allograft meniscus transplantation *Sports Med Arthrosc* 20 106-14
- [10] Liu C, Toma I, Mastrogiacomo M, Krettek C, von Lewinski G and Jagodzinski M 2013 Meniscus reconstruction: Today's achievements and premises for the future *Arch Orthop Trauma Surg* 133 95-109
- [11] Cook J L, Fox D B, Malaviya P, Tomlinson J L, Kuroki K, Cook C R and Kladakis S 2006 Long-term outcome for large meniscal defects treated with small intestinal submucosa in a dog model *The American journal of sports medicine* 34 32-42
- [12] Heijkants R G, van Calck R V, De Groot J H, Pennings A J, Schouten A J, van Tienen T G, Ramrattan N, Buma P and Veth R P 2004 Design, synthesis and properties of a degradable polyurethane scaffold for meniscus regeneration *J Mater Sci Mater Med* 15 423-7
- [13] Kobayashi M, Chang Y S and Oka M 2005 A two year in vivo study of polyvinyl alcohol-hydrogel (pva-h) artificial meniscus *Biomaterials* 26 3243-8

- [14] Sweigart M A and Athanasiou K A 2001 Toward tissue engineering of the knee meniscus *Tissue Eng* 7 111-29
- [15] Baker B M and Mauck R L 2007 The effect of nanofiber alignment on the maturation of engineered meniscus constructs *Biomaterials* 28 1967-77
- [16] Ionescu L C and Mauck R L 2013 Porosity and cell preseeding influence electrospun scaffold maturation and meniscus integration in vitro *Tissue engineering Part A* 19 538-47
- [17] Kumbar S G, James R, Nukavarapu S P and Laurencin C T 2008 Electrospun nanofiber scaffolds: Engineering soft tissues *Biomed Mater* 3 034002
- [18] Platt M A 2005 Tendon repair and healing *Clin Podiatr Med Surg* 22 553-60
- [19] Gloria A, De Santis R and Ambrosio L 2010 Polymer-based composite scaffolds for tissue engineering. *J Appl Biomater Biomech* 8 57-67
- [20] Athanassiou K, Agrawal C, Barber F and Burkhart S 1998 Orthopaedic applications for pla-pga biodegradable polymers *Arthroscopy* 14 726-37
- [21] Barber F A 1999 Meniscus repair aftercare *Sports Med Arthrosc* 7 43-7
- [22] Arnoczky S P and Lavagnino M 2001 Tensile fixation of absorbable meniscal repair devices as a function of hydrolysis time *The American journal of sports medicine* 29 118-23
- [23] Asik M and Atalar A C 2002 Failed resorption of bioabsorbable meniscus repair devices *Knee surgery, sports traumatology, arthroscopy : official journal of the ESSKA* 10 300-4
- [24] Becker R, Schroder M, Starke C, Urbach D and Nebelung W 2001 Biomechanical investigations of different meniscal repair implants in comparison with horizontal sutures on human meniscus *Arthroscopy* 17 439-44
- [25] Athanasiou K A, Niederauer G G and Agrawal C M 1996 Sterilization, toxicity, biocompatibility and clinical applications of polylactic acid/polyglycolic acid copolymers *Biomaterials* 17 93-102
- [26] Oksman K, Skrifvars M and Selin J F 2003 Natural fibres as reinforcement in polylactic acid (pla) composites *Compos Sci Technol* 63 1317-24
- [27] Petersen W and Tillmann B 1998 Collagenous fibril texture of the human knee joint menisci *Anat Embryol* 197 317-24
- [28] Pauli C, Grogan S P, Patil S, Otsuki S, Hasegawa A, Koziol J, Lotz M K and D'Lima D D 2011 Macroscopic and histopathologic analysis of human knee menisci in aging and osteoarthritis *Osteoarthr Cartil* 19 1132-41

- [29] Barbero A, Grogan S, Schäfer D, Heberer M, Mainil-Varlet P and Martin I 2004 Age related changes in human articular chondrocyte yield, proliferation and post-expansion chondrogenic capacity *Osteoarthritis and cartilage / OARS, Osteoarthritis Research Society* 12 476-84
- [30] Grogan S P, Aklin B, Frenz M, Brunner T, Schaffner T and Mainil-Varlet P 2002 In vitro model for the study of necrosis and apoptosis in native cartilage *The Journal of pathology* 198 5-13
- [31] Roberts S, Menage J, Sandell L J, Evans E H and Richardson J B 2009 Immunohistochemical study of collagen types i and ii and procollagen iia in human cartilage repair tissue following autologous chondrocyte implantation *Knee* 16 398-404
- [32] Grogan S P, Miyaki S, Asahara H, D'Lima D D and Lotz M K 2009 Mesenchymal progenitor cell markers in human articular cartilage: Normal distribution and changes in osteoarthritis *Arthritis research & therapy* 11 R85
- [33] Martin I, Jakob M, Schäfer D, Dick W, Spagnoli G and Heberer M 2001 Quantitative analysis of gene expression in human articular cartilage from normal and osteoarthritic joints *Osteoarthritis and cartilage / OARS, Osteoarthritis Research Society* 9 112-8
- [34] Baker B M, Handorf A M, Ionescu L C, Li W J and Mauck R L 2009 New directions in nanofibrous scaffolds for soft tissue engineering and regeneration *Expert review of medical devices* 6 515-32
- [35] Li W J, Mauck R L, Cooper J A, Yuan X and Tuan R S 2007 Engineering controllable anisotropy in electrospun biodegradable nanofibrous scaffolds for musculoskeletal tissue engineering *Journal of biomechanics* 40 1686-93
- [36] Metter R B, Ifkovits J L, Hou K, Vincent L, Hsu B, Wang L, Mauck R L and Burdick J A 2010 Biodegradable fibrous scaffolds with diverse properties by electrospinning candidates from a combinatorial macromer library *Acta biomaterialia* 6 1219-26
- [37] Nerurkar N L, Elliott D M and Mauck R L 2007 Mechanics of oriented electrospun nanofibrous scaffolds for annulus fibrosus tissue engineering *Journal of orthopaedic research : official publication of the Orthopaedic Research Society* 25 1018-28
- [38] McCullen S D, Stevens D R, Roberts W A, Clarke L I, Bernacki S H, Gorga R E and Lobo E G 2007 Characterization of electrospun nanocomposite scaffolds and biocompatibility with adipose- derived human mesenchymal stem cells *Int J Nanomedicine* 2 253-63
- [39] Deitzel J M, Kleinmeyer J, Harris D and Tan N C B 2001 The effect of processing variables on the morphology of electrospun nanofibers and textiles *Polymer* 42 261-72

- [40] Li W-J, Jiang Y J and Tuan R S 2006 Chondrocyte phenotype in engineered fibrous matrix is regulated by fiber size *Tissue Eng* 12 1775-85
- [41] Grogan S P, Chung P H, Soman P, Chen P, Lotz M K, Chen S and D'Lima D D 2013 Digital micromirror device projection printing system for meniscus tissue engineering *Acta biomaterialia* 9 7218-26
- [42] Mandal B B, Park S H, Gil E S and Kaplan D L 2011 Multilayered silk scaffolds for meniscus tissue engineering *Biomaterials* 32 639-51
- [43] Lannutti J, Reneker D, Ma T, Tomasko D and Farson D 2007 Electrospinning for tissue engineering scaffolds *Mater Sci Eng C Mater Biol Appl* 27 504-9
- [44] Kai D, Prabhakaran M P, Stahl B, Eblenkamp M, Wintermantel E and Ramakrishna S 2012 Mechanical properties and in vitro behavior of nanofiber-hydrogel composites for tissue engineering applications *Nanotechnology* 23 095705
- [45] Han N, Johnson J K, Bradley P A, Parikh K S, Lannutti J J and Winter J O 2012 Cell attachment to hydrogel-electrospun fiber mat composite materials *J Funct Biomater* 3 497-513
- [46] Xu T, Binder K W, Albanna M Z, Dice D, Zhao W, Yoo J J and Atala A 2013 Hybrid printing of mechanically and biologically improved constructs for cartilage tissue engineering applications *Biofabrication* 5 015001

CHAPTER 3: REPAIR OF AVASCULAR MENISCUS TEARS WITH ELECTROSPUN COLLAGEN SCAFFOLDS SEEDED WITH HUMAN CELLS.

*“I can’t change the direction of the wind,
but I can adjust my sails to always reach my destination.”*

—Jimmy Dean

3.1 Introduction

Knee injuries, resulting in meniscal tears, are the most frequent injuries to the meniscus and are an important factor of knee disability [1-3], accounting for up to 15% of all injuries of the knee in younger active individuals [4]. Partial or total meniscectomy is currently the most common recommended treatment approach for meniscus tears[5]. A number of techniques have been developed to repair meniscal tears: involving sutures, screws, arrows, and darts[6]. These meniscal repair procedures can relieve pain, locking, and instability in the short-term. However, in the long term, no significant benefit has been documented with respect to preventing degenerative joint changes and accelerated osteoarthritis (OA) due to deficient meniscal function[7-9].

The predominant issue with meniscal tears is absence of self-healing capacity of the meniscus due to lack of vasculature[10, 3]. While fully vascularized at birth, adult menisci are usually only vascularized in the outer one-third to two-thirds [3]. The

vascularized periphery of the meniscus possesses some self-healing capacity, and minor or simple tears can be repaired[11]. However, large or complex tears, especially those within the avascular region are extremely difficult to repair.

Numerous approaches have attempted to enhance repair or replace injured meniscal tissue. Transplantation of meniscus allografts can relieve pain and enhance function in the short term[12-14]. Others have explored replacement of meniscal tissue using natural biomaterials, including periosteal tissue[15], small intestine submucosa (SIS)[16], acellular porcine meniscal tissue[17], perichondral tissue[18], and bacterial cellulose[19]. However, these approaches have not been translated to clinical application largely due to poor replication of the organization, structure, biological and mechanical properties of meniscal tissue.

Electrospinning makes it feasible to fabricate nano-scale fibers composed of synthetic materials such as polylactic acid (PLA), polycaprolactone (PCL)[20-23]; and natural materials such as collagen, gelatin, and chitosan[24-26]. Electrospun fiber matrices have been used successfully in drug delivery and wound healing as well as other biomedical applications[27]. These nanofibrous scaffolds possess the advantages of tunable mechanical strength with a large biomimetic surface area. Cell attachment, cell proliferation, and transport of nutrients through the scaffold can be accelerated by the high surface-to-volume ratio and porous structure of the scaffold [28, 29]. We previously demonstrated that electrospun PLA scaffolds can replicate meniscus nano- and microstructural organization with appropriate mechanical properties and high cell compatibility[30].

Although synthetic polymers are biocompatible, they can cause significant inflammation and foreign body reaction when implanted *in vivo*[31]. For example, biodegradation products (lactic acid) released from PLA reduce pH within the knee joint [32]. Natural polymers may circumvent these complications and a scaffold comprised of collagen may be optimal since it is the main fibrillar component of the meniscus, it is biocompatible, and is approved for clinical use[33, 34].

The objective of this study was to develop biomimetic scaffolds that replicate the collagen fibrils of native menisci, seeded with cells derived from human meniscogenic cells, and with biomechanical properties approaching that of native meniscal tissue. Towards this objective, we electrospun scaffolds comprised of collagen type I with different fiber arrangements (random and aligned) to emulate the regional distribution of meniscus fibers. These electrospun scaffolds were then cross-linked to enhance mechanical properties and seeded with human meniscal fibrochondrocytes. The scaffolds were characterized by fiber morphology and biomechanical properties. Meniscogenic potential was assessed by cell viability, proliferation, gene expression, and matrix synthesis. To determine potential for clinical translation, we also evaluated *ex-vivo* repair by implanting cell-seeded electrospun scaffolds in tears created in the avascular region of live meniscus explants.

3.2 Materials and Methods

3.2.1 Fabrication of electrospun collagen type I scaffolds

Sixteen percent w/v Bovine Collagen type I (Semed S, acid-soluble, DSM, NL) was dissolved in 20x Phosphate buffered Saline (PBS) and ethanol at a ratio of 1:1 v/v as described previously[37]. ES scaffolds were created in a similar way as previously described for electrospun PLA scaffolds[20]. The collagen solution was placed in a syringe, actuated by a syringe pump (KDS200, KD Scientific Inc., USA) at a feeding rate of 0.1-0.2 mL/h into a Teflon tube that was connected to a 21-G needle with an inner diameter of 0.5 mm. Collagen fibers were electrospun onto collectors covered by aluminum foil. For fabricating random fibers, a flat plate was used as a collector with a tip-to-collector distance of 16 cm. For fabricating aligned fibers, a drum, rotating at 2400 rpm was placed at 12 cm from the needle tip (to the tangent surface of the drum). The applied voltage was varied from 15 to 20 kV by a voltage regulated DC power supply (NNC-30kV-2mA portable type, NanoNC, South Korea) to generate the polymer jet. Electrospun collagen scaffolds were crosslinked by submerging in 0.25% glutaraldehyde (Sigma-Aldrich) in 1x PBS for 1 hour. After fixation, scaffolds were washed three times for 10 min each with absolute ethanol and store at 4 °C.

3.2.2 Structural morphology of collagen type I scaffold

To examine the ultrastructural morphology of electrospun collagen type I scaffolds, scanning electron microscopy (SEM) was performed. The ES collagen scaffolds were coated with iridium using a sputter coater (Emitech K575X, EM

Technologies Ltd, England). The prepared scaffolds were examined under SEM (Philips XL30, FEI Co., Andover, MA) with an accelerating voltage of 10 kV. The diameter of the electrospun fibers for each scaffold was calculated from the SEM images via an image processing software (Image J, National Institutes of Health, USA).

3.2.3 Tissues harvesting and cell isolation

Normal human menisci (medial and lateral) were obtained from tissue banks (approved by Scripps Health review board), from six donors (mean age: 29.8 ± 4.7 ; age range: 23–35 years; two females and four males). To grade and select the menisci a macroscopic and histologic grading system was used [38]. The avascular region was defined as the 1/3 outer portion and the remaining 2/3 was considered the vascular region. These regions were separated by scalpel and enzymatically digested using collagenase (2mg/mL; C5138, Sigma-Aldrich, St. Louis, MO) in DMEM (Mediatech Inc, Manassas, VA) and 1% Penicillin-Streptomycin-Fungizone (Life Technologies, Carlsbad, CA) for 5-6 hours. Digested tissues were filtered through 100 μm cell strainers (BD Biosciences, San Jose, CA) and seeded in monolayer culture in DMEM (Mediatech) supplemented with 10% calf serum (Omega Scientific Inc. Tarzana, CA) and 1% Penicillin/Streptomycin/Gentamycin (Life Technologies). The isolated meniscus cells were cultured for one passage before seeding onto electrospun scaffolds.

3.2.4 Cell seeding in electrospun collagen type I scaffolds

Isolated human meniscus cells (passage 1) derived from the vascular and avascular regions were seeded onto 2 cm x 1 cm rectangular random and aligned collagen

scaffolds at a cell density of 0.5×10^6 per scaffold. Cell-seeded scaffolds were cultured in 6-well plates and maintained in 2 mL of monolayer culture medium for 3 days to permit initial cell attachment and scaffold colonization. The medium was then changed to serum-free ITS+ medium (Sigma) supplemented with 10 ng/mL TGF β 1 (Peprotech, Rocky Hill, NJ). The serum-free ITS+ medium used for electrospun scaffolds culture consisted of DMEM (Mediatech), 1 x ITS+ medium(Sigma-Aldrich) (i.e. 10 mg ml⁻¹ insulin 5.5 mg ml⁻¹ transferrin, 5 ng ml⁻¹ selenium, 0.5 mg ml⁻¹ bovine serum albumin, 4.7 mg ml⁻¹ linoleic acid), 1.25 mg ml⁻¹ human serum albumin (Bayer, Leverkusen, Germany), 100 nM dexamethasone (Sigma-Aldrich), 0.1 mM ascorbic acid 2-phosphate (Sigma-Aldrich), and penicillin/streptomycin/gentamycin (Gibco, Carlsbad, CA)[39]. The scaffolds and cells were cultured for 2 weeks in the ITS+ medium with medium changes every 3 to 4 days. At 2 weeks, scaffolds were assessed for cell viability and for cell distribution and morphology by histology and SEM.

3.2.5 Mechanical properties of collagen type I scaffold

The electrospun collagen scaffold mechanical properties were quantified via tensile testing (n=6 per group) as previously described [20]. The scaffolds were tested under three different conditions: i) random and aligned electrospun dry scaffolds; ii) aligned scaffolds seeded with avascular human meniscus cells and cultured for 1 and 3 weeks; and iii) aligned scaffolds without cells and cultured for 1 and 3 weeks. Scaffolds were cut into dog-bone shaped specimens with a gauge length of 8 mm and gauge width of 2 mm using a custom-made aluminum template. The thickness of each scaffold was measured using a digital caliper. For mechanical testing of cultured cell-seeded scaffolds,

human avascular cells (0.5×10^6 cells/each sample) were seeded on the dog-bone shaped aligned collagen scaffold. Scaffolds were cultured as described in the previous section.

The specimens were mounted in the grips of a uniaxial testing machine (Instron® Universal Testing Machine, 3342 Single Column Model; Norwood, MA) with a 500 N load cell and tested to failure at a displacement rate of 1 mmsec^{-1} . Samples that failed outside the gauge length were discarded. Young's modulus was calculated as the slope of the linear segment of the stress-strain curve. The maximum load before failure was recorded as the ultimate tensile strength (UTS).

3.2.6 Cell viability assessments

The viability of cells cultured on aligned collagen scaffolds was observed using Calcein-AM and Ethidium Homodimer-1 (Live/Dead kit, Life Technologies) and a laser confocal microscope (LSM-510, Zeiss, Jena, Germany) as previously reported[40].

3.2.7 Cellular morphology of meniscus cells on collagen type I scaffolds by SEM

SEM was employed in order to observe high-resolution features of cells grown on the electrospun collagen scaffolds. After 2 weeks in culture cell-seeded scaffolds were washed with 1x PBS and fixed with 2.5% w/v glutaraldehyde (Sigma-Aldrich) in 1x PBS for 1 h. After fixation specimens were washed three times with PBS for 10 min each wash. Then the specimens were dehydrated in a graded series of ethanol (50%, 70%, and 90%) for 30 min each and left in 100% ethanol for 24 h at temperatures below zero. Next, the specimens were kept in 100% ethanol until they were completely dried in a critical point dryer (Autosamdri-815, Series A, Tousimis Inc., Rockville, MD). The surface of

dried samples was then metalized by sputter coating with iridium. The morphology of the scaffolds as well as that of the adherent cells was observed by SEM (Philips XL30).

3.2.8 Measurement of newly deposited collagen type I

Human meniscus avascular cells were cultured on discs of aligned collagen scaffolds (6 mm in diameter, 0.125×10^6 cells per disc) in serum free ITS+ medium (Sigma-Aldrich) supplemented with 10 ng/mL TGF β 1 (Peprotech). After 3 weeks in culture with medium changes every 3 to 4 days. To evaluate newly deposited collagen, an ELISA was performed ELISA (Human collagen type I ELISA, MD Bioproducts, Zurich, Switzerland). Briefly, the scaffold and cells were solubilized with pepsin (1-10 mg/ml dissolved in 0.05M Acetic Acid) under acidic conditions and further digested with pancreatic elastase at neutral pH to convert polymeric collagen to monomeric collagen at 2-8 °C as outlined by the manufacturer's protocol. The plate was read on a SpectraMax 384 Plate Reader (Molecular Devices, Sunnyvale, CA, USA) at 450 nm (650 nm reference). Non-specific ELISA readings were controlled by using non-cell seeded scaffolds cultured under the same conditions and times.

3.2.9 RNA isolation and RT-PCR

Total RNA was isolated using the RNeasy mini kit (Qiagen, Hilden, Germany) and first strand cDNA was made as reported by the manufacturer's protocol (Applied Biosystems, Foster City, CA). Quantitative RT-PCR was performed using TaqMan® gene expression reagents. COL1A1, SOX9, COMP, CHAD, aggrecan (AGG) and GAPDH were detected using Assays-on-Demand™ primer/probe sets (Applied

Biosystems). Expression levels were normalized to GAPDH using the recommended ΔCt method, and fold-change was calculated using the $2^{-\Delta\Delta\text{CT}}$ formula[42].

3.2.10 *Ex-vivo meniscal repair*

Avascular bovine meniscal tissue explants were harvested from fresh adult bovine knees (Figure 3.1) and cultured in medium for 5 days in 6 well plates with DMEM supplemented with 10% calf serum and 1% Penicillin, Streptomycin, and Gentamycin. To simulate a longitudinal meniscal tear, a scalpel was used to cut the explant parallel to the circumferential direction of the collagen bundles. Aligned collagen scaffolds seeded with avascular meniscus cells were first cultured in serum free ITS+ medium (Sigma-Aldrich) supplemented with 10 ng/mL TGF β 1 (PeproTech) (3 mL/well) for 4 weeks and then inserted in the meniscal tear with the scaffold fibers aligned parallel to the circumferential collagen fibers of the host meniscal tissue. The repaired meniscal explants were maintained in serum free ITS+ medium (Sigma-Aldrich) supplemented with 10 ng/mL TGF β 1 (PeproTech) (8 mL/well) for an additional 3 weeks (with medium changes every 4-5 days) and processed for histology, MRI, and mechanical testing to assess filling of meniscal tear with neotissue and scaffold-host integration.

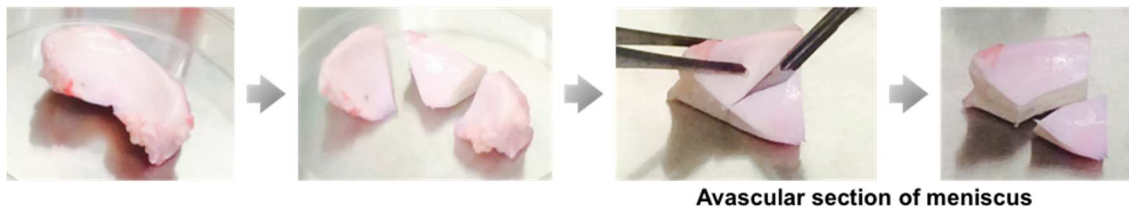


Figure 3.1 Fabrication of avascular section of meniscus

3.2.11 Histology, immunohistochemistry (IHC), and histomorphometry

Ex-vivo meniscal explants with meniscal tears repaired with cell-seeded or acellular electrospun collagen scaffolds were fixed in Z-Fix (ANATECH, Battle Creek, MI) for 9 days and embedded in paraffin. Sections (5–7 μm thick) were stained with hematoxylin and eosin (H&E) for the study of morphological details, while Safranin O-fast green staining was used to assess glycosaminoglycan distribution. For detection of collagen type I by immunohistochemistry, cut sections were treated with hyaluronidase for 2 h[35] and incubated overnight at 4°C with a primary antibody against collagen type I (clone: I-8H5; MP Biomedicals, Santa Ana, CA) at 10 $\mu\text{g}/\text{mL}$. Secondary antibody staining and detection procedures were followed as previously described [30, 38]. An isotype control was used to monitor nonspecific staining. To detect cells, sections were stained with Vectashield mounting medium containing 4',6-diamidino-2-phenylindole (DAPI) (Vector Laboratories, Burlingame, CA).

Microphotographs of all histological sections were captured using a microscope (Olympus BX60; Shinjuku, Tokyo, Japan) mounted with a calibrated charge-coupled device camera (Macrofire Optronics, Goleta, CA). Histomorphometric analysis was performed using the image processing software (Image J, National Institutes of Health, USA). The total length of the interface between the meniscal tissue and the scaffold was measured and classified as integration, disintegration, and apposition as described by Pabbruwe et al[41, 42]. Briefly, the presence of a gap between the scaffold and adjacent host tissue was classified as “disintegration”; apposition of scaffold to adjacent host tissue with clear demarcation of the interface was classified as “apposition”; and a continuous interface with absence of a clear boundary between scaffold and adjacent host

tissue, and presence of cell migration and matrix remodeling, was classified as “integration”. Each type of interface was expressed as a percentage of the total interface.

3.2.12 MRI for ex-vivo model with coronal defect

Bovine meniscus explants with surgically created tears were implanted with collagen scaffolds and cultured for 3 weeks as described above. Explants were divided into three groups: i) untreated tears, ii) tears repaired with acellular scaffolds, and iii) tears repaired with cell-seeded scaffolds. Explants were then placed in custom syringe coils for MRI imaging at 3T.

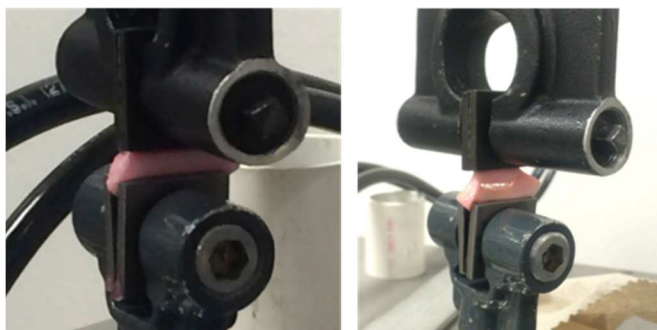


Figure 3.2 Images of the cell/collagen scaffold implant during the tensile testing process.

3.2.13 Mechanical testing of repair in ex-vivo model

Bovine meniscus explants with tears repaired with cell-seeded or acellular scaffolds were trimmed as shown in Figure 3.2. Each end of the specimen (with the longitudinal tear in the center) was mounted in the clumps of an Instron mechanical testing frame (Instron ® Universal Testing Machine, 3342 Single Column Model; Norwood, MA). Tensile force was monitored using a 1000 N load cell as samples were

tested to failure in tension at a constant displacement rate of 1 mm/min. Young's modulus was calculated from the slope of the linear segment of the stress-strain curve. Ultimate tensile strength (UTS) was calculated at the maximum load before failure.

3.2.14 Statistical analysis

Analysis of variance (ANOVA) and post hoc student's t-tests were used to detect statistically significant differences in fiber diameter, mechanical properties, and gene expression levels. P-values less than 0.05 were considered significant.

3.3 Results

3.3.1 Controlled production of ES collagen fibrous scaffolds

The morphological structure of aligned and random ES collagen fibers is shown in Figure 3.3. The rotating drum speed (~ 2400 rpm) and delivery parameters used produced scaffold structures with a high degree of alignment. The average diameter of aligned fibers was 496 ± 97 nm (range: 340–860 nm) and that for random collagen fibers was 467 ± 76 nm (range: 250–720 nm). The thickness of GA crosslinked random scaffolds was 0.25 ± 0.04 mm while crosslinked aligned scaffolds were 0.25 ± 0.03 mm.

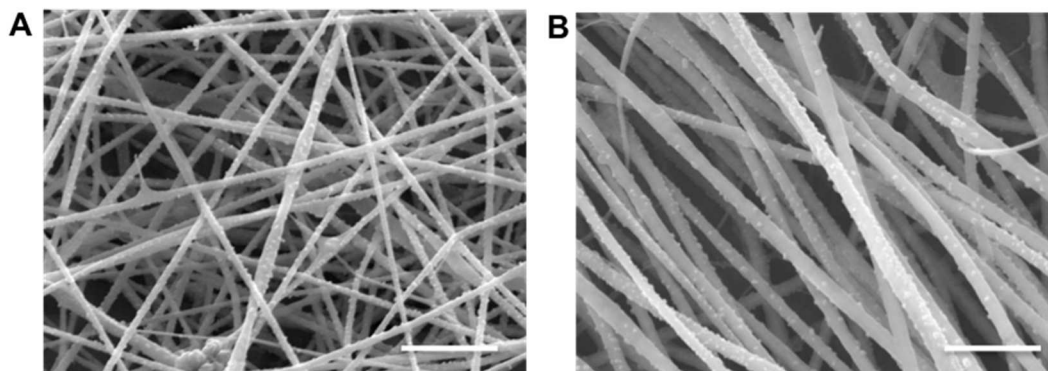


Figure 3.3 Scanning electron micrographs (SEM) of electrospun (ES) collagen scaffolds. (A) SEM of random and (B) aligned ES collagen fibers (Mag. 1250x; scale bar: 10 μ m).

3.3.2 Scaffold organization influences cell response while maintaining high cell viability

Meniscus avascular and vascular cells seeded upon randomly oriented ES collagen scaffolds were flattened and spread-out with multi-directional extensions (Figures 3.4A, 3.4C, and 3.4E). Cells on aligned collagen scaffolds were elongated in line

with the direction of the fibers (Figures. 3.4B, 3.4D, and 3.4F). These differences in morphology and alignment were also seen in the confocal images (Figures 3.4E and 3.4F), which provided evidence of high cell viability in aligned scaffolds.

3.3.3 Mechanical properties of scaffolds influenced by fiber alignment and culture conditions

Crosslinking with glutaraldehyde increased the average tensile modulus of dry random scaffolds from 32.48 ± 11.84 (non-crosslinked) to 57.56 ± 28.11 MPa (Figures 3.5A and Table 3.1). Crosslinking also increased the average tensile modulus of dry aligned collagen fibers when tested in tension parallel to or perpendicular to the direction of aligned fibers (Figures 3.5A and Table 3.1). Aligned scaffolds, when tested in the direction parallel to the aligned nanofibers generated a significantly greater tensile modulus compared to random scaffolds regardless of crosslinking ($p < 0.001$). On the other hand, the tensile modulus perpendicular to the direction of the aligned fibers was 32.18 ± 21.68 MPa after crosslinking, significantly weaker than random scaffolds ($p < 0.001$). Similar to the tensile modulus, the UTS of crosslinked aligned scaffolds was significantly ($p < 0.001$) higher: 4.97 ± 2.01 MPa (parallel to direction of alignment) compared to 1.19 ± 0.63 MPa measured in the crosslinked random scaffolds.

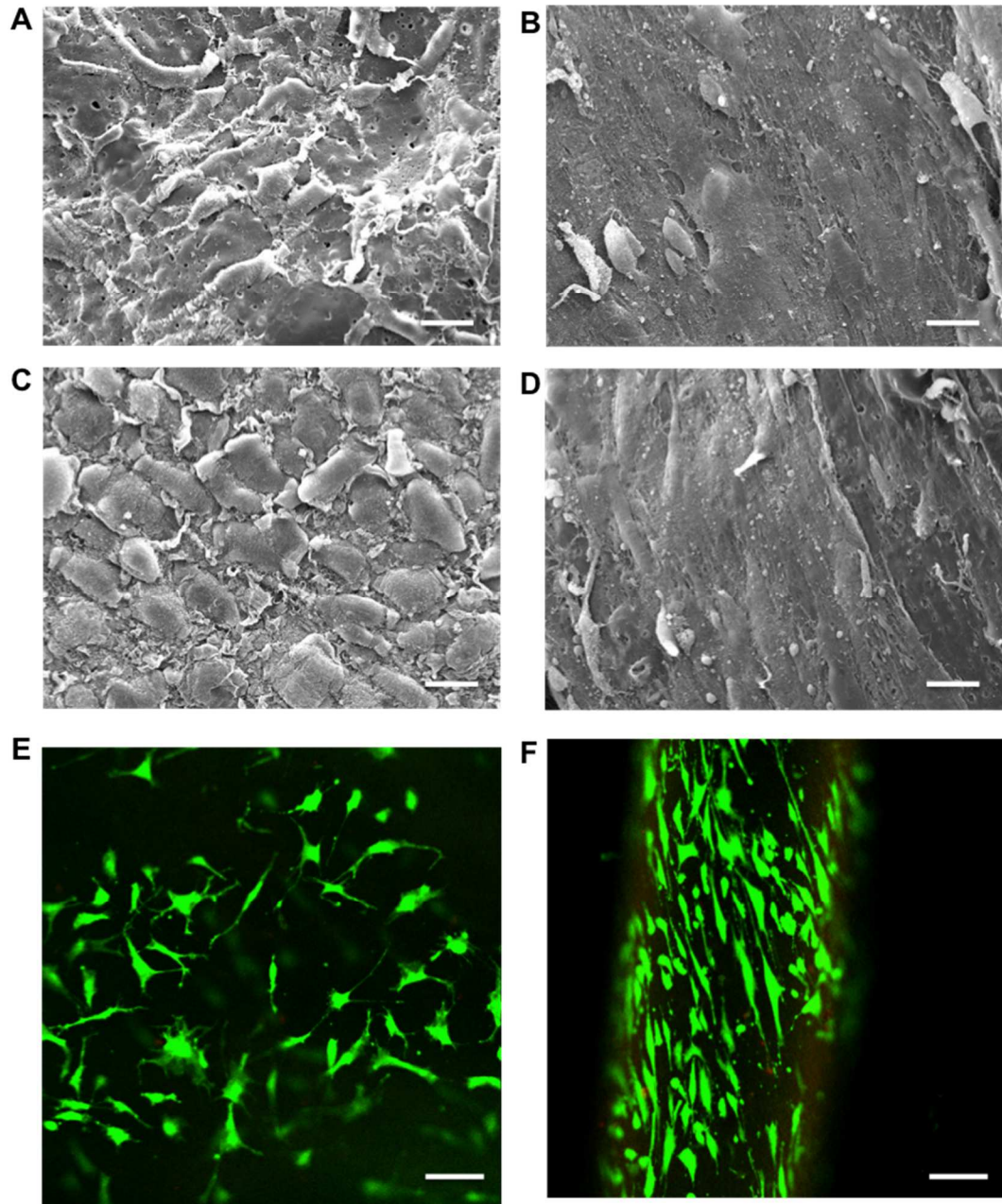


Figure 3.4 Scanning electron micrographs (SEM) of cellular response on electrospun (ES) collagen scaffolds (A) SEM of vascular human meniscus cells cultivated on random and (B) aligned electrospun collagen fibers (C) Avascular human meniscus cells seeded on random and (D) aligned electrospun collagen fibers (Mag. 625x; scale bar: 5 μ m). (E) Vascular human meniscus cells cultivated on random scaffolds and (F) avascular human meniscus cells on aligned scaffolds demonstrating viability (live/dead) and aligned cells cultivated on collagen scaffolds (Mag. 10x; scale bar: 200 μ m in confocal images).

Table 3.1 Ultimate tensile strength and Young's modulus (MPa) of freshly made and non-cultured random and aligned ES collagen scaffolds. (NC, noncrosslinked scaffolds; CL, crosslinked scaffolds)

ES nanofiber [type]	Noncrosslinked[NC] /Crosslinked[CL]	Tensile Strength [MPa]	Young's Modulus [MPa]
Random collagen	NC	1.16 ± 0.88	32.48 ± 11.84
	CL	1.19 ± 0.63	57.56 ± 28.11
Aligned collagen	NC	4.20 ± 1.81	178.72 ± 78.53
	CL	4.97 ± 2.01	214.76 ± 75.41
Perpendicular to aligned collagen	NC	1.44 ± 0.91	12.15 ± 8.42
	CL	1.51 ± 0.97	32.18 ± 21.68

Mechanical properties of cell-seeded and acellular scaffolds in culture were significantly ($P < 0.0001$) lower than dry scaffolds (Table 3.2). The stiffness of both cellular and acellular scaffolds decreased with time in culture. However, cell-seeded scaffolds were consistently stiffer and reached a higher ultimate tensile stress than acellular scaffolds ($p < 0.0001$).

To determine whether the increased mechanical property of cell-seeded scaffolds was due to the deposition of newly formed collagen, we used ELISA to measure newly synthesized collagen type I (Figure. 3.6A). No collagen was detected in the cell free-scaffolds since the antibody does not recognize denatured collagen in the scaffold (as detailed by the manufacturer) and by our immunostains (Figure 3.8L and 3.8M). In addition, cells seeded on collagen I scaffolds generated greater levels of collagen I than cells seeded on PLA (Figure 3.6A).

Table 3.2 Ultimate tensile strength and Young's modulus (MPa) of random & aligned ES collagen scaffolds over time in culture with or without cells (1 week and 3 weeks).

Time In Culture	Cells & Fiber Type	Tensile Strength [MPa]	Young's Modulus [MPa]
1 week	No cells and Aligned	0.48 ± 0.27	0.78 ± 0.48
	Cells and Aligned	0.63 ± 0.53	1.51 ± 0.90
3 week	No cells and Aligned	0.024 ± 0.029	0.26 ± 0.10
	Cells and Aligned	0.41 ± 0.67	0.90 ± 0.62

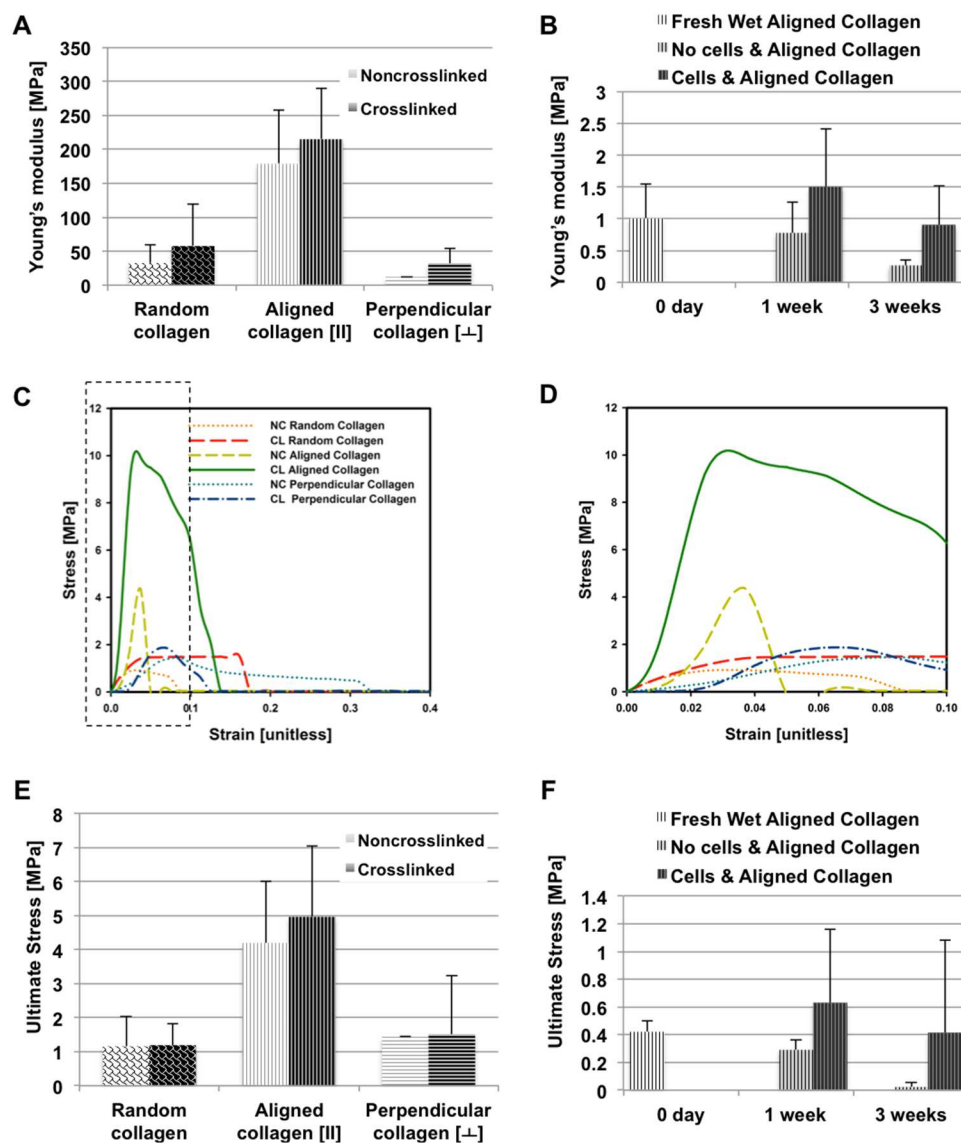


Figure 3.5 Mechanical testing of random and aligned ES collagen scaffolds. (A) Young's modulus (MPa) for random, aligned (along fiber orientation), and perpendicular to fiber orientation with and without crosslinking. (B) Young's modulus (MPa) of aligned electrospun collagen scaffolds over time in culture with or without cells (0 day after soaking in 1x PBS for 1 hour, one week, and three weeks). (C) Stress/strain curve for each condition (NC: noncrosslinked, CL: crosslinked). (D) Dotted outlined area of stress/strain curve in (C). (E) Ultimate stress readings (MPa) for each condition either crosslinked or noncrosslinked. (F) Ultimate stress (MPa) for aligned electrospun collagen scaffolds over time in culture with or without cells (0 day after soaking in PBS for 1 hour, one week, and three weeks).

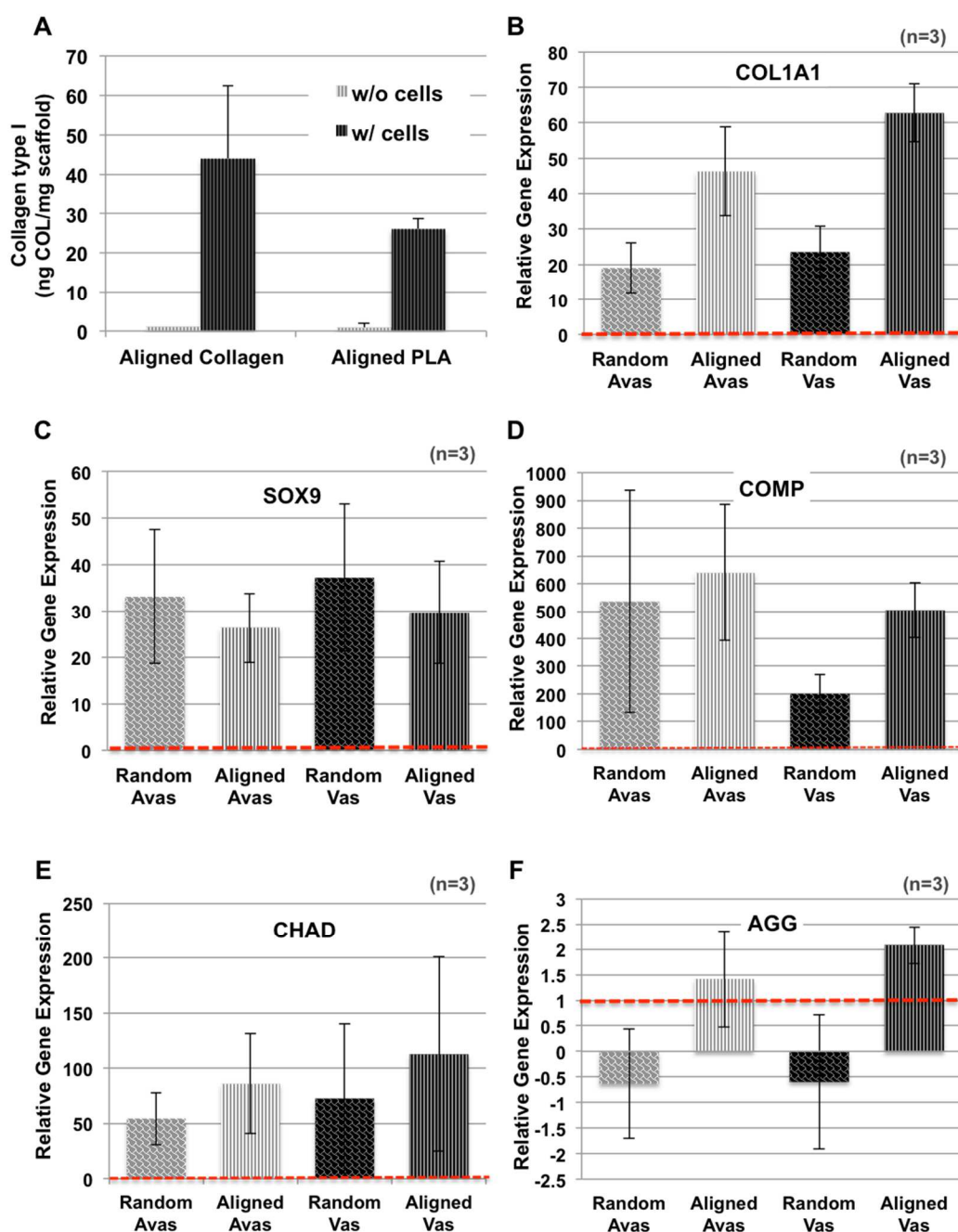


Figure 3.6 ELISA quantification for collagen type I and gene expression levels of human vascular and avascular meniscus cells cultivated on either random or aligned collagen electrospun scaffolds. (A) ELISA quantification of Collagen type I for cell and non-cell seeded aligned collagen and PLA scaffolds. (B) COL1A1 gene expression. (C) SOX9 gene expression. (D) COMP gene expression. (E) CHAD gene expression (F) Aggrecan gene expression (n = 3 donors) relative to monolayer controls. Expression levels are relative to monolayer controls (dotted line).

3.3.4 *A meniscus-like phenotype supported by scaffold and specific gene responses differed between cell source and scaffold organization*

In comparison to meniscal cells in monolayer culture (baseline gene expression levels indicated by dotted line in Figures 3.6B to 3.6F), cells that were derived from either vascular or avascular regions cultivated on both random and aligned collagen scaffolds expressed ($p < 0.05$) higher levels of COL1A1, SOX9, COMP, CHAD, and aggrecan mRNA expression relative monolayer cultured cells. Although COL1A1 and aggrecan mRNA expression levels were higher for both meniscus cell sources on aligned scaffolds relative to random oriented scaffolds ($p < 0.05$) (Figures 3.6B and 3.6F), no significant differences in gene expression levels were found between vascular and avascular cells.

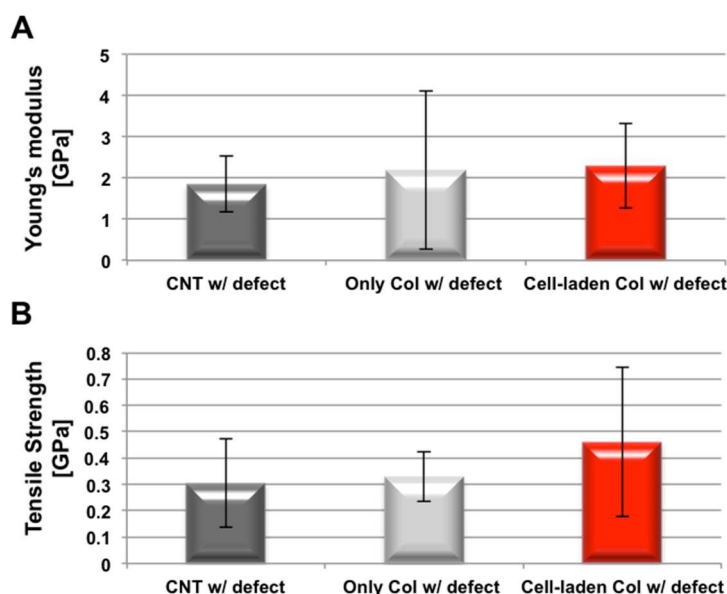


Figure 3.7 Mechanical strength of bovine meniscus ex-vivo repair model. Collagen membranes were seeded with human meniscus avascular cells to create a human meniscus avascular cells/electrospun collagen scaffold implant, as described under material and methods. (A) Young's modulus and (B) ultimate tensile strength of meniscal repair model using only defect without any membrane and cells as control, a membrane only control (i.e. no implanted cells), and the cells/collagen scaffold implant.

3.3.5 Integration and neotissue formation of ES cell seeded scaffolds in an ex vivo meniscus defect model.

Human meniscus cells seeded on collagen aligned scaffolds and pre-cultured for 4 weeks were implanted in surgically created longitudinal tears in bovine meniscus tissue explants. After 3 weeks of post-repair culture in 6-well plates histological analysis revealed the generation of newly formed tissue within the tear with elongated cellular morphology and collagen type I immunohistochemistry, between the implanted scaffolds and the native tissue, and with integration of neotissue for improving defects (Figure 3.8). Also, on histomorphometry, collagen electrospun scaffolds seeded with human meniscus avascular cells resulted in 90% integration with host meniscus tissue, significantly greater than acellular collagen scaffolds (Figure 3.9). MRI of the ex vivo repair (Figure 3.10) revealed persistence of the surgical tear in the unrepaired group, apposition without integration of the interface in the acellular scaffold group, and integration of the scaffold into host tissue in the cell-seeded scaffold group. On mechanical testing of the repaired defects, cell-seeded scaffolds tended towards a greater tensile strength than either unrepaired defects or defects repaired with acellular scaffolds (though not reaching statistical significance).

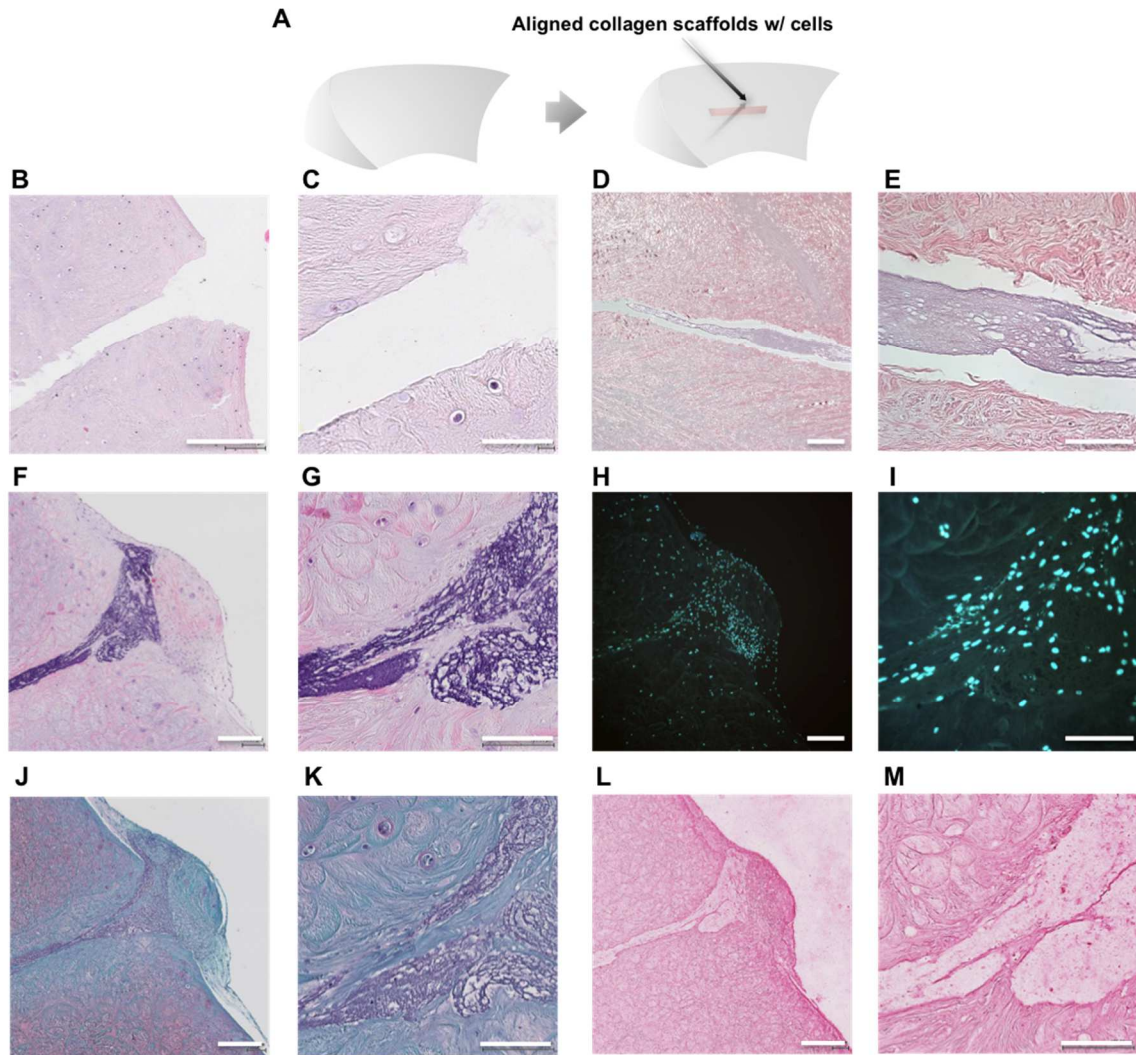


Figure 3.8 Overview of defect formation, histology and immunohistochemistry of bovine meniscus ex-vivo repair model (A) Coronal defects were surgically produced in bovine meniscus white zone tissue i) only defect without both cells and scaffolds, ii) only collagen scaffolds without cells, iii) cell-laden scaffolds. (B–C) H&E stain of only defect in meniscus. (D–E) H&E stain of only collagen implant. (F–G) H&E stain of the cells/aligned collagen scaffold implant within the defect of meniscus. (H–I) DAPI stain of the cells/aligned collagen scaffold implant. (J–K) Safranin O/fast-green stain of the cells/aligned collagen scaffold implant. (L–M) Collagen type I immunostain of the cells/aligned collagen scaffold implant. (Mag. B, D, F, H, J, and L = 10x, scale bar: 200 μm ; Mag. C, E, G, I, K, and M = 40x, scale bar: 100 μm).

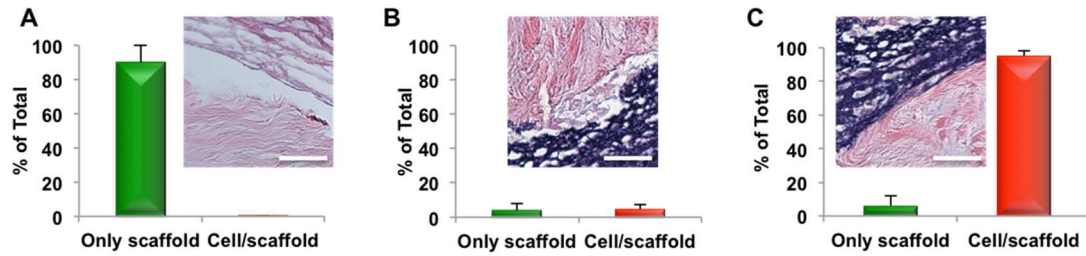


Figure 3.9 Histomorphometric analysis of integration was significantly different between acellular and cell-seeded scaffolds (A) the % disintegration ($p < 0.0001$), (B) the % apposition ($p < 0.5$), and (C) the % integration ($p < 0.0001$). Histologic images are show as representative of each morphometric feature (scale bar: 50 μm). The % of disintegration, apposition, or integration was calculated as reported by Pabbruwe et al.

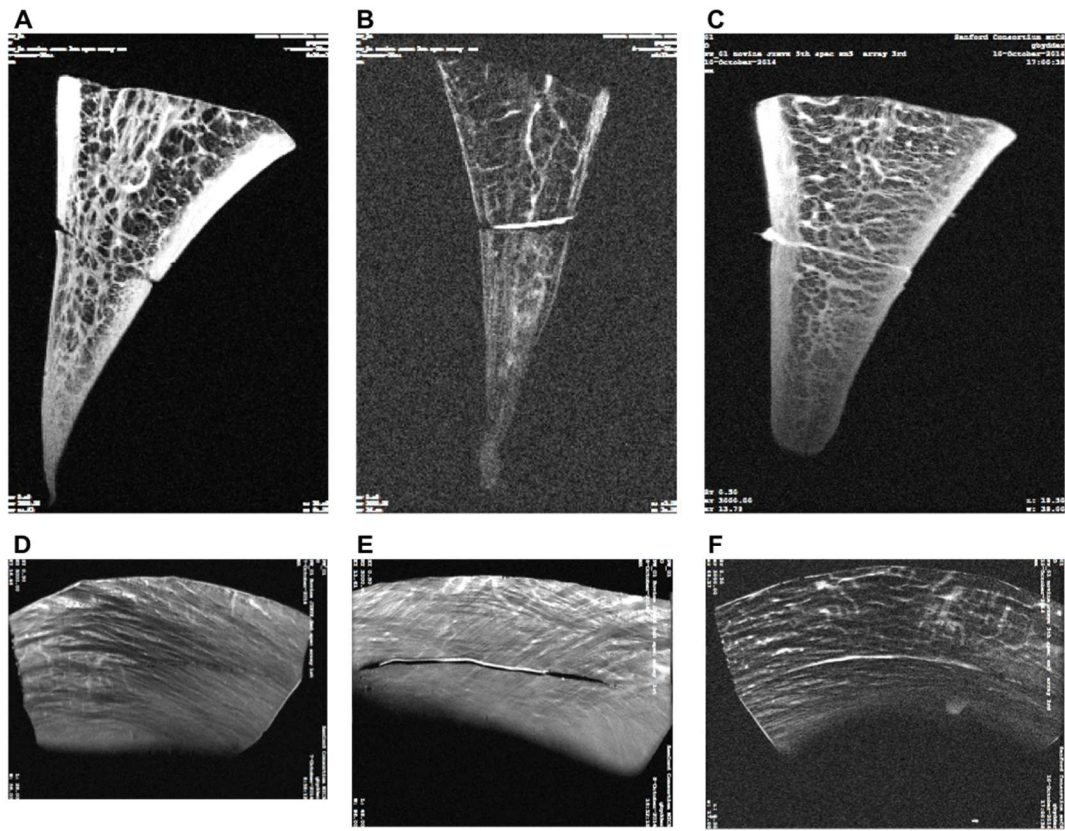


Figure 3.10 MRI images of bovine meniscus ex-vivo repair model. Collagen membranes were seeded with human meniscus avascular cells to create a human meniscus avascular cells/electrospun collagen scaffold implant, as described under material and methods. The scaffolds were inserted into incisions made in a bovine meniscus avascular section and cultured for 3 weeks. Imaging of meniscal specimens using a spin echo (SE) sequence with T_{es} of 9.8 ms and multi-slice, in the coronal plane to the meniscus with (A) empty defect, (B) acellular electrospun scaffold, and (C) cell-seeded electrospun scaffold. Imaging of a meniscus specimens using gradient echoes (GRE) in the axial plane to the meniscus with (D) empty defect, (E) acellular electrospun scaffold, and (F) cell-seeded electrospun scaffold.

3.4 Discussion

A meniscal tear is the most frequently recorded diagnosis of all orthopaedic diagnoses, and partial or total meniscectomy remain the most common of all orthopaedic procedures[43]. Electrospinning is an attractive tissue fabrication process to generate nano-fibrous scaffolds that emulate the structure of native meniscal tissue. We have shown that collagen electrospun scaffolds produced in this study support the viability of human meniscus cells, induce an organized cellular alignment reflecting the scaffold microstructure, and promote the formation of meniscus-like tissues. Prefabrication of organized collagen scaffolds with an architecture mimicking the meniscus collagen bundle organization shows promise for the repair of meniscal tears, as demonstrated by the formation and integration of new tissue in the ex-vivo meniscus defect model.

Fabrication of scaffolds for meniscus tissue engineering via electrospinning has been accomplished with numerous synthetic as well as natural biopolymers[44]. We have also previously shown proof of concept of engineering meniscogenic tissue by electrospinning PLA[30]. Despite the biocompatibility and mechanical properties of electrospun PLA, there is some concern about the reduction in pH induced by biodegradation products (lactic acid) within the knee joint as noted by others using this material [32]. In this study we selected collagen type I to more closely mimic the dominant structural protein in native meniscal tissue. Using collagen type I scaffolds also appeared to be advantageous for tissue engineering since it leads to a higher production of collagen type I compared to PLA scaffolds. Similar to our previous report on PLA scaffolds[30], we also observed that the aligned ES collagen scaffolds possessed greater

mechanical properties relative to randomly electrospun scaffolds and generated a higher quality of neo-tissue (based on gene expression) as well.

The neo tissue produced on the collagen scaffolds appeared meniscus-like with a characteristic deposition of collagen type I, high expression of SOX9, COMP, CHAD and low GAG content as reported elsewhere for native[45-47] and engineered meniscus[30, 48-50]. Although scaffolds were composed of collagen type I, we confirmed that the antibody for immunostaining and ELISA was specific to newly synthesized collagen type I by comparing results to acellular scaffolds. In addition, meniscal cells seeded on collagen I electrospun scaffolds generated greater levels of collagen I than cells seeded on PLA, supporting our rationale for selecting a naturally occurring polymer.

Electrospinning is a convenient manufacturing technique for tuning the anisotropy of tissue engineering scaffolds and mechanical properties. Dry extruded collagen fibers have a wide range of reported tensile moduli: from 2 – 46 MPa[51] to 1.7 – 3.3 GPa[52]. Dry electrospun collagen scaffolds had a reported tensile modulus of 52 MPa in the dominant direction of fiber alignment and 26 MPa in the direction perpendicular to fiber alignment[53]. The moduli of our dry electrospun mats, even before crosslinking, were substantially greater. Single electrospun collagen fibers have a reported bending modulus of 1.3 – 7.8 GPa. However, the bending modulus decreased dramatically after hydration in PBS buffer (to 0.07 – 0.26 MPa)[54]. Cross-linking with glutaraldehyde almost doubled the shear modulus of single electrospun collagen fibers and rendered the fibers insoluble[54]. Glutaraldehyde has also been shown to effectively increase the tensile strength of extruded collagen threads[55]. In our study, crosslinking with glutaraldehyde

doubled the stiffness of randomly aligned collagen and increased the stiffness of aligned collagen by 120 %.

Upon hydration non-crosslinked scaffolds quickly lost most of their structural integrity, while glutaraldehyde crosslinked scaffolds remained intact. However, the mechanical properties of hydrated scaffolds were significantly reduced (Figure 3.5). Furthermore, the stiffness continued to decrease with time in culture. Nevertheless, cell-seeded scaffolds consistently generated higher stiffness than acellular scaffolds and reached a high ultimate tensile stress. In addition, this difference between the mechanical properties of cell-seeded (Young's modulus are 1.51 ± 0.90 at 1 week and 0.90 ± 0.62 MPa at 3 weeks) and acellular scaffolds (Young's modulus are 0.78 ± 0.48 at 1 week and 0.26 ± 0.10 MPa at 3 weeks) increased over time. This relative increase in mechanical properties can be attributed to the collagen synthesis measured in the cell-seeded scaffolds via ELISA. Furthermore, these cell-laden collagen aligned ES scaffolds had a much higher tensile mechanical property than other reported studies using protein polymer scaffolds with cells. For example, Grogan et al.[50] reported that methacrylated gelatin scaffolds patterned via projection stereolithography possessed a Young's modulus of about 0.01 MPa. Kai et al.[56] measured tensile properties of a blend of coaxial PCL/gelatin ES nanofibers. After soaking in PBS for 3 h, the Young's modulus was only 0.13 ± 0.04 MPa and 0.56 ± 0.09 MPa. Grover et al.[57] varied the ratio of collagen to gelatin in their scaffolds to tailor their mechanical and degradation properties. Pure collagen, pure gelatin, and mixed collagen-gelatin 1:1 scaffolds had a Young's modulus of 81 ± 8 kPa, 4.6 ± 0.1 kPa, and 19 ± 3 kPa, respectively. The Young's modulus of pure collagen scaffolds was the highest measured among seven different scaffolds tested on

that study. The tensile moduli of our cell-seeded collagen scaffolds were consistently higher than that previously reported for scaffolds of collagen origin.

Cell-seeded scaffolds can generate additional ECM after implantation and therefore tend to integrate better into host tissue[58]. Kobayashi et al reported that meniscal grafts from the vascular region had a better repair capacity than grafts from the avascular region, suggesting an intrinsic repair capacity independent of blood supply[59]. On the other hand, Hennerbichler et al did not find any significant difference in the repair capacity between vascular and avascular zones[60]. In our experiments, we also did not find significant differences in gene expression between meniscal cells harvested from vascular and avascular regions. We therefore chose to only study avascular cells in the ex vivo repair model.

The ex-vivo model developed in this study with electrospun collagen scaffold supports the potential for cell-seeded collagen scaffolds to integrate with native tissues. Others have reported on ex vivo repair of meniscal tears. Pabbruwe et al seeded commercial sources of collagen membranes or sponges with bone marrow derived MSC with promising results[42]. More recently, Shimomura et al, reported on repair of radial meniscal tears using electrospun PCL scaffolds made porous by sacrificial PEO and seeded with bovine meniscal fibrochondrocytes[61]. In that study, however, the meniscal explants were wrapped by the scaffolds at the site of the tear. Comparison of mechanical properties of the repair among different studies is difficult because of the differences in the creation of tears or meniscal defects, the repair procedure, and the methods of testing. However, we found a trend towards increased mechanical strength (not statistically

significant) when the tear was repaired with cell-seeded scaffolds relative to untreated tears or tears repaired with acellular scaffolds.

Despite the positive interaction of human meniscus cells with the collagen scaffolds, the low toxicity, and encouraging new tissue formation, several issues remain to be addressed. The mechanical properties of cultured electrospun collagen mats may not be sufficient to survive implantation in the loaded environment of the knee as required for a meniscal tissue replacement. We therefore chose to assess potential application for enhancement of meniscal tissue repair. We are continuing to enhance the biomechanical function by optimizing electrospinning and crosslinking conditions, enhancing cell culture, and combining collagen with other biomaterials. While fibrochondrocytes have been extensively tested with some success, we are also exploring other cell sources, such as bone marrow derived mesenchymal stem cells that are more attractive because the source of meniscal fibrochondrocytes is limited[42].

3.5 Conclusion

In summary, we electrospun collagen scaffolds to induce a cellular alignment with scaffold microstructure and to stimulate meniscogenic neo-tissue generation. Collagen scaffolds mimicking the collagen bundle organization of the native meniscus have promise for the repair of meniscal tears, as indicated by the generation and integration of new tissue in ex-vivo meniscal tears in the avascular region.

3.6 Acknowledgments

This chapter, in full, is currently being prepared for submission for publication. Jihye Baek, Sujata Sovani, Nicholas E. Glembofski, Jiang Du, Sungho Jin, Shawn P. Grogan, Darryl D. D'Lima. The dissertation author was the primary investigator and author of this paper.

3.7 References

- [1] Baker P, Coggon D, Reading I, Barrett D, McLaren M, Cooper C. Sports injury, occupational physical activity, joint laxity, and meniscal damage. *The journal of Rheumatology*. 2002;3:557-63.
- [2] Boyd KT, Myers PT. Meniscus preservation; rationale, repair techniques and results. *The Knee*. 2003;10:1-11.
- [3] Sweigart MA, Athanasiou KA. Toward tissue engineering of the knee meniscus. *Tissue Eng*. 2001;7:111-29.
- [4] Majewski M, Susanne H, Klaus S. Epidemiology of athletic knee injuries: A 10-year study. *The Knee*. 2006;13:184-8.
- [5] van Tienen TG, Hannink G, Buma P. Meniscus replacement using synthetic materials. *Clinics in Sports Medicine*. 2009;28:143-56.
- [6] Lozano J, Ma Cb Fau - Cannon WD, Cannon WD. All-inside meniscus repair: a systematic review. *Clin Orthop Relat Res*. 2007:134-41.
- [7] Chang A, Moisio K, Chmiel J S, Eckstein F, Guermazi A, Almagor O, Cahue S, Wirth W, Prasad P and Sharma L. Subregional effects of meniscal tears on cartilage loss over 2 years in knee osteoarthritis. *Annals of the Rheumatic Diseases*. 2011;70:74-49.
- [8] Englund M, Guermazi A, Roemer FW, Yang M, Zhang Y, Nevitt MC, Lynch JA, Lewis CE, Torner J and Felson DT. Meniscal pathology on MRI increases the risk for both incident and enlarging subchondral bone marrow lesions of the knee: the MOST Study. *Annals of the Rheumatic Diseases*. 2010;69:1796-802.
- [9] Roos H, Lauren M, Adalberth T, Roos EM, Jonsson K, Lohmander LS. Knee osteoarthritis after meniscectomy: prevalence of radiographic changes after twenty-one years, compared with matched controls. *Arthritis and Rheumatism*. 1998;41:687-93.

- [10] Ibarra C, Koski J, Warren RF. Tissue engineering meniscus: cells and matrix. *Orthopedic Clinics of North America*. 2000;31:411-8.
- [11] McCarty EC, Marx RG, DeHaven KE. Meniscus repair: considerations in treatment and update of clinical results. *Clinical Orthopaedics and Related Research*. 2002;402:122-34.
- [12] Peretti GM. Cell-based therapy for meniscal repair: a large animal study. *American Journal of Sports Medicine*. 2004;32:146-58.
- [13] Port J, Jackson DW, Lee TQ, Simon TM. Meniscal repair supplemented with exogenous fibrin clot and autogenous cultured marrow cells in the goat model. *American Journal of Sports Medicine*. 1996;24:547-55.
- [14] Izuta Y, Ochi M, Adachi N, Deie M, Yamasaki T, Shinomiya R. Meniscal repair using bone marrow-derived mesenchymal stem cells: experimental study using green fluorescent protein transgenic rats. *Knee*. 2005;12:217-23.
- [15] Walsh CJ, Goodman D, Caplan AI, Goldberg VM. Meniscus regeneration in a rabbit partial meniscectomy model. *Tissue Engineering*. 1999;5:327-37.
- [16] Cook J L, Fox DB, Malaviya P, Tomlinson JL, Kuroki K, Cook CR and Kladakis S Long-term outcome for large meniscal defects treated with small intestinal submucosa in a dog model. *The American journal of sports medicine*. 2006;34:32-42.
- [17] Stapleton TW, Ingram J, Fisher J, Ingham E. Investigation of the regenerative capacity of an acellular porcine medial meniscus for tissue engineering applications. *Tissue Engineering Part A*. 2011;17:231-42.
- [18] Bruns J, Kahrs J, Kampen J, Behrens P, Plitz W. Autologous perichondral tissue for meniscal replacement. *The Journal of Bone & Joint Surgery Br*. 1998;80:918-23.
- [19] Bodin A, Concaro S, Brittberg M, Gatenholm P. Bacterial cellulose as a potential meniscus implant. *Journal of Tissue Engineering and Regenerative Medicine*. 2007;1:406-8.

- [20] Calve S, Dennis RG, Kosnik PE, Baar K, Grosh K, Arruda EM. Engineering of functional tendon. *Tissue Engineering*. 2004;10:755-61.
- [21] Kumbar SG, Nukavarapu SP, James R, Nair LS, Laurencin CT. Electrospun poly(lactic acid-co-glycolic acid) scaffolds for skin tissue engineering. *Biomaterials*. 2008;29:4100-7.
- [22] Park K, Ju YM, Son JS, Ahn KD, Han DK. Surface modification of biodegradable electrospun nanofiber scaffolds and their interaction with fibroblasts. *J Biomater Sci Polym Ed* 2007;18:369-82.
- [23] Zhang YZ, Su B, Venugopal J, Ramakrishna S, Lim CT. Biomimetic and bioactive nanofibrous scaffolds from electrospun composite nanofibers. *Int J Nanomed*. 2007;47:264-70.
- [24] McClure MJ, Sell SA, Simpson DG, Bowlin GL. Electrospun Polydioxanone, Elastin, and Collagen Vascular Scaffolds: Uniaxial Cyclic Distension. *Journal of Engineered Fibers and Fabrics* 2009;4:18.
- [25] Li M, Mondrinos MJ, Gandhi MR, Ko FK, Weiss AS, Lelkes PI. Electrospun protein fibers as matrices for tissue engineering. *Biomaterials*. 2005;26:5999-6008.
- [26] Homayoni H, Ravandi SAH, Valizadeh M. Electrospinning of chitosan nanofibers: Processing optimization. *Carbohydrate Polymers*. 2009;77:656-61.
- [27] Kumbar SG, Nukavarapu SP, James R, Hogan MV, Laurencin CT. Recent patents on electrospun biomedical nanostructures: an overview. *Recent Patents on Biomedical Engineering*. 2008;1:68-78.
- [28] Dong B, Arnoult O, Smith ME, Wnek GE. Electrospinning of collagen nanofiber scaffolds from benign solvents. *Macromolecular rapid communications*. 2009;30:539-42.
- [29] Platt MA. Tendon repair and healing. *Clinics in Podiatric Medicine and Surgery*. 2005;22:553-60.

- [30] Baek J, Chen X, Sovani S, Jin S, Grogan SP, D'Lima DD. Meniscus tissue engineering using a novel combination of electrospun scaffolds and human meniscus cells embedded within an extracellular matrix hydrogel. *Journal of Orthopaedic Research*. 2015;33:572-83.
- [31] Bergsma EJ, Rozema FR, Bos RRM, Bruijn WCD. Foreign body reactions to resorbable poly(l-lactide) bone plates and screws used for the fixation of unstable zygomatic fractures. *Journal of Oral and Maxillofacial Surgery*. 1993;51:666-70.
- [32] Spain TL, Agrawal CM, Athanasiou KA. New technique to extend the useful life of a biodegradable cartilage implant. *Tissue Engineering*. 1998;4:343-52.
- [33] Makris EA, Hadidi P, Athanasiou KA. The knee meniscus: structure-function, pathophysiology, current repair techniques, and prospects for regeneration. *Biomaterials*. 2011;32:7411-31.
- [34] Lei Huang, Karthik Nagapudi, Robert P. Apkarian, Chaikof EL. Engineered collagen-PEO nanofibers and fabrics. *Journal of Biomaterials Science Polymer Edition*. 2001;12:979-93.
- [35] Roberts S, Menage J, Sandell LJ, Evans EH, Richardson JB. Immunohistochemical study of collagen types I and II and procollagen IIA in human cartilage repair tissue following autologous chondrocyte implantation. *The Knee*. 2009;16:398-404.
- [36] Pauli C, Grogan SP, Patil S, Otsuki S, Hasegawa A, Koziol J, Lotz MK and D'Lima DD. Macroscopic and histopathologic analysis of human knee menisci in aging and osteoarthritis. *Osteoarthritis and cartilage / OARS, Osteoarthritis Research Society*. 2011;19:1132-41.
- [37] Barbero A, Grogan S, Schäfer D, Heberer M, Mainil-Varlet P, Martin I. Age related changes in human articular chondrocyte yield, proliferation and post-expansion chondrogenic capacity. *Osteoarthritis and Cartilage*. 2004;12:476-84.

- [38] Grogan SP, Miyaki S, Asahara H, D'Lima DD, Lotz MK. Mesenchymal progenitor cell markers in human articular cartilage: normal distribution and changes in osteoarthritis. *Arthritis research & therapy*. 2009;11:R85.
- [39] Grogan SP, Aclin B, Frenz M, Brunner T, Schaffner T, Mainil-Varlet P. In vitro model for the study of necrosis and apoptosis in native cartilage. *The Journal of pathology*. 2002;198:5-13.
- [40] Martin I, Jakob M, Schäfer D, Dick W, Spagnoli G, Heberer M. Quantitative analysis of gene expression in human articular cartilage from normal and osteoarthritic joints. *Osteoarthritis and Cartilage*. 2001;9:112-8.
- [41] Pabbruwe MB, Esfandiari E, Kafienah W, Tarlton JF, Hollander AP. Induction of cartilage integration by a chondrocyte/collagen-scaffold implant. *Biomaterials*. 2009;30:4277-86.
- [42] Pabbruwe MB, Kafienah W, Tarlton JF, Mistry S, Fox DJ, Hollander AP. Repair of meniscal cartilage white zone tears using a stem cell/collagen-scaffold implant. *Biomaterials*. 2010;31:2583-91.
- [43] Garrett WE, Swiontkowski MF, Weinstein JN, Callaghan J, Rosier RN, Berry DJ, Harrast J and Derosa GP. American Board of Orthopaedic Surgery Practice of the Orthopaedic Surgeon: Part-II, Certification Examination Case Mix. *The Journal of Bone & Joint Surgery*. 2006;88:660-7.
- [44] Rim NG, Shin CS, Shin H. Current approaches to electrospun nanofibers for tissue engineering. *Biomedical Materials*. 2013;8:014102.
- [45] Cheung H. Distribution of type I, II, III and V in the pepsin solubilized collagens in bovine menisci. *Connect Tissue Res*. 1987;16:343-56.
- [46] Eyre DR, Wu JJ. Collagen of fibrocartilage: a distinctive molecular phenotype in bovine meniscus. *FEBS Letters*. 1983;158:265-70.
- [47] Kambic HE, McDevitt CA. Spatial organization of types I and II collagen in the canine meniscus. *Journal of Orthopaedic Research*. 2005;23:142-9.

- [48] Freymann U, Endres M, Neumann K, Scholman HJ, Morawietz L, Kaps C. Expanded human meniscus-derived cells in 3-D polymer–hyaluronan scaffolds for meniscus repair. *Acta Biomaterialia*. 2012;8:677-85.
- [49] Xu T, Binder KW, Albanna MZ, Dice D, Zhao W, Yoo JJ, Atala A. Hybrid printing of mechanically and biologically improved constructs for cartilage tissue engineering applications. *Biofabrication*. 2013;5:015001.
- [50] Grogan SP, Chung PH, Soman P, Chen P, Lotz MK, Chen S, D'Lima DD. Digital micromirror device projection printing system for meniscus tissue engineering. *Acta Biomater*. 2013;9:7218-26.
- [51] Pins GD, Christiansen DL, Raj Patel, Silver FH. Self-assembly of collagen fibers. Influence of fibrillar alignment and decorin on mechanical properties. *Biophysical Journal*. 1997;73:2164-72.
- [52] Zeugolis DI, Paul GR, Attenburrow G. Cross-linking of extruded collagen fibers—A biomimetic three-dimensional scaffold for tissue engineering applications. *Journal of Biomedical Materials Research Part A*. 2009;89A:895-908.
- [53] Matthews JA, Wnek GE, Simpson DG, Bowlin GL. Electrospinning of Collagen Nanofibers. *Biomacromolecules*. 2002;3:232-8.
- [54] Yang L, Fitié CFC, van der Werf KO, Bennink ML, Dijkstra PJ, Feijen J. Mechanical properties of single electrospun collagen type I fibers. *Biomaterials*. 2008;29:955-62.
- [55] Cavallaro JF, Kemp PD, Kraus KH. Collagen fabrics as biomaterials. *Biotechnology and Bioengineering*. 1994;43:781-91.
- [56] Kai D, Prabhakaran MP, Stahl B, Eblenkamp M, Wintermantel E, Ramakrishna S. Mechanical properties and in vitro behavior of nanofiber-hydrogel composites for tissue engineering applications. *Nanotechnology*. 2012;23:095705.
- [57] Grover CN, Cameron RE, Best SM. Investigating the morphological, mechanical and degradation properties of scaffolds comprising collagen, gelatin and elastin for

- use in soft tissue engineering. *Journal of the Mechanical Behavior of Biomedical Materials*. 2012;10:62-74.
- [58] Angele P, Johnstone B, Kujat R, Zellner J, Nerlich M, Goldberg V, Yoo J. Stem cell based tissue engineering for meniscus repair. *Journal of Biomedical Materials Research Part A*. 2008;85A:445-55.
- [59] Kobayashi K, Fujimoto E, Deie M, Sumen Y, Ikuta Y, Ochi M. Regional differences in the healing potential of the meniscus—an organ culture model to eliminate the influence of microvasculature and the synovium. *The Knee*. 2004;11:271-8.
- [60] Hennerbichler A, Moutos FT-, Hennerbichler D, Weinberg JB, Guilak F. Repair response of the inner and outer regions of the porcine meniscus in vitro. *The American journal of sports medicine*. 2007;35:754-62.
- [61] Shimomura K, Bean AC, Lin H, Nakamura N, Tuan RS. In vitro Repair of Meniscal Radial Tear Using Aligned Electrospun Nanofibrous Scaffold. *Tissue Engineering part A*. 2015.

CHAPTER 4: MENISCAL TISSUE ENGINEERING USING ELECTROSPUN NATURAL/COLLAGEN: COMPARISON OF DIFFERENT CELL SOURCES.

“Attitude is a little thing that makes a big difference.”

—Winston Churchill

4.1 Introduction

Meniscus tears are the most frequently recorded orthopaedic diagnosis and a common cause of knee impairment and dysfunction [1-4]. Traumatic or degenerative meniscal lesions and tears that occur in the inner avascular region of meniscus are commonly more extensive, are more complex and due to the lack of vascularity possess limited self-healing properties [5]. Such lesions and tears disrupt the fibrous architecture of the meniscus which impairs normal load transmission within the joint [6] and results in osteoarthritis [7]. Hence, partial or total meniscectomy is a common procedure in symptomatic patients[8].

To overcome the need for partial or total meniscectomy following development of a tear in the avascular region, alternative means to restore native tissue function may be achieved by improving surgical repair techniques (sutures and implants) and by encouraging cell growth and new reparative tissue formation. However, tears located in

the avascular region or spanning vascular and avascular regions still pose a significant challenge. Tissue-engineered acellular collagen constructs, such as collagen meniscus implant (CMI)[9], have been implanted in four human patients with various results[10, 11] despite the absence of cells or growth factor. A number of cell-based strategies have been tested in order to improve the bonding of a torn meniscus using cultured meniscus cells or stem cells. Collagen scaffolds combined with human bone marrow-derived stem cells (hMSC) were used to sandwich constructs of two white zone ovine meniscus discs[12]. A swine chondrocyte-fibrin glue suspension was utilized as a biological glue to improve bonding between two meniscal slices obtained from swine menisci[13]. Vicryl mesh scaffold seeded with chondrocytes from different sources (articular, auricular, and costal) were implanted into a porcine bucket handle lesion model to produce mainly scar-like tissue [14, 15]. Ibarra et al. used bovine meniscus fibrochondrocytes seeded on polyglycolic acid scaffolds which were implanted in nude mice to investigate the use of allografts in meniscus transplantation. These studies illustrate the potential of cell-based meniscus alternatives to improve meniscus repair.

Several cell sources have been tested for meniscus healing, along with meniscus fibrochondrocytes[16-18], chondrocytes[19-21], bone marrow-derived mesenchymal progenitor cells (BM-MSC)[22, 23], synovium derived stem cells[24], infra patellar fat pad progenitors (IPFP)[24], and adipose derived stem cells (ADSC)[25, 26]. However identification of the ideal cell type for meniscus repair has not yet been established.

Hydrogels and electrospun scaffolds materials can be tuned to structurally and mechanically resemble native ECM by altering either electrospun fiber or hydrogel properties. Hydrogel-based biomaterial systems have shown potential for tissue

engineering approaches. Hydrogels[27] are biocompatible crosslinkable hydrophilic polymers, with a high water content and a low mechanical modulus making them attractive as soft tissue engineering constructs[28]. Wu et al. studied tissue-derived ECM hydrogels for meniscus regeneration to treat meniscus injuries and disease[29]. For the creation of nano-fibrous scaffolds to emulate the structure of native tissue architectures like meniscus, application of electrospinning is an attractive and efficient method [30]. Electrospun fibers are produced by applying a voltage to charged polymer solutions by electrospinning [31, 32], which has attracted interest as tissue engineered scaffolds due to their fibrous structure, which mimics components of the extracellular matrix (ECM) (e.g., nm- μ m fiber diameters)[33, 34], and possesses a high surface area-to-volume ratio to increase cell contact area. Similarly, these materials can be tuned to structurally and mechanically resemble native ECM by altering either electrospun fiber or hydrogel properties; both can support cell attachment and proliferation[33, 35]. We previously demonstrated that polylactic acid (PLA) electrospun scaffolds can be specifically made to have either random or aligned electrospun fibers, which indicated potential suitability for meniscus tissue engineering[36].

To move towards production of meniscus like tissue with natural ECM materials, in this study we utilize the electrospinning process to produce scaffolds comprised of collagen type I with a fiber arrangement that emulates circumferential meniscus fiber structures. Scaffold compatibility was assessed by examining cell viability and whether these scaffolds permitted the development of meniscus like tissues when seeded with either human meniscus cells (derived from vascular and avascular regions), bone-marrow mesenchymal stem cells (hMSC), synovial cells, or infrapatellar fat pad (IPFP), to

produce (histological and gene expression based assessments). Finally, in order to produce tissues at a clinically relevant scale, we created layered constructs composed of ES scaffolds stacked with each of the aforementioned human cells embedded in an ECM hydrogel.

4.2 Materials and Methods

4.2.1 Fabrication of electrospun collagen type I scaffolds

Bovine Collagen type I (Semed S, acid-soluble, DSM, NL) at 16% (w/v) was dissolved in 20x phosphate buffered Saline (PBS) in ethanol at a ratio of 1:1 v/v as described previously[37]. The collagen solution was placed in a syringe controlled by a syringe pump (KDS200, KD Scientific Inc., USA) at a feeding rate of 0.1 mL/h. A Teflon tube was used to connect the syringe and a 21-gauge needle. All collector surfaces were covered by an aluminum foil. For spin random fibers, the tip-to-collector distance (TCD) was set to 16 cm on a flat plate as a collector. To spin aligned fibers, a rotating drum (~2400 rpm) was placed at 12 cm from the tangent of the drum to the needle tip. The applied voltage was varied from 15 to 20 kV using a voltage regulated DC power supply (NNC-30kV-2mA portable type, NanoNC, South Korea) to generate the polymer jet. Electrospun collagen scaffolds were crosslinked by soaking the mats in 0.25% glutaraldehyde (Sigma-Aldrich) in 1x PBS for 1 hour. After fixation scaffolds were washed three times with ethanol for 10 min each wash and stored at 4°C.

4.2.2 Tissues and cell isolation

Normal human meniscus (medial and lateral) was obtained from tissue banks (approved by Scripps institutional review board), from three donors (mean age: 34.6 ± 3.21 ; age range: 31–37 years; two males and one female). A macroscopic and histologic grading system[38] was used to select normal menisci. The outer 1/3 (avascular) portion of the meniscus and inner 2/3 was separated (using a surgical scalpel) and enzymatically

digested using collagenase (2mg/mL; C5138, Sigma-Aldrich, St. Louis, MO) in DMEM (Mediatech Inc, Manassas, VA) and 1% Penicillin-Streptomycin-Fungizone (Life Technologies, Carlsbad, CA) for 5-6 hours. Digested tissues were filtered through 100 μ m cell strainers (BD Biosciences, San Jose, CA) and seeded in monolayer culture in DMEM (Mediatech) supplemented with 10% calf serum (Omega Scientific Inc. Tarzana, CA) and 1% Penicillin/Streptomycin/Gentamycin (Life Technologies). Meniscus cells were cultured for one passage before use in scaffold seeding experiments.

Human MSC were purchased from Lonza (Alpharetta, GA) or from Texas A&M (Texas A&M Health Science Center College of Medicine Institute for Regenerative Medicine at Scott & White). MSC were cultured in Lonza MSC medium (Lonza, Basel Switzerland), and used at passage 4.

Human infrapatellar fat pad (IPFP) and synovium cells (from the suprapatellar pouch of the knee) were harvested and isolated from tissue banks or human knees (IPFP donor- mean age: 41 ± 11.53 ; age range: 29–52 years; two males and one female, synovial donor- mean age: 40.66 ± 29.77 ; age range: 22–75 years; two males and one female) within 22–72 h after death. IPFP and synovial tissues were rinsed with phosphate-buffered saline (PBS), and placed for overnight digestion under constant rotation at 37 °C with collagenase (2mg/mL; C5138, Sigma-Aldrich) in DMEM (Mediatech) and 1% Penicillin-Streptomycin-Fungizone (Life Technologies). The digested tissues were filtered through cell strainer with pore size of 100 μ m (BD Biosciences) and the cells were isolated by centrifugation (1500 rpm for 5 minutes, 3 times). The isolated synovial and IPFP cells were suspended in expansion medium,

DMEM (Mediatech) supplemented with 10% calf serum (Omega Scientific Inc.) and 1% Penicillin/Streptomycin/Gentamycin(Life Technologies). Cells were expanded for two passages before initiation of experiments.

4.2.3 Single layer scaffold cell culturing

Isolated human meniscus cells derived from the vascular and avascular regions, MSCs, synovial cells, and IPFP were seeded onto 1 cm x 0.5 cm rectangular aligned collagen scaffolds at a density of 0.25×10^6 per scaffold and maintained in 3 mL of monolayer culture medium for 3 days to allow cell attachment and scaffold colonization. The medium was changed to serum free ITS+ medium (Sigma) supplemented with 10 ng/mL TGF β 1 (Peprotech, Rocky Hill, NJ). After 1 week in culture with medium changes every 3-4 days, the cells on the scaffolds were assessed for cell viability (live/dead assay via confocal microscopy). After 2 weeks cell morphology was assessed by SEM.

4.2.4 Multi-layer construct formation

We used two approaches to produce multi-layer cell-seeded scaffolds: i) cells encapsulated in a hydrogel or ii) cell seeded directly on the scaffolds. For the former, cells were encapsulated in ECM molecules including collagen type II, chondroitin sulfate and hyaluronan (1 mg each). Isolated human vascular and avascular meniscus cells, MSCs, synovial cells, and IPFP were encapsulated in the ECM hydrogel at 6.25×10^6 cells per ml. Aligned collagen scaffolds were cut into discs (5 mm in diameter). Cells were seeded onto each disc and three discs were layered and encapsulated with 2%

alginate (PRONOVA UP LVG; Novamatrix, Sandvika, Norway) crosslinked in calcium chloride (120 mM; Sigma) for 20 minutes [36].

To seed cells directly onto aligned collagen scaffolds, two cell-laden scaffold layers were stacked and covered by a layer of 2 % alginate (PRONOVA UP LVG; Novamatrix) and soaked in calcium chloride (120mM; Sigma) in order to crosslink for 20 minutes. Constructs seeded with each cell type were cultured in 3 mL of monolayer culture medium, DMEM (Mediatech) supplemented with 10% calf serum (Omega Scientific Inc.) and 1% Penicillin/Streptomycin/Gentamycin (Life Technologies) for 3 days to permit cell attachment and scaffold colonization. The medium was changed every 3-4 days for 1 week to serum free ITS+ medium (Sigma) supplemented with 10 ng/mL TGF β 1 (Peprotech), TGF β 3 (Peprotech), or no growth factor (controls).

4.2.5 Cell viability assessments

Viability assessments were made single layer constructs after 7 days. Cells cultured in multilayered constructs (with and without the ECM hydrogel) were assessed for viability after 14 days of culture. The live/dead kit consisting of Calcein-AM and Ethidium Homodimer-1 (Life Technologies) was used for viability assessments using a laser confocal microscope (LSM-510, Zeiss, Jena, Germany)[36].

4.2.6 Cellular morphology of avascular meniscus cells on collagen type I scaffolds by

SEM

SEM was employed to observe high-resolution features of different cells grown on a single layer of an electrospun collagen scaffold. After a culture time of 14 day the

cell-seeded substrates were washed with 1x PBS and fixed with 2.5% w/v glutaraldehyde (Sigma-Aldrich) in 1x PBS for 1 h. After fixation the samples were washed three times with PBS for 10 min each wash. Following dehydration in a graded series of ethanol (50%, 70%, and 90%) for 30 min each, the samples were maintained in 100% ethanol for 24 h at 4 °C. While in 100% ethanol, the samples were completely dried in a critical point dryer (Autosamdri-815, Series A, Tousimis Inc., Rockvile, MD). The surface of the dried samples were metalized by sputter coating with iridium for SEM examination. The morphology of the samples as well as that of the adherent cells was observed by SEM (Philips XL30, FEI Co., Andover, MA)

4.2.7 Histology

Multilayered constructs seeded were fixed in Z-Fix (ANATECH, Battle Creek, MI) and embedded in paraffin. Sections (5–7µm thick) were stained with hematoxylin and eosin (H&E) to assess neotissue formation or with Safranin O-fast green to assess glycosaminoglycan distribution.

4.2.8 RNA isolation and RT-PCR

Total RNA was isolated from multilayered constructs with human meniscus cells, MSCs, synovial cells, and IPFP, using the RNeasy mini kit (Qiagen, Hilden, Germany). First strand cDNA was made according to the manufacturer's protocol (Applied Biosystems, Foster City, CA). Quantitative RT-PCR was performed using TaqMan® gene expression reagents. COL1A1, SOX9, COMP, CHAD, AGG, THY-1 and GAPDH

were detected using Assays-on-Demand™ primer/probe sets (Applied Biosystems). Gene expression was normalized relative to GAPDH expression using the Δ Ct method[41].

4.2.9 Mechanical properties of multilayered constructs

The mechanical properties of multilayered construct were measured via tensile testing (n=6 per group) under 4 conditions: i) freshly constructed multilayered constructs without hydrogel; ii) acellular multilayered construct with hydrogel; iii) human avascular meniscus cells encapsulated in hydrogel (avascular meniscal cells-laden multilayered constructs); iv) human IPFP cell layers (IPFP cells-laden multilayered constructs). Electrospun scaffolds were cut into dog-bone shaped specimens with a gauge length of 8 mm and width of 2 mm as previously described[36]. The thickness of each construct was measured using a digital caliper. The specimens were mounted in the grips of a uniaxial testing machine (Instron® Universal Testing Machine, 3342 Single Column Model; Norwood, MA) with a 500 N load cell and tested to failure at a crosshead speed of 1mm min⁻¹. Young's modulus was calculated from the slope of the linear segment of the stress-strain curve. Ultimate tensile strength (UTS) was calculated at the maximum load before failure. Values were presented as mean \pm SD.

4.2.10 Statistical analysis

Analysis of variance (ANOVA) and post hoc student's t-tests were used to assess statistically significance of differences in fiber diameter, mechanical properties, and gene expression levels. P-values less than 0.05 were considered significant.

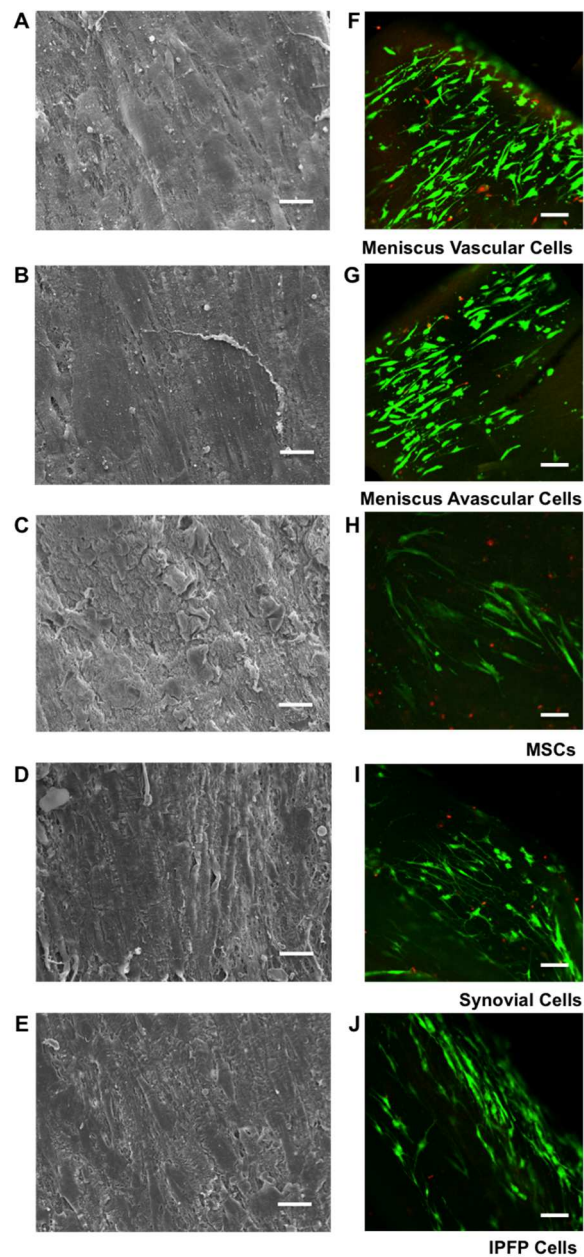


Figure 4.1 Scanning electron micrographs (SEM) of cellular response to aligned collagen fibrous scaffolds. SEM of (A) vascular, (B) avascular human meniscus cells, (C) MSCs, (D) synovial, and (E) IPFP cells cultivated on aligned electrospun collagen fibers (Mag. 625x; scale bar: 5 μm). (F) vascular, (G) avascular human meniscus cells, (H) MSCs, (I) synovial, and (J) IPFP cells on aligned scaffolds demonstrating viability (live/dead) and aligned cells cultivated on collagen scaffolds (Mag. 10x; scale bar: 200 μm in confocal images).

4.3 Results

4.3.1 Cell morphology and organization on a single layer of scaffold

Human meniscus cells, MSCs, synovial cells, and IPFP were seeded on aligned scaffolds of collagen type I collagen fibers. The cells were elongated and aligned parallel to the direction of the fibers as shown by SEM images on 14 day (Figures 4.1A, 4.1C, 4.1E, 4.1G, and 4.1I) or when assessed by confocal microscopy (after 7 days) using the live/dead assay (Figure 4.1B, 4.1D, 4.1F, 4.1H, and 4.1J).

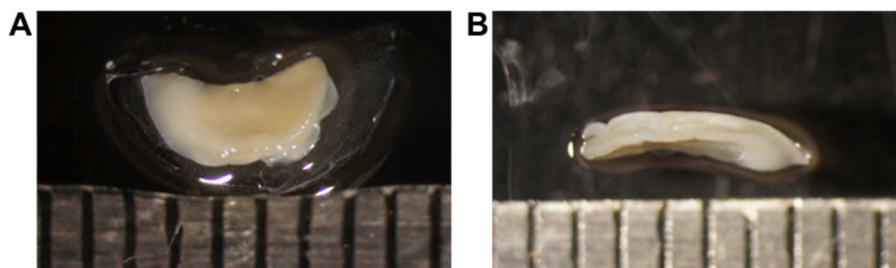


Figure 4.2 Three –dimensional cultures of human meniscus and BM-MSC on electrospun collagen scaffolds embedded in the tricomponent hydrogel As a screening tool, hBM-MSC were seeded upon electrospun collagen scaffold sheets I the hydrogel. (A) Macro top-view showing half a disc (scale in millimeters) (B) Macro side-view of half a disc

4.3.2 Multi-layer collagen scaffolds encapsulated cells with or without hydrogel

To create thicker meniscus-like graft tissues, multilayer constructs consisting of aligned ES collagen scaffolds, an ECM hydrogel and each of the human cells examined in this study were created. For each cell type, two conditions were examined. In one condition, the cells were either encapsulated with an ECM hydrogel and seeded onto the aligned ES scaffolds in layers, all held together within 2% alginate, crosslinked with

sodium citrate (Figure 4.3A). To assess the effect of the hydrogel, the second condition consisted on directly seeding the appropriate cell type on the scaffold (no ECM hydrogel) and two cell-laden collagen scaffolds were stacked, followed by an upper third collagen scaffold without cells and a covering layer of 2% alginate (Figure 4.4A). Cell viability of both multilayered constructs with or without the ECM hydrogel including human meniscus cells was captured via confocal images showing high viability between each scaffold (Figure 4.3B-C and 4.4B-C).

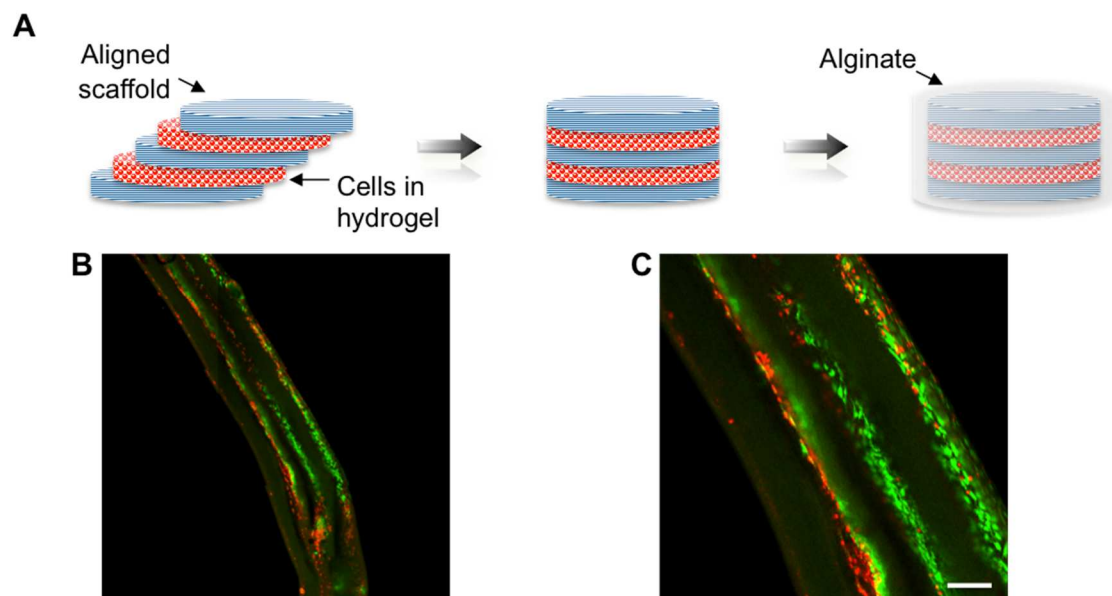


Figure 4.3 Layers of scaffold (square or disc shaped) and cells within hydrogel were constructed. The constructs were maintained in serum-free medium with either TGF β 1, TGF β 3 (10 ng/ml) or without growth factors (control) for 14 days. (A) Schematic representation of the three-layered constructs of collagen aligned fibrous scaffolds with cells encapsulated within the tricomponent hydrogel. Meniscus cells were seeded onto one disc-shaped aligned collagen scaffold, followed by layering another scaffold sheet on top. Another cell layer was applied, followed by a final third scaffold on the top. To stabilize the layers, a layer of 2% alginate dispensed over the construct. (B) Meniscus cells between aligned collagen fibrous scaffolds demonstrating viability (live/dead) aligned cells encapsulated with hydrogel within multilayered constructs (Mag. 10x; scale bar: 200 μ m in confocal images). (C) 3x3 of (B)

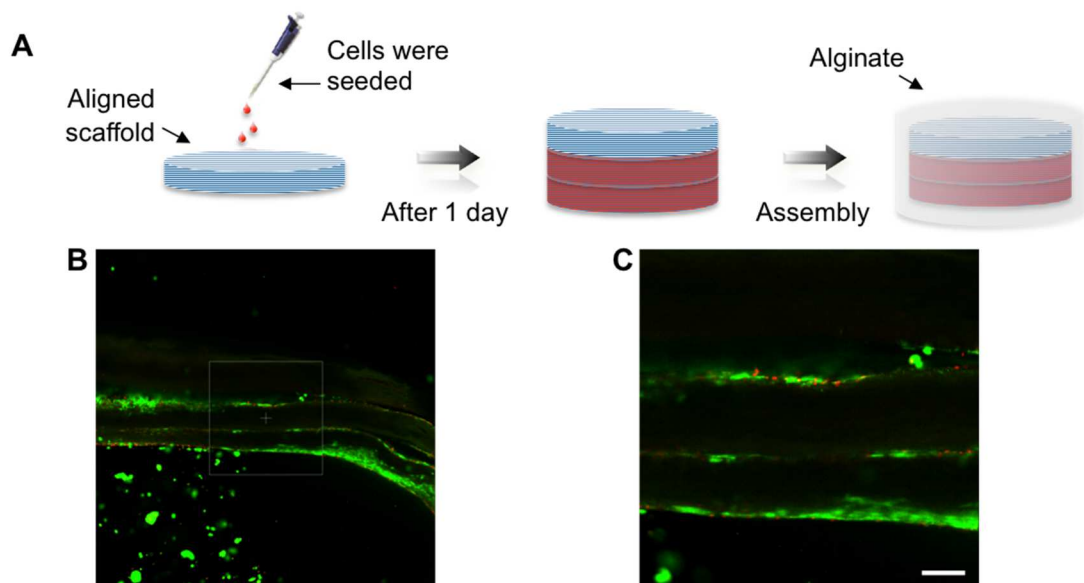


Figure 4.4 Layers of scaffold (square or disc shaped) and cells without hydrogel were constructed. The constructs were maintained in serum-free medium with either TGF β 1, TGF β 3 (10 ng/ml) or without growth factors (control) for 14 days. (A) Schematic representation of the three-layered constructs of collagen aligned fibrous scaffolds with cells. Meniscus cells were seeded on aligned collagen scaffolds. After one day, two cell-laden scaffold layers were stacked up with organized parallel to fibrous alignment of scaffold and covered with acellular scaffold layer. The layer of 2% alginate covered over the construct to hold the layers. (B) Meniscus cells between aligned collagen fibrous scaffolds demonstrating viability (live/dead) aligned cells without the hydrogel cultured within multilayered constructs (Mag. 10x; scale bar: 200 μ m in confocal images). (C) 3x3 of (B)

4.3.3 Multilayered collagen construct support meniscus-like neotissue formation

Histological analysis using Safranin O and H&E staining indicated that the multilayered constructs, with and without ECM hydrogels, formed new tissue between the layers consisting of extracellular matrix that was Safranin O negative and of cells that were aligned within the new tissue (Figure 4.5 and 4.6).

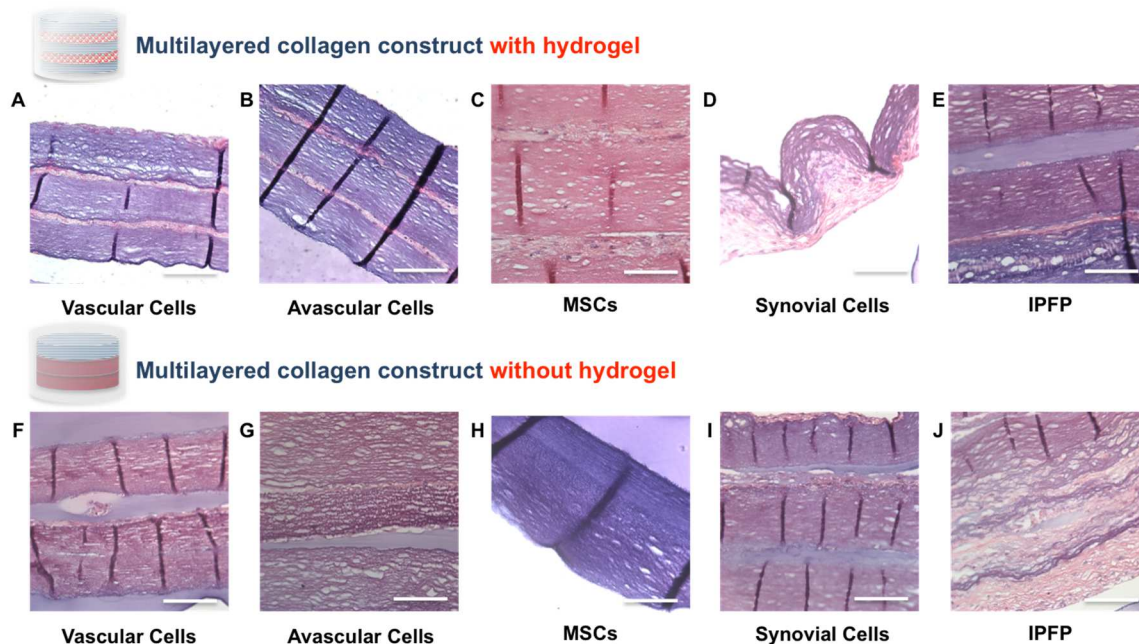


Figure 4.5 Histological analysis of three-dimensional cultures of human meniscus, BM-MSCs, Synovial, and IPFP cells on electrospun collagen scaffolds embedded in the tricomponent hydrogel. H&E stain of (A) human meniscus vascular, (B) avascular, (C) MSCs, (D) synovial, and (E) IPFP cells encapsulated within hydrogel for multilayered constructs. All different types of cell-laden aligned collagen scaffolds stacked without hydrogel for multilayered constructs. H&E stain of (F) human meniscus vascular, (G) avascular, (H) MSCs, (I) synovial, and (J) IPFP cells cultured between multilayered constructs.

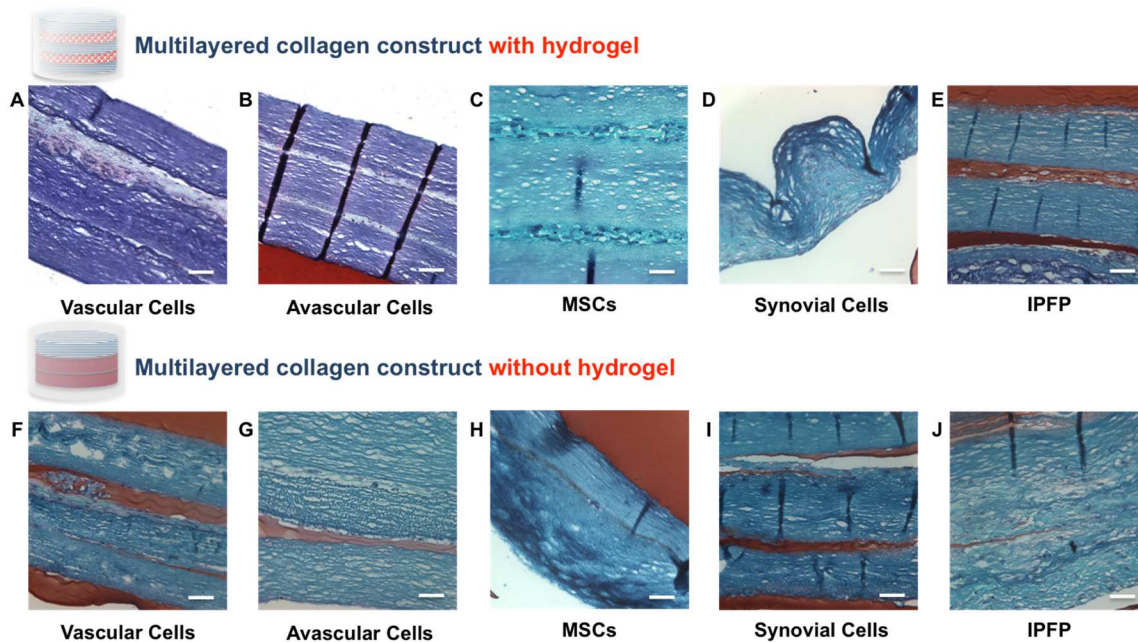


Figure 4.6 Histological analysis of three-dimensional cultures of human meniscus, BM-MSCs, Synovial, and IPFP cells on electrospun collagen scaffolds embedded in the tricomponent hydrogel. Safranin o fast green stain of (A) human meniscus vascular, (B) avascular, (C) MSCs, (D) synovial, and (E) IPFP cells encapsulated within hydrogel for multilayered constructs. All different types of cell-laden aligned collagen scaffolds stacked without hydrogel for multilayered constructs. Safranin O fast green stain of (F) human meniscus vascular, (G) avascular, (H) MSCs, (I) synovial, and (J) IPFP cells cultured between multilayered constructs.

4.3.4 A meniscus-like phenotype supported by scaffold and specific gene responses differed between cell source and scaffold organization.

Relative gene expression levels of neo-tissues formed under either TGF β 1 or TGF β 3 stimulation of cells relative to baseline control gene expression levels are shown in Figures 4.7 and 4.8. High expression of meniscus like-genes, especially collagen type I and COMP genes was induced by TGF β 1 stimulation of vascular and avascular meniscus cells, and MSC cells in multilayered constructs. However, synovial and IPFP cells produced high expression of meniscus like-genes when exposed to TGF β 3. Synovial cells without hydrogel expressed higher meniscus like-genes compared to multilayered construct with hydrogel. We could not detect any collagen type II expression in any cell type examined in this study.

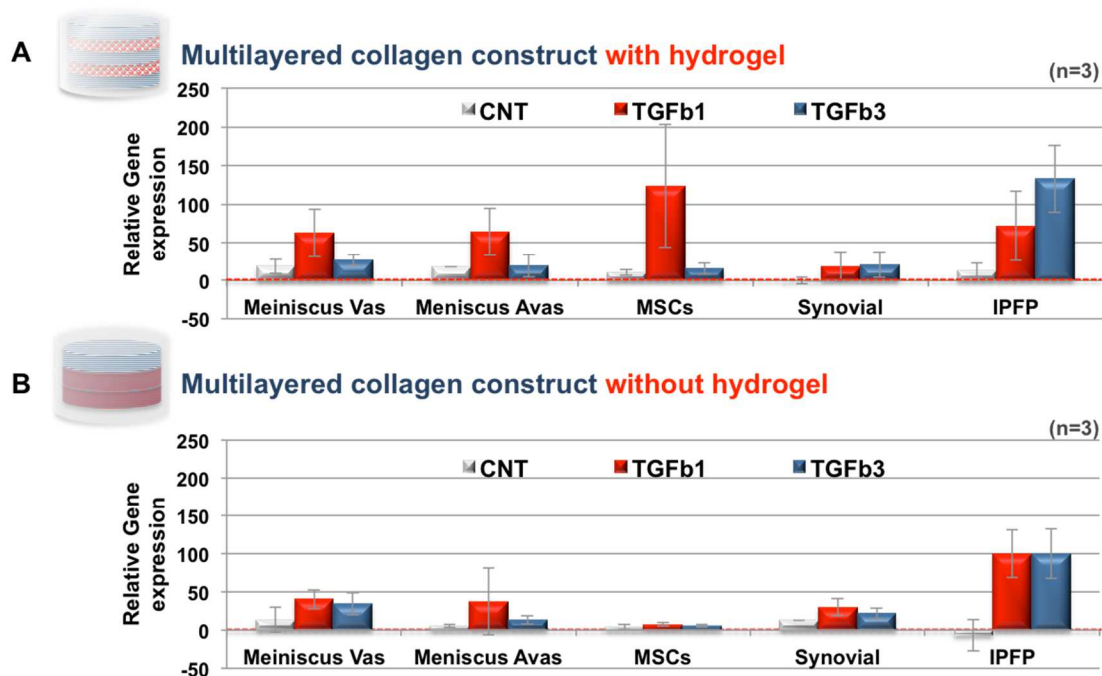


Figure 4.7 Relative fold change in COL1A1 gene expression of human vascular and avascular meniscus cells, MSCs, synovial, and IPFP cells of multilayered collagen constructs. (A) Gene expression of human meniscus vascular, avascular, MSCs, synovial, and IPFP cells encapsulated within hydrogel for multilayered constructs (n = 3 donors) relative to monolayer controls. And (B) gene expression of human meniscus vascular, avascular, MSCs, synovial, and IPFP cells cultured within multilayered constructs except for hydrogel (n = 3 donors) relative to monolayer controls. Expression levels are relative to monolayer controls (dotted line).

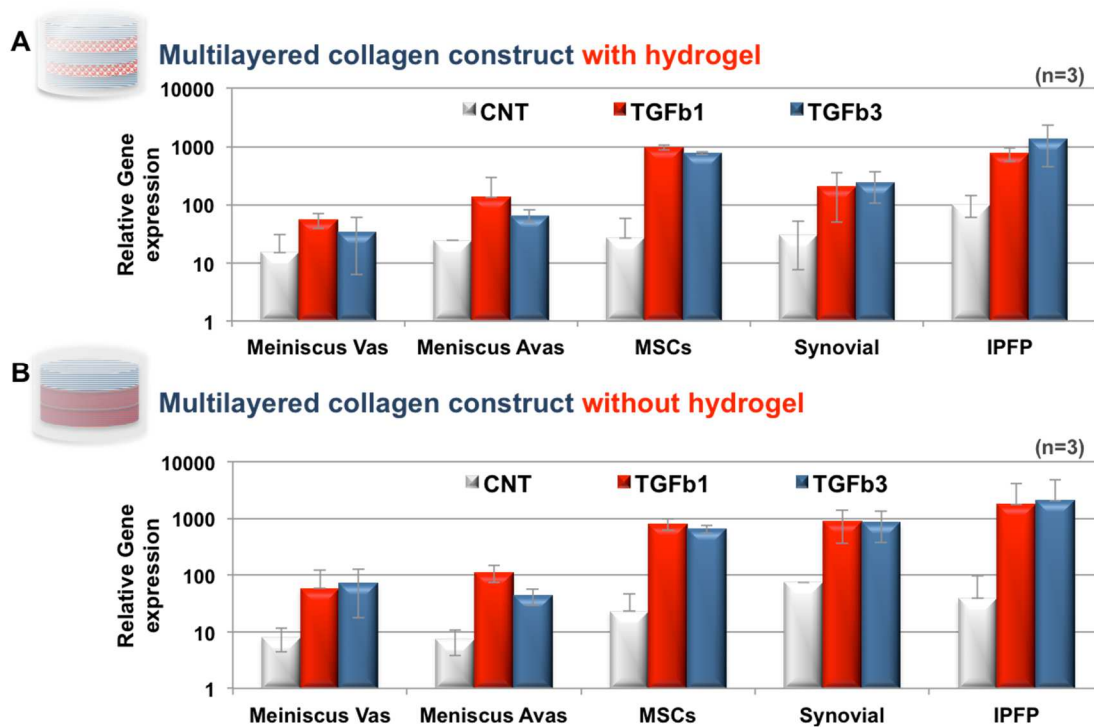


Figure 4.8 Relative fold change in COMP gene expression of human vascular and avascular meniscus cells, MSCs, synovial, and IPFP cells of multilayered collagen constructs. (A) Gene expression of human meniscus vascular, avascular, MSCs, synovial, and IPFP cells encapsulated within hydrogel for multilayered constructs (n = 3 donors) relative to monolayer controls. And (B) gene expression of human meniscus vascular, avascular, MSCs, synovial, and IPFP cells cultured within multilayered constructs except for hydrogel (n = 3 donors) relative to monolayer controls. Expression levels are relative to monolayer controls (dotted line).

4.3.5 Tensile mechanical property of multilayered construct dependent on existing cells or cell types

We compared the tensile modulus and ultimate tensile strength of the different multilayered constructs in Figure 4.9. Mechanical properties of human meniscus avascular and IPFP cell-seeded and acellular scaffolds were assessed after 1 week in culture. All constructs decreased in stiffness over time in culture, however, IPFP cell-seeded constructs generated higher stiffness and reached a higher ultimate tensile stress relative to scaffolds seeded with human meniscus avascular cells ($p < 0.05$).

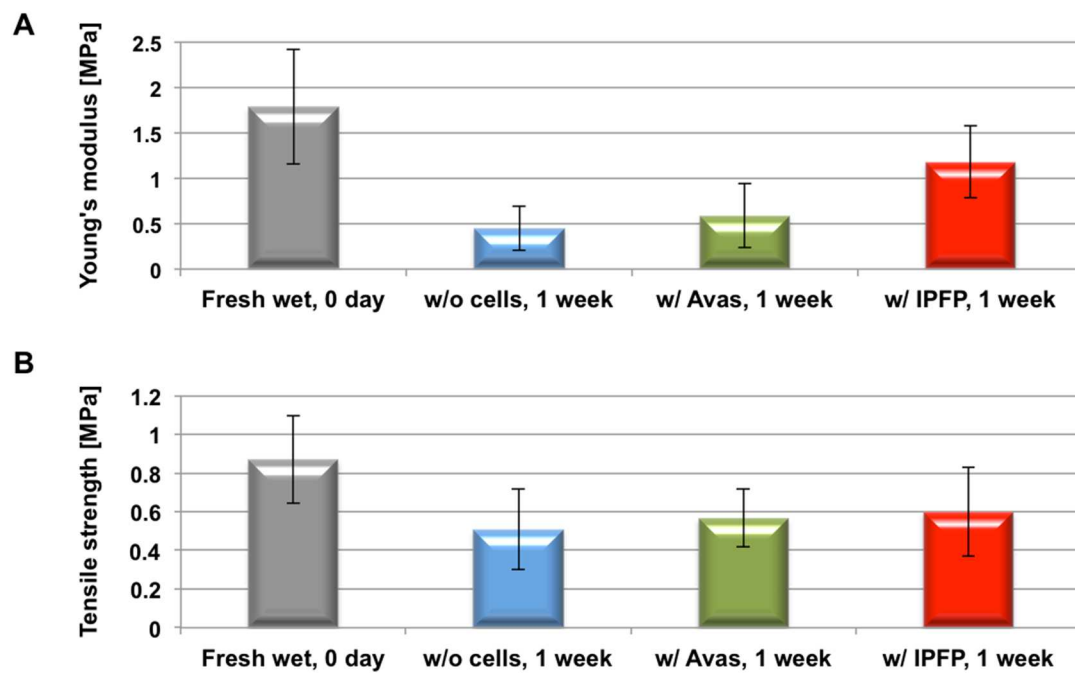


Figure 4.9 The mechanical properties of multilayered construct were quantified via tensile testing ($n = 9$ per group). (A) Young's modulus ($p < 0.05$) and (B) ultimate tensile strength of three-dimensional constructs (no significant difference)

4.4 Discussion

This study explored the potential for electrospun collagen scaffolds seeded with human cells of different sources to generate tissue capable of repairing or regenerating meniscal tears or degeneration. Since meniscal cells are difficult to obtain for tissue engineering we studied the meniscogenic potential of mesenchymal, cells from infrapatellar fat pad, and synovial cells. We demonstrated that layers of electrospun scaffolds could be combined with hydrogels to produce meniscus-like tissue constructs that structurally mimic native ECM of meniscus

Tissue obtained during meniscectomy can be a source of meniscal cells[42]. Previously, we have shown the potential for tissue engineering using meniscus cells isolated from meniscus tissue seeded in biodegradable electrospun scaffolds[36]. Baker et al.[43] also demonstrated that expansion and seeding of meniscal debris-derived cells onto nanofibrous biodegradable scaffolds results in engineered constructs with mechanical properties approaching native tissue levels. However, due to the limited source of meniscal cells, it is critical that alternate cell sources be investigated for meniscogenic potential[42]. In this present study, we investigated several cell types assess their capacity for meniscus tissue formation. We demonstrated high cell compatibility with electrospun collagen scaffolds and ECM hydrogel.

An ideal engineered meniscus construct will eventually be replaced in its entirety by newly deposited ECM produced by cells implanted along with the scaffold, or by cells that invade the scaffold in situ. In the present study, a single collagen ES layer was too thin to emulate the tissue thickness desired for a meniscus graft. Therefore, thicker

constructs were fabricated by layering up to 3 aligned collagen scaffolds for proof-of-concept in engineering fiber-reinforced meniscal tissues. Reinforcement with nanofibers are an attractive approach for improving the poor mechanical properties of hydrogels. For example, Kai et al.[44] fabricated nanofiber reinforced composite hydrogels by combined electrospun poly(e-caprolactone) (PCL)/gelatin ‘blend’ or ‘coaxial’ nanofibers into gelatin hydrogels. The Young’s modulus of the composite hydrogels increased from 3.29 ± 1.02 kPa to 20.30 ± 1.79 kPa by increasing the amount of nanofibers incorporated into the hydrogel.

All the cells in our study developed an elongated morphology and followed the alignment of the ES fibers. As evidence of ECM production we observed high COL1A1 and COMP mRNA levels, and collagen type I deposition between the electrospun collagen fibers and throughout the multiple electrospun collagen layers within 14 days of culture. Overall, multilayer constructs with the ECM hydrogel produced tissue with higher COMP and COL1A1 gene expression levels compared to multi-layered constructs without the ECM hydrogel. In terms of cell source, the IPFP cells revealed much higher meniscus-like neotissue formation in terms of COL1A1 and COMP gene expression, and were equally responsive to both TGF β 1 and TGF β 3 in comparison to other cell types tested, which only responded to TGF β 1.

Electrospinning is a suitable manufacturing technique for adjusting the mechanical properties and anisotropy of tissue engineering scaffolds. We showed that such scaffolds could be formed with a range of anisotropic behavior of collagen fibrous scaffolds using a rotating drum cylinder as an electrospun fiber collecting plate. The mechanical response of multilayered constructs also differed markedly between human

meniscus avascular and IPFP cells encapsulated between collagen scaffolds. Interestingly, IPFP cell-encapsulated multilayered constructs had higher mechanical property than any other cell type within 7 days of culture. The higher mechanical property in construct correlated with the amount of neo-tissue generated by the cells according to gene expression data and histology.

These cell-laden multilayered constructs also had a much higher tensile mechanical property compared to 3D constructs reported in other studies. Kai et al.[44] studied mechanical properties of nanofiber-hydrogel composite blending of two different materials or co-axial electrospinning methods. Tensile properties of their blend and coaxial polycaprolactone (PCL)/gelatin nanofibers after soaking in PBS for 3 hour was 0.13 ± 0.04 and 0.56 ± 0.09 MPa respectively, which were lower than our wet fresh 0 day specimen's mechanical property (Young's modulus: 1.79 ± 0.63 MPa). Also, Grogan et al. [45] analyzed the tensile strength of three-dimensional methacrylated gelatin (GelMA) constructs fabricated via projection stereolithography and cultured with human meniscus cells and reported a Young's modulus about 10.5 kPa. Xu et al.[46] investigated the multilayered construction of a hybrid inkjet printing/PCL electrospinning system for cartilage tissue engineering applications and reported a tensile modulus of 1.76 MPa for their printed hybrid constructs. This value is similar to ours; however, we used natural protein polymers and hydrogel to mimic the environment of native human meniscus avascular zone for a more meniscus-like tissue formation.

We generated promising results from five different cell types: meniscus cells derived from vascular and avascular sections, MSCs, synovial, and IPFP cells; and showed potential for tissue engineering by layering multiple collagen scaffolds. However,

several issues remain to be addressed to translate our approach to clinical application. Layers tend to delaminate under shear and therefore shear testing has to be conducted. The mechanical properties of the collagen scaffolds, while encouraging, were still lower than the optimal levels required to survive loading in vivo in the knee. Hence, research is ongoing to develop methods to improve structural and mechanical properties of the construct. One such approach is co-axial core/shell electrospinning with a synthetic biodegradable polymer as the core to enhance structural and mechanical property and protein polymer as the shell to improve cell compatibility.

4.5 Conclusion

In summary, this study demonstrates the potential of combination of cells and scaffolds with hydrogel to create meniscus-like neo-tissue. Future studies to enhance mechanical properties of these constructs are required before translation to the repair of meniscal defects.

4.6 Acknowledgments

This chapter, in full, is currently being prepared for submission for publication of the material. Jihye Baek, Sujata Sovani, Wonchul Choi, Sungho Jin, Shawn P. Grogan, Darryl D. D'Lima. The dissertation author was the primary investigator and author of this paper.

4.7 References

- [1] Baker P, Coggon D, Reading I, Barrett D, McLaren M, Cooper C. Sports injury, occupational physical activity, joint laxity, and meniscal damage. *The Journal of Rheumatology*. 2002;3:557-63.
- [2] Boyd KT, Myers PT. Meniscus preservation; rationale, repair techniques and results. *The Knee*. 2003;10:1-11.
- [3] Sweigart MA, Athanasiou KA. Toward tissue engineering of the knee meniscus. *Tissue Eng*. 2001;7:111-29.
- [4] Poulsen MR, Johnson DL. Meniscal injuries in the young, athletically active patient. *Phys Sportsmed*. 2011;39:123-30.
- [5] Setton LA, Guilak F, Hsu EW, Vail TP. Biomechanical factors in tissue engineered meniscal repair. *Clinical Orthopaedics and Related Research*. 1999;367(Suppl):S254-72.
- [6] Jones RS, Keene GCR, Learmonth DJA, Bickerstaff D, Nawana NS, Costi JJ and Percy MJ. Direct measurement of hoop strains in the intact and torn human medial meniscus. *Clinical Biomechanics*. 1996;11:295-300.
- [7] Roos H, Lauren M, Adalberth T, Roos EM, Jonsson K, Lohmander LS. Knee osteoarthritis after meniscectomy: prevalence of radiographic changes after twenty-one years, compared with matched controls. *Arthritis and Rheumatism*. 1998;41:687-93.
- [8] Garrett W E, Swiontkowski M F, Weinstein J N, Callaghan J, Rosier R N, Berry D J, Harrast J and Derosa G P American Board of Orthopaedic Surgery Practice of the Orthopaedic Surgeon: Part-II, Certification Examination Case Mix. *The Journal of Bone & Joint Surgery*. 2006;88:660-7.
- [9] Reguzzoni M, Manelli A, Ronga M, Raspanti M, Grassi FA. Histology and ultrastructure of a tissue-engineered collagen meniscus before and after implantation. *Journal of Biomedical Materials Research Part B: Applied Biomaterials*. 2005;74B:808-16.
- [10] Ronga M, Grassi FA, Manelli A, Bulgheroni P. Tissue Engineering Techniques for the Treatment of a Complex Knee Injury. *Arthroscopy: The Journal of Arthroscopic & Related Surgery*. 2006;22:576.e1-.e3.
- [11] Zaffagnini S, Giordano G, Vascellari A, Bruni D, Neri M, Iacono F, Kon E, Presti M and Maccacci M Arthroscopic collagen meniscus implant results at 6 to 8 years follow up. *Knee Surg Sports Traumatol Arthrosc*. 2007;15:175-83.

- [12] Pabbruwe MB, Kafienah W, Tarlton JF, Mistry S, Fox DJ, Hollander AP. Repair of meniscal cartilage white zone tears using a stem cell/collagen-scaffold implant. *Biomaterials*. 2010;31:2583-91.
- [13] Peretti G, Scotti C, Pozzi A, Mangiavini L, Vitari F, Domeneghini C, Frascini G. Bonding of meniscal tissue: a nude mouse repair model. *Sport Sci Health*. 2008;3:47-52.
- [14] Weinand C, Peretti G, Adams S, Jr., Randolph M, Savvidis E, Gill T. Healing potential of transplanted allogeneic chondrocytes of three different sources in lesions of the avascular zone of the meniscus: a pilot study. *Arch Orthop Trauma Surg*. 2006;126:599-605.
- [15] Weinand C, Peretti GM, Adams SBJ, Bonassar LJ, Randolph MA, Gill TJ. An allogenic cell-based implant for meniscal lesions. *Am J Sports Med*. 2006;34:1779-89.
- [16] Ibarra C, Jannetta C, Vacanti CA, Cao Y, Kim TH, Upton J, Vacanti JP. Tissue engineered meniscus: A potential new alternative to allogeneic meniscus transplantation. *Transplantation Proceedings*. 1997;29:986-8.
- [17] Martinek V, Ueblacker P, Bräun K, Nitschke S, Mannhardt R, Specht K, Gansbacher B, Imhoff AB. Second generation of meniscus transplantation: in-vivo study with tissue engineered meniscus replacement. *Arch Orthop Trauma Surg*. 2006;126:228-34.
- [18] Hidaka C, Ibarra C, Hannafin JA, Torzilli PA, Quitoriano M, Jen S-S, Warren RF, Crystal RG. Formation of Vascularized Meniscal Tissue by Combining Gene Therapy with Tissue Engineering. *Tissue Engineering*. 2004;8:93-105.
- [19] Weinand C, Randolph M, Peretti G, Adams S, Gill T. Cellular repair of meniscal tears in avascular region (Abstract). *Trans Orthop Res Soc*. 2005.
- [20] Peretti GM, Gill T, Xu J-W, Randolph MA, Morse KR, Zaleske DJ. Cell-based therapy for meniscal repair: a large animal study. *The American Journal of Sports Medicine*. 2004;32:146-58.
- [21] Peretti GM, Caruso EM, Randolph MA, Zaleske DJ. Meniscal repair using engineered tissue. *Journal of Orthopaedic Research*. 2001;19:278-85.
- [22] Dave LYH, Nyland J, McKee PB, Caborn DNM. Mesenchymal Stem Cell Therapy in the Sports Knee: Where Are We in 2011? *Sports Health*. 2012;4:252-7.
- [23] Ferris D, Frisbie D, Kisiday J, McIlwraith CW. In Vivo Healing of Meniscal Lacerations Using Bone Marrow-Derived Mesenchymal Stem Cells and Fibrin Glue. *Stem Cells International*. 2012;2012:691605.

- [24] Marsano A, Millward-Sadler SJ, Salter DM, Adesida A, Hardingham T, Tognana E, Kon E, Chiari-Grisar C, Nehrer S, Jakob M, Martin I. Differential cartilaginous tissue formation by human synovial membrane, fat pad, meniscus cells and articular chondrocytes. *Osteoarthritis and Cartilage*. 2007;15:48-58.
- [25] Pak J, Lee JH, Lee SH. Regenerative repair of damaged meniscus with autologous adipose tissue-derived stem cells. *BioMed Research International*. 2014; 436029.
- [26] Ruiz-Ibán MÁ, Díaz-Heredia J, García-Gómez I, Gonzalez-Lizán F, Elías-Martín E, Abaira V. The Effect of the Addition of Adipose-Derived Mesenchymal Stem Cells to a Meniscal Repair in the Avascular Zone: An Experimental Study in Rabbits. *Arthroscopy*. 2011;27:1688-96.
- [27] Kashyap N, Kumar N, Kumar MN. Hydrogels for pharmaceutical and biomedical applications. *Critical Reviews in Therapeutic Drug Carrier Systems*. 2005;22:107-49.
- [28] Peppas NA, Hilt JZ, Khademhosseini A, Langer R. Hydrogels in Biology and Medicine: From Molecular Principles to Bionanotechnology. *Advanced Materials*. 2006;18:1345-60.
- [29] Wu J, Ding Q, Dutta A, Wang Y, Huang Y-h, Weng H, Tang L, Hong Y. An injectable extracellular matrix derived hydrogel for meniscus repair and regeneration. *Acta biomaterialia*. 2015;16:49-59.
- [30] Sill TJ, von Recum HA. Electrospinning: Applications in drug delivery and tissue engineering. *Biomaterials*. 2008;29:1989-2006.
- [31] Chew SY, Wen Y, Dzenis Y, Leong KW. The Role of Electrospinning in the Emerging Field of Nanomedicine. *Current pharmaceutical design*. 2006;12:4751-70.
- [32] Murugan. R, Ramakrishna. S. Nano-featured scaffolds for tissue engineering- A review of spinning methodologies. *Tissue Engineering*. 2006;12:435-47.
- [33] Liang D, Hsiao BS, Chu B. Functional Electrospun Nanofibrous Scaffolds for Biomedical Applications. *Advanced drug delivery reviews*. 2007;59:1392-412.
- [34] Yoo HS, Kim TG, Park TG. Surface-functionalized electrospun nanofibers for tissue engineering and drug delivery. *Advanced Drug Delivery Reviews*. 2009;61:1033-42.
- [35] Lee KY, Mooney DJ. Hydrogels for Tissue Engineering. *Chemical Reviews*. 2001;101:1869-80.
- [36] Baek J, Chen X, Sovani S, Jin S, Grogan SP, D'Lima DD. Meniscus tissue engineering using a novel combination of electrospun scaffolds and human meniscus cells embedded within an extracellular matrix hydrogel. *Journal of Orthopaedic Research*. 2015;33:572-83.

- [37] Dong B, Arnoult O, Smith ME, Wnek GE. Electrospinning of collagen nanofiber scaffolds from benign solvents. *Macromolecular rapid communications*. 2009;30:539-42.
- [38] Pauli C, Grogan SP, Patil S, Otsuki S, Hasegawa A, Koziol J, Lotz MK and D'Lima DD Macroscopic and histopathologic analysis of human knee menisci in aging and osteoarthritis. *Osteoarthritis and cartilage / OARS, Osteoarthritis Research Society*. 2011;19:1132-41.
- [39] Roberts S, Menage J, Sandell LJ, Evans EH, Richardson JB. Immunohistochemical study of collagen types I and II and procollagen IIA in human cartilage repair tissue following autologous chondrocyte implantation. *The Knee*. 2009;16:398-404.
- [40] Grogan SP, Miyaki S, Asahara H, D'Lima DD, Lotz MK. Mesenchymal progenitor cell markers in human articular cartilage: normal distribution and changes in osteoarthritis. *Arthritis research & therapy*. 2009;11:R85.
- [41] Martin I, Jakob M, Schäfer D, Dick W, Spagnoli G, Heberer M. Quantitative analysis of gene expression in human articular cartilage from normal and osteoarthritic joints. *Osteoarthritis and Cartilage*. 2001;9:112-8.
- [42] Scotti C, Hirschmann MT, Antinolfi P, Martin I, Peretti GM. Meniscus repair and regeneration: review on current methods and research potential. *Eur Cell Mater*. 2013;26:150-70.
- [43] Baker BM, Nathan AS, Huffman GR, Mauck RL. Tissue Engineering With Meniscus Cells Derived From Surgical Debris. *Osteoarthritis and cartilage / OARS, Osteoarthritis Research Society*. 2009;17:336-45.
- [44] Kai D, Prabhakaran MP, Stahl B, Eblenkamp M, Wintermantel E, Ramakrishna S. Mechanical properties and in vitro behavior of nanofiber-hydrogel composites for tissue engineering applications. *Nanotechnology*. 2012;23:095705.
- [45] Grogan SP, Chung PH, Soman P, Chen P, Lotz MK, Chen S and D'Lima DD Digital micromirror device projection printing system for meniscus tissue engineering. *Acta biomaterialia*. 2013;9:7218-26.
- [46] Xu T, Binder KW, Albanna MZ, Dice D, Zhao W, Yoo JJ and Atala A Hybrid printing of mechanically and biologically improved constructs for cartilage tissue engineering applications. *Biofabrication*. 2013;5:015001.

CHAPTER 5: CONCLUSIONS

In this work, electrospun materials alone or in combination with an ECM hydrogel was capable of supporting the development of meniscus-like neotissue, which show potential for use in cell-based meniscus regeneration strategies.

Firstly, we electrospun PLA to generate biodegradable and biomimetic nanofibrous scaffolds. Aligned electrospun PLA fibers developed an anisotropic tensile modulus that better approximated the properties of meniscal tissue than random electrospun PLA fibers. Cells from avascular and vascular regions of human menisci survived, attached, and infiltrated the PLA nanofibrous scaffold, and secreted the major proteins found in native meniscal matrix. We were also able to demonstrate feasibility of a novel approach of combining nanofibrous scaffolds with human meniscus cells in an ECM hydrogel to fabricate thicker multilayered constructs with the dimensions necessary for partial meniscus replacement.

Secondly, we used electrospun collagen scaffolds to induce a cellular alignment with scaffold microstructure and to stimulate meniscogenic neo-tissue. Collagen scaffolds mimicking the organization of collagen bundles in the native meniscus have promise for the repair of meniscal tears, as indicated by the generation and integration of new tissue in ex-vivo meniscal tears in the avascular region. Such cell-based scaffolds may be translated to enhance surgical treatments to heal meniscal tears in the avascular zone.

Lastly, the results of this study demonstrated the potential of different human cell types in combination with collagen scaffolds to create meniscus like neotissues resembling native tissue. Because it is difficult to obtain human meniscal cells, other cells

that are more readily available clinically were investigated. Cells harvested from infrapatellar fat pad had the most meniscogenic potential compared to mesenchymal cells harvested from bone marrow or cells harvested from the synovial membrane. With optimization of scaffold and cell function to enhance tissue properties, such constructs may have promise in the repair and replacement of meniscal defects.

Overall, electrospun materials that can support neotissue formation show potential for use in cell-based meniscus regeneration strategies. When combined with biomimetic materials to support the production of meniscus-like phenotype, cells harvested from infrapatellar fat pad have greater potential compared to other cell types.